Flasher calibration of the T1 and T2 CANGAROO telescopes and TeV gamma ray observation of Markarian 421 and EXO 055625-3838.6 BL Lacertae blazars

David Swaby

This thesis is submitted as a Master of Science (Research) to the

School of Chemistry and Physics (High Energy Astrophysics),
University of Adelaide

Supervisor:
Prof. Roger Clay

Adelaide, December 2010

Appendix A

Circuit diagrams of the flasher apparatus and PIN diode monitor

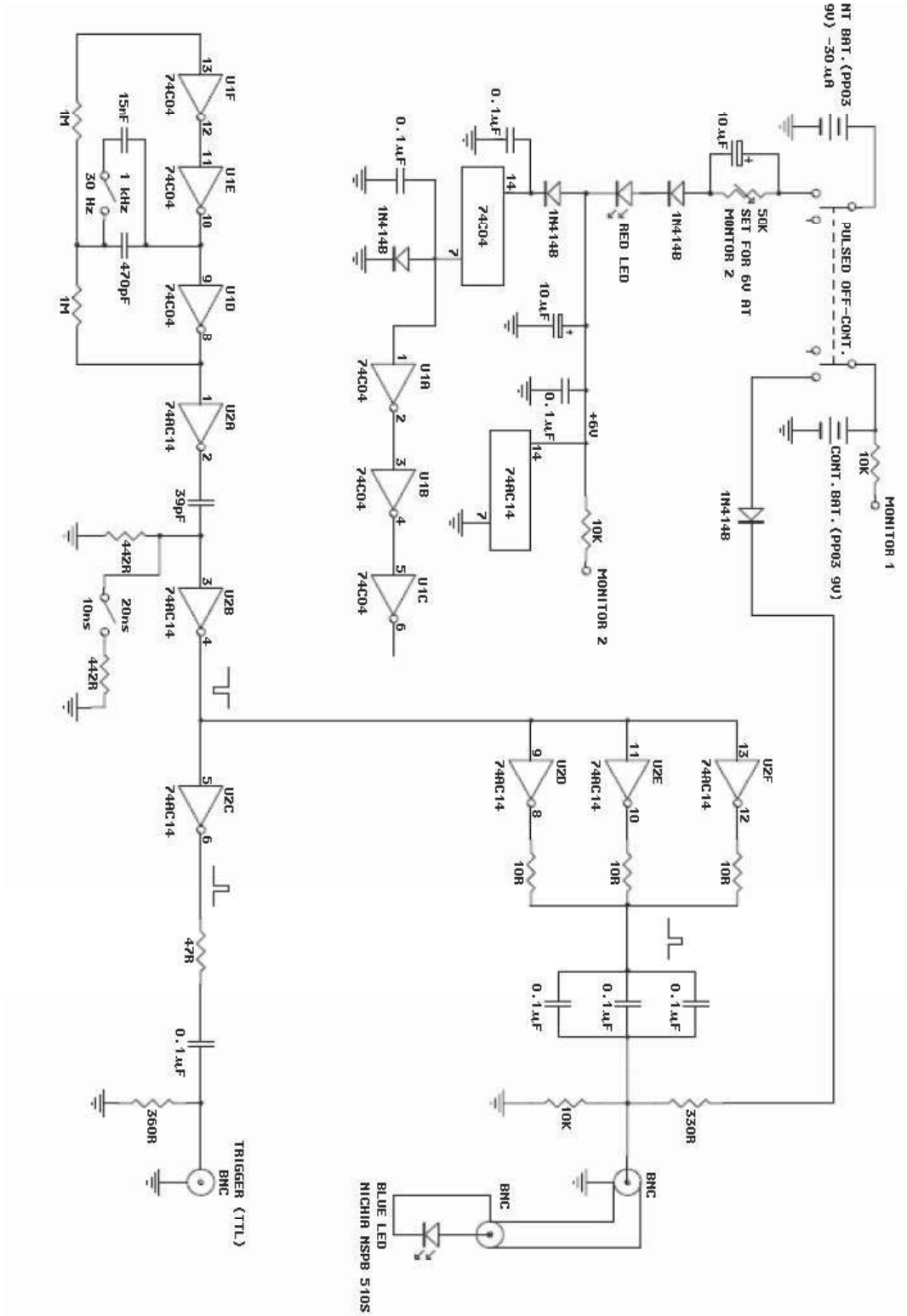

Figure A.1: Circuit diagram (rotated 90°) of the *Nichia* blue LED flasher calibration apparatus.

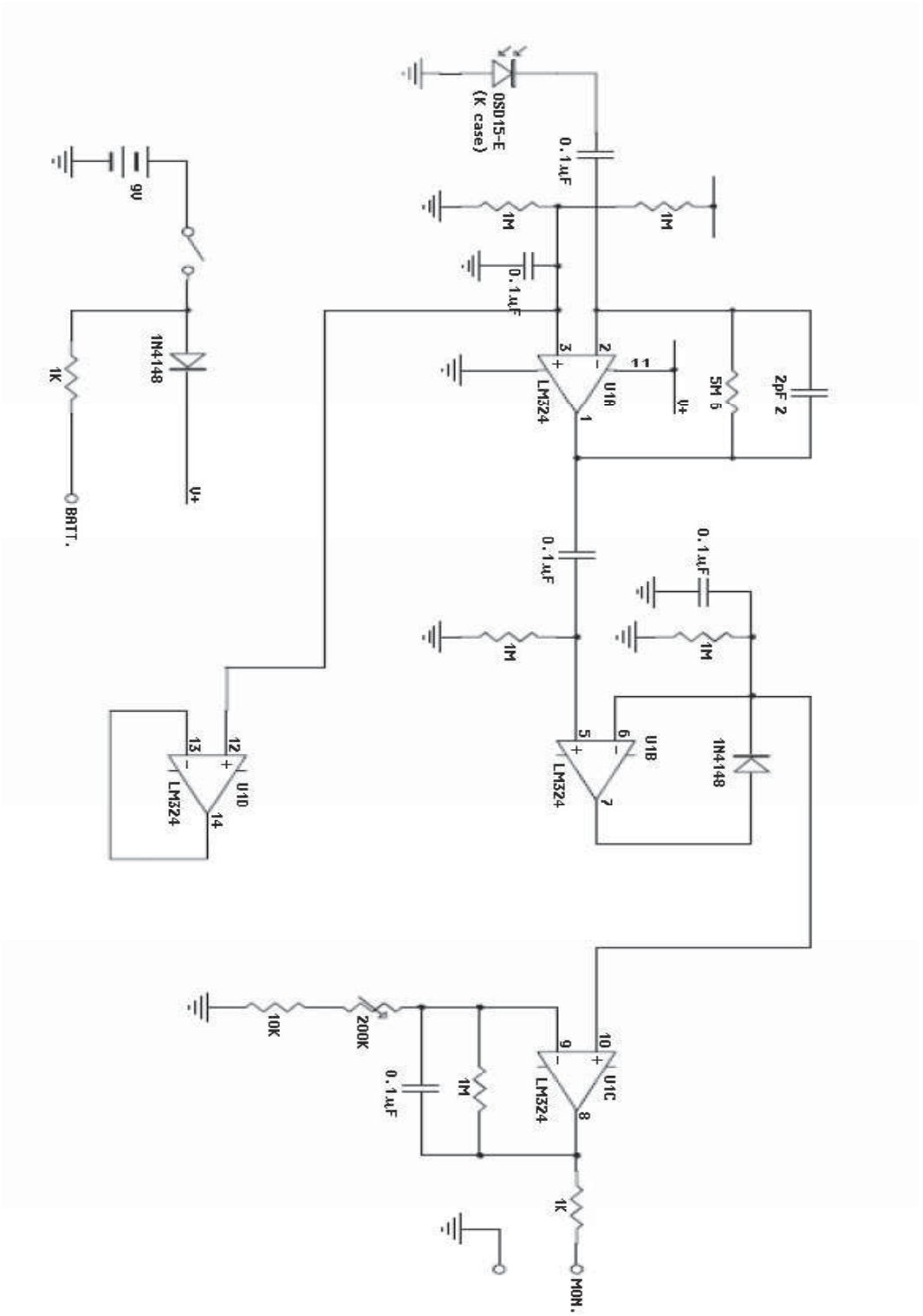

Figure A.2: Circuit diagram (rotated 90°) of pin diode monitor apparatus to measure the flasher output.

Appendix B

T1 and T2 flasher calibration data files

Calibration data file no.	Month(Year)	Flasher setting	No. of events
1042007	Apr. 2001	10 ns	7401
1042008	Apr. 2001	20 ns	10081
1042009	Apr. 2001	10 ns	7036
1042010	Apr. 2001	Background (random trig.)	19162
1071711	July 2001	20 ns	3239
1071712	July 2001	10 ns	2716
1071713	July 2001	20 ns ND 0.8	3188
1071714	July 2001	10 ns ND 0.8	2185
1071724	July 2001	10 ns ND 1.0 ?	4124
1071725	July 2001	10 ns ?	17803
1071726	July 2001	Background (random trig.)	5399
2020704	Feb. 2002	20 ns	13589
2020705	Feb. 2002	20 ns	10315
2020706	Feb. 2002	10 ns	12260
2020709	Feb. 2002	Background (random trig.)	11320
2060406	June 2002	10 ns ND 0.4	3922
2060410	June 2002	20 ns	9128
2060411	June 2002	10 ns	9518
2060412	June 2002	10 ns ND 0.1	8217
2060413	June 2002	10 ns ND 0.2	8519
2060414	June 2002	10 ns ND 0.6	4946
2060415	June 2002	10 ns ND 0.8	4129
2060416	June 2002	10 ns ND 1.0	2599
2060417	June 2002	10 ns	4423
2060418	June 2002	20 ns	3961
2060421	June 2002	Background (random trig.)	3168

Table B.1: Table 1 of 2: T1 flasher calibration data files from unit 2. Data file numbers in bold indicate 10 ns setting used in two-dimensional cross-correlation calibration by month, see Fig E.4 Appendix E. The question marks for data runs 1071724 & 1071725, indicate some uncertainty about the flasher settings for these two calibrations.

Calibration data file no.	Month(Year)	Flasher setting	No. of events
2110703	Nov. 2002	20 ns	7906
2110704	Nov. 2002	10 ns	4300 car lights
2110705	Nov. 2002	20 ns ND 0.4	4225
2110706	Nov. 2002	10 ns ND 0.4	4481
2110707	Nov. 2002	20 ns	3663
2110708	Nov. 2002	10 ns	3629
2110713	Nov. 2002	Background (random trig.)	10517
3010904	Jan. 2003	20 ns	13855
3010905	Jan. 2003	10 ns	7105
3010907	Jan. 2003	10 ns ND 0.4	7412
3010908	Jan. 2003	20 ns ND 0.4	8639
3010913	Jan. 2003	Background (random trig.)	10547
3060607	June 2003	20 ns	7794
3060608	June 2003	10 ns	10218
3060609	June 2003	20 ns ND 0.4	10543
3060612	June 2003	10 ns ND 0.4	19595
3060613	June 2003	Background (random trig.)	14910
3101604	Oct. 2003	20 ns ND 0.8	10076
3101605	Oct. 2003	10 ns ND 0.8	9151
3101606	Oct. 2003	20 ns	3312
3101607	Oct. 2003	10ns	3279
3101608	Oct. 2003	20 ns ND 0.4	3557
3101609	Oct. 2003	10 ns ND 0.4	4183
3101610	Oct. 2003	Background (random trig.)	10105

Table B.2: Table 2 of 2: T1 flasher calibration data files from unit 2. Data file numbers in bold indicate 10 ns setting used in two-dimensional cross-correlation calibration by month, see Fig E.4 Appendix E.

Calibration data file no.	**Month(Year)**	**Flasher setting**	**No. of events**
3010905	Jan. 2003	20 ns	25625
3010906	Jan. 2003	10 ns	16151
3010911	Jan. 2003	10 ns ND 0.4	13347
3010912	Jan. 2003	20 ns ND 0.4	8722
3010914	Jan. 2003	20 ns	19786
3010915	Jan. 2003	10 ns	12228
3010916	Jan. 2003	Background (random trig.)	11607
3060609	June 2003	20 ns	8294
3060610	June 2003	10 ns	27266
3060611	June 2003	20 ns ND 0.4	12098
3060612	June 2003	10 ns ND 0.4	8838
3060613	June 2003	Background (random trig.)	10396
3101603	Oct. 2003	20 ns	44802
3101604	Oct. 2003	20 ns	17809
3101605	Oct. 2003	10 ns	4203
3101606	Oct. 2003	10 ns ND 0.4	5809
3101607	Oct. 2003	20 ns ND 0.4	5230
3101608	Oct. 2003	20 ns ND 0.8	7934
3101609	Oct. 2003	10 ns ND 0.8	7462
3101611	Oct. 2003	Background (random trig.)	11037

Table B.3: T2 flasher calibration data files from unit 2. Data file numbers in bold indicate 10 ns setting used in checking flasher signal amplitude, month by month. Data file numbers in italics indicate 10 ns ND 0.4 setting, also used for checking flasher signal amplitude for T2.

Appendix C

T1 flasher calibration: Mean ADC Pedestals

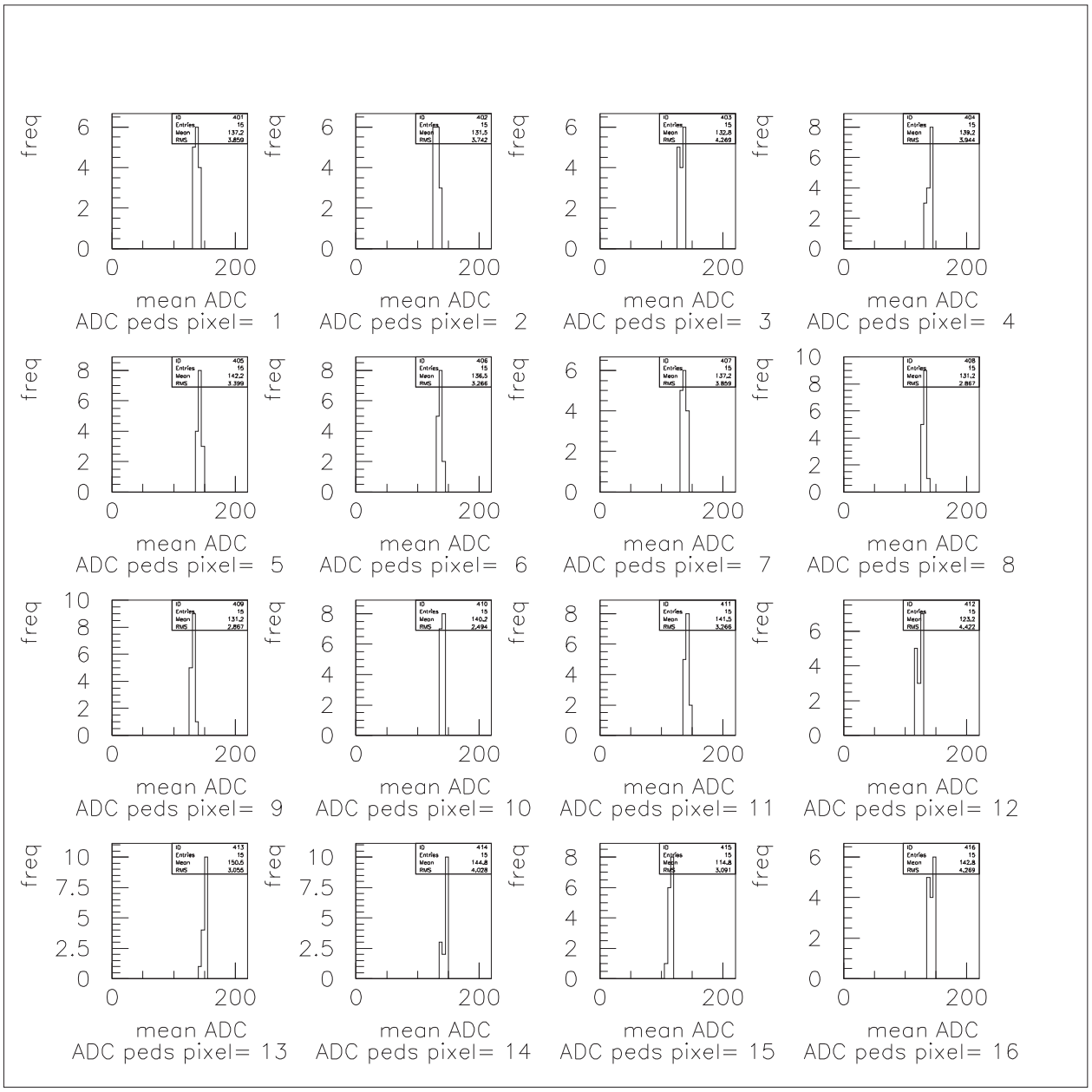

Figure C.1: ADC pedestals over 15 months. Box 1. Each figure shows 1-16 boxes of the T1 inner camera (16 pixels per box). ADC pixel number is shown below each histogram.

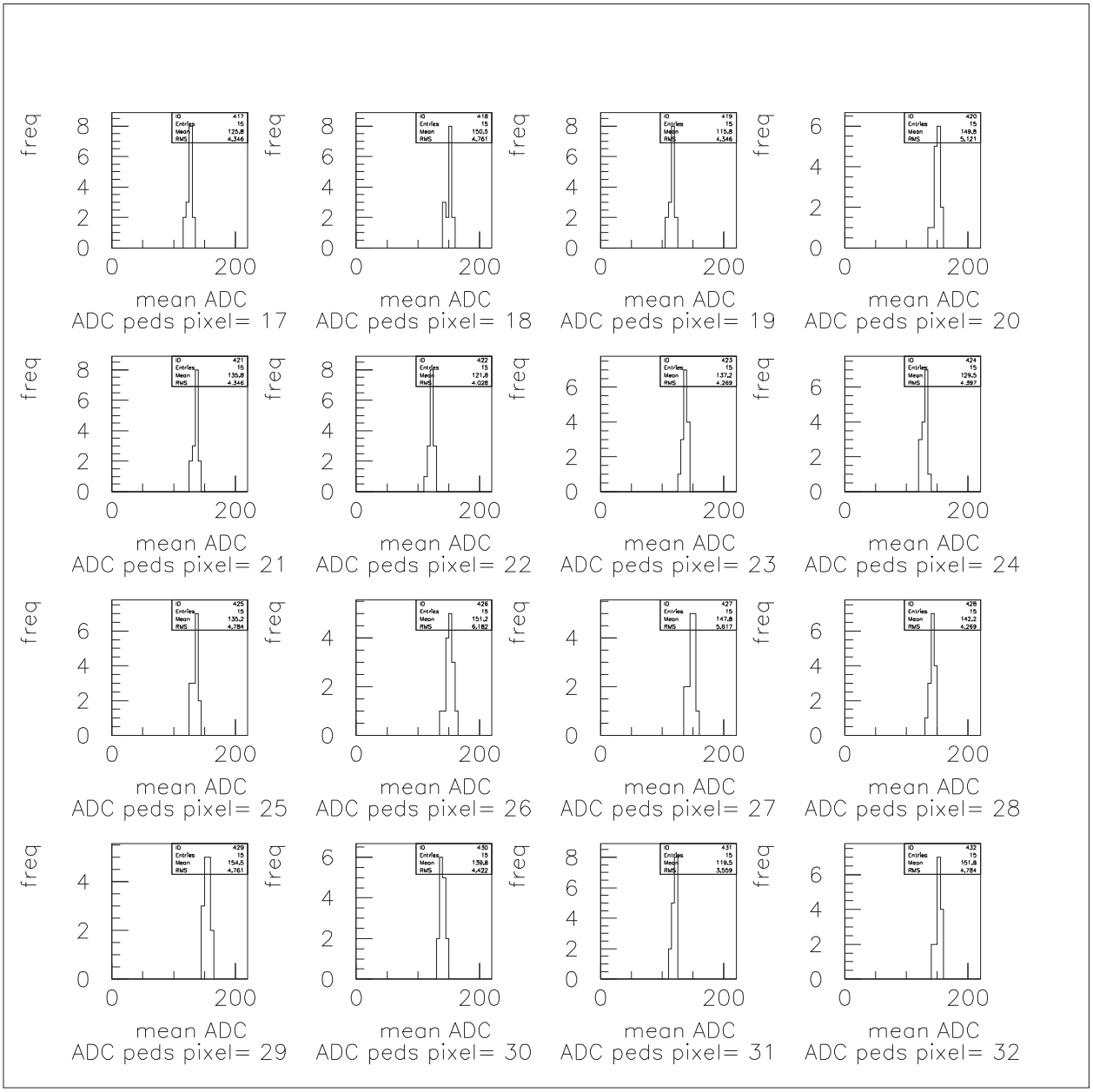

Figure C.2: Box 2. ADC pixel number is shown below each histogram.

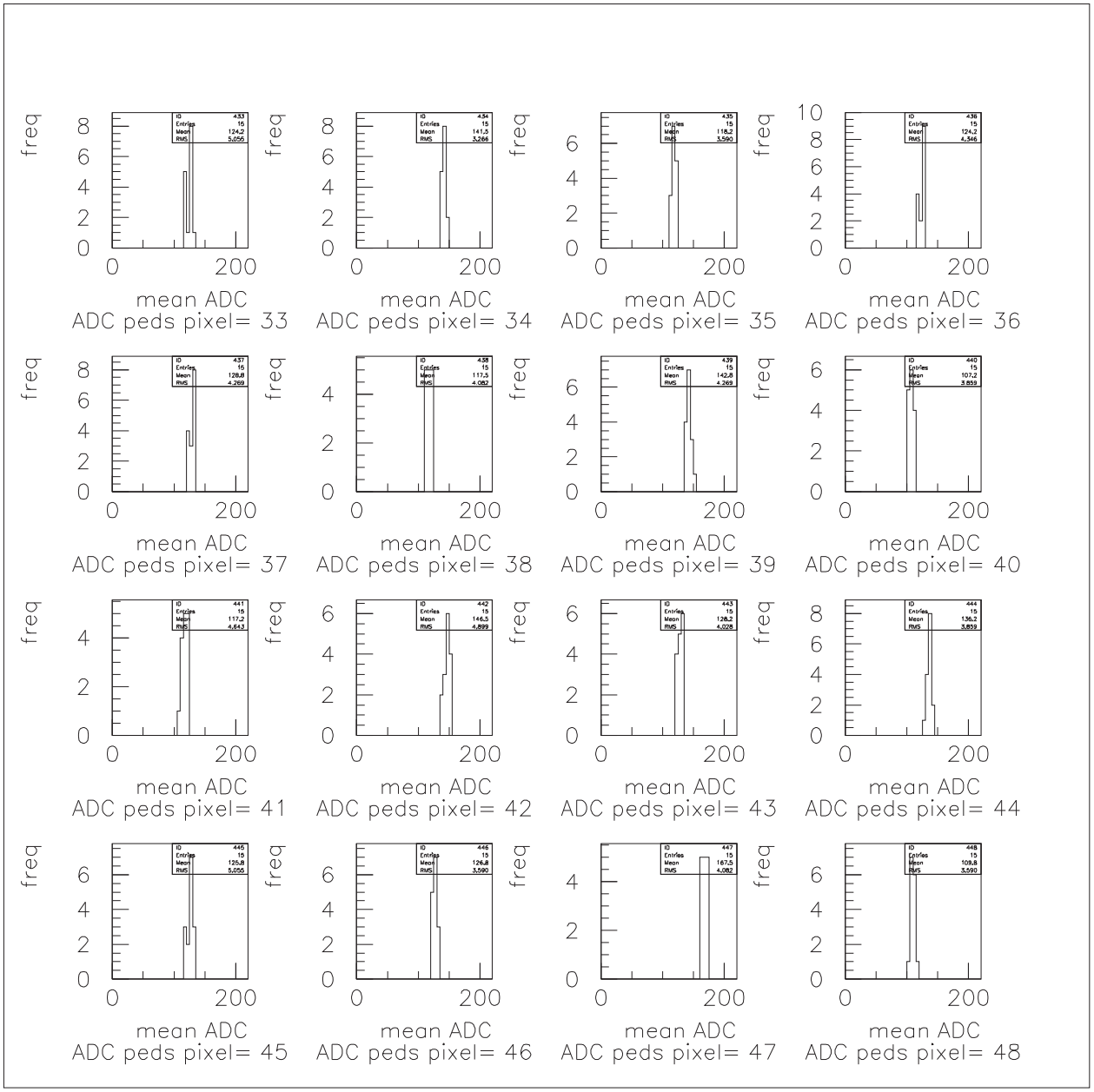

Figure C.3: Box 3. ADC pixel number is shown below each histogram.

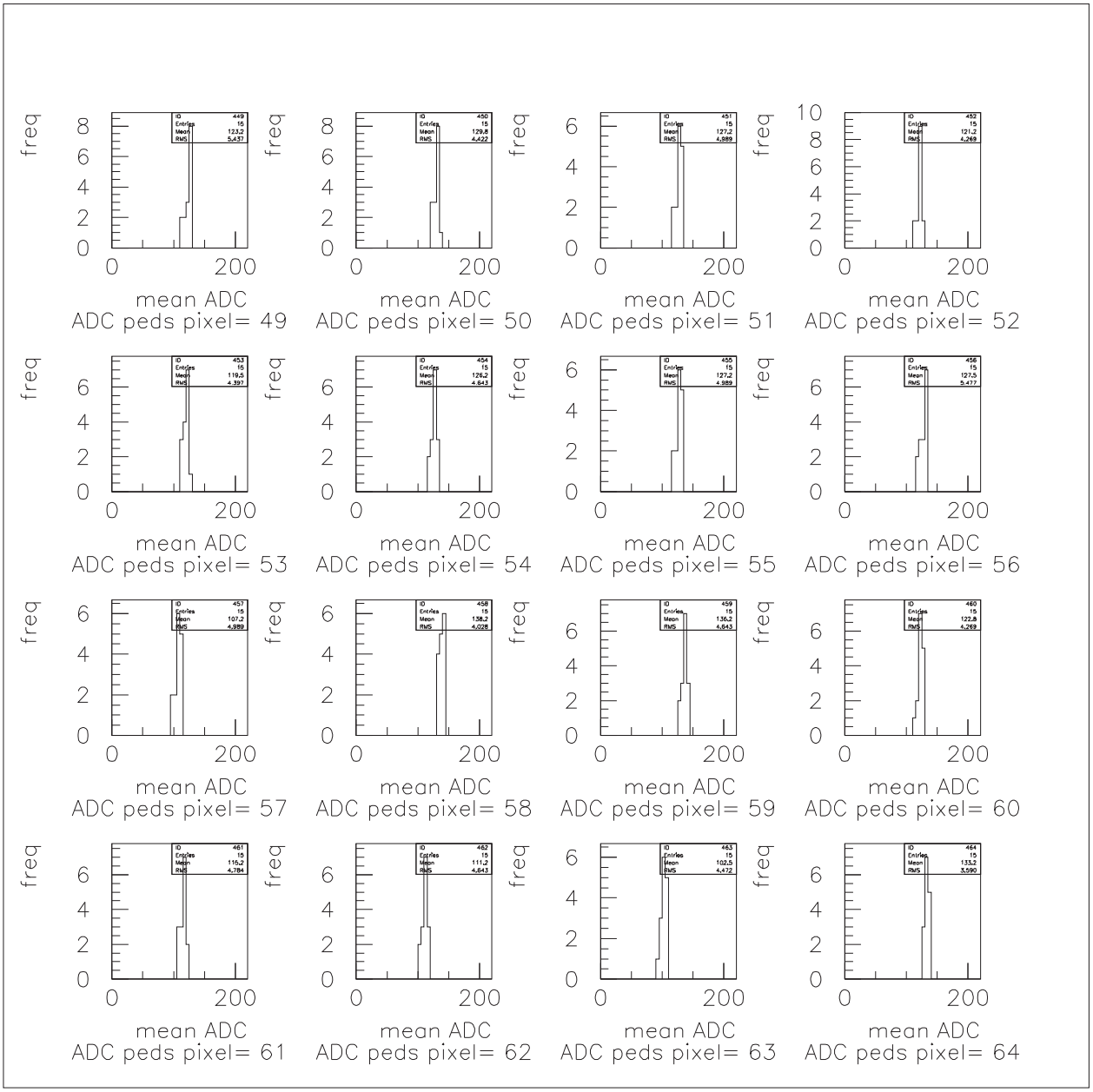

Figure C.4: Box 4. ADC pixel number is shown below each histogram.

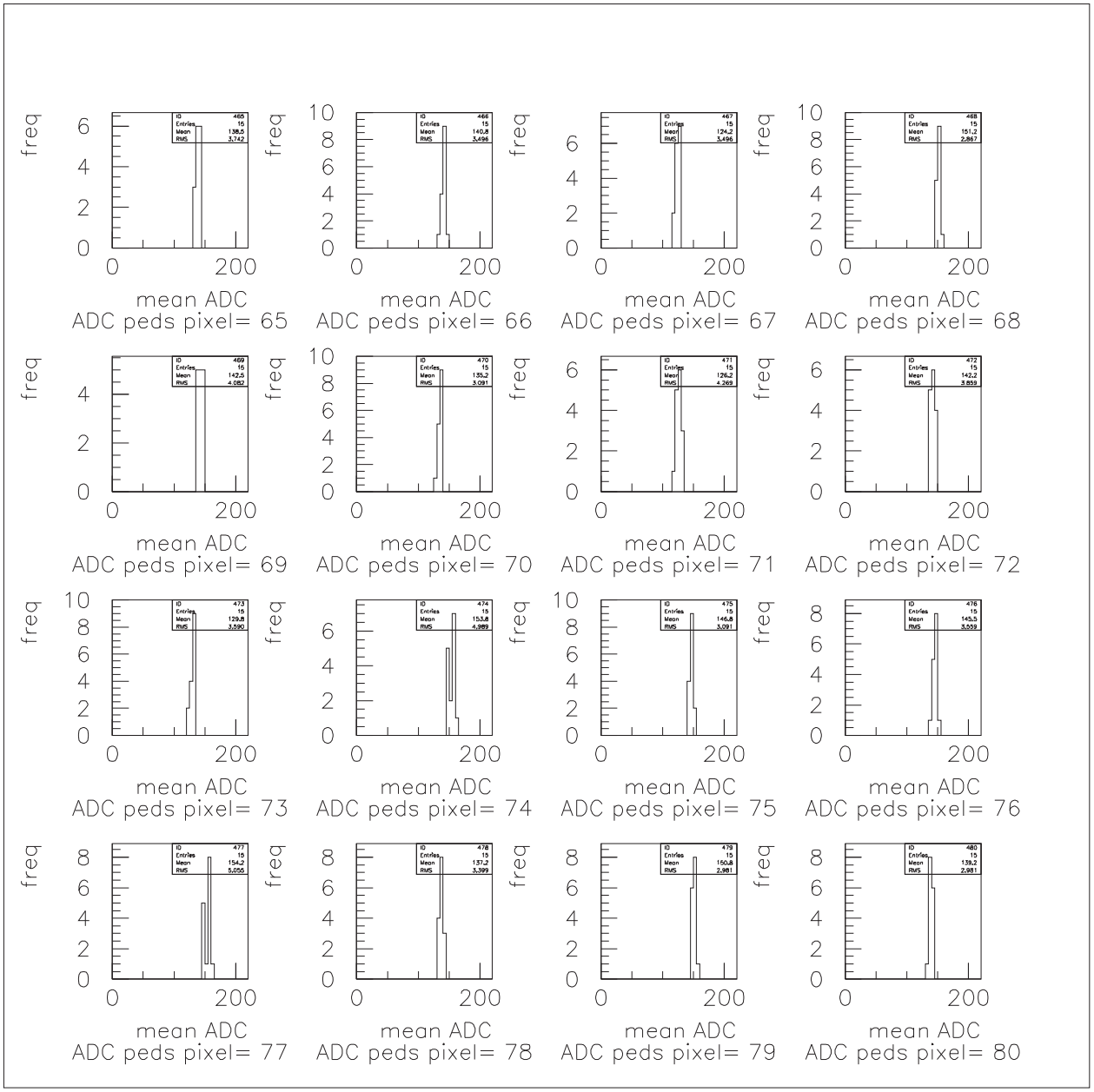

Figure C.5: Box 5. ADC pixel number is shown below each histogram.

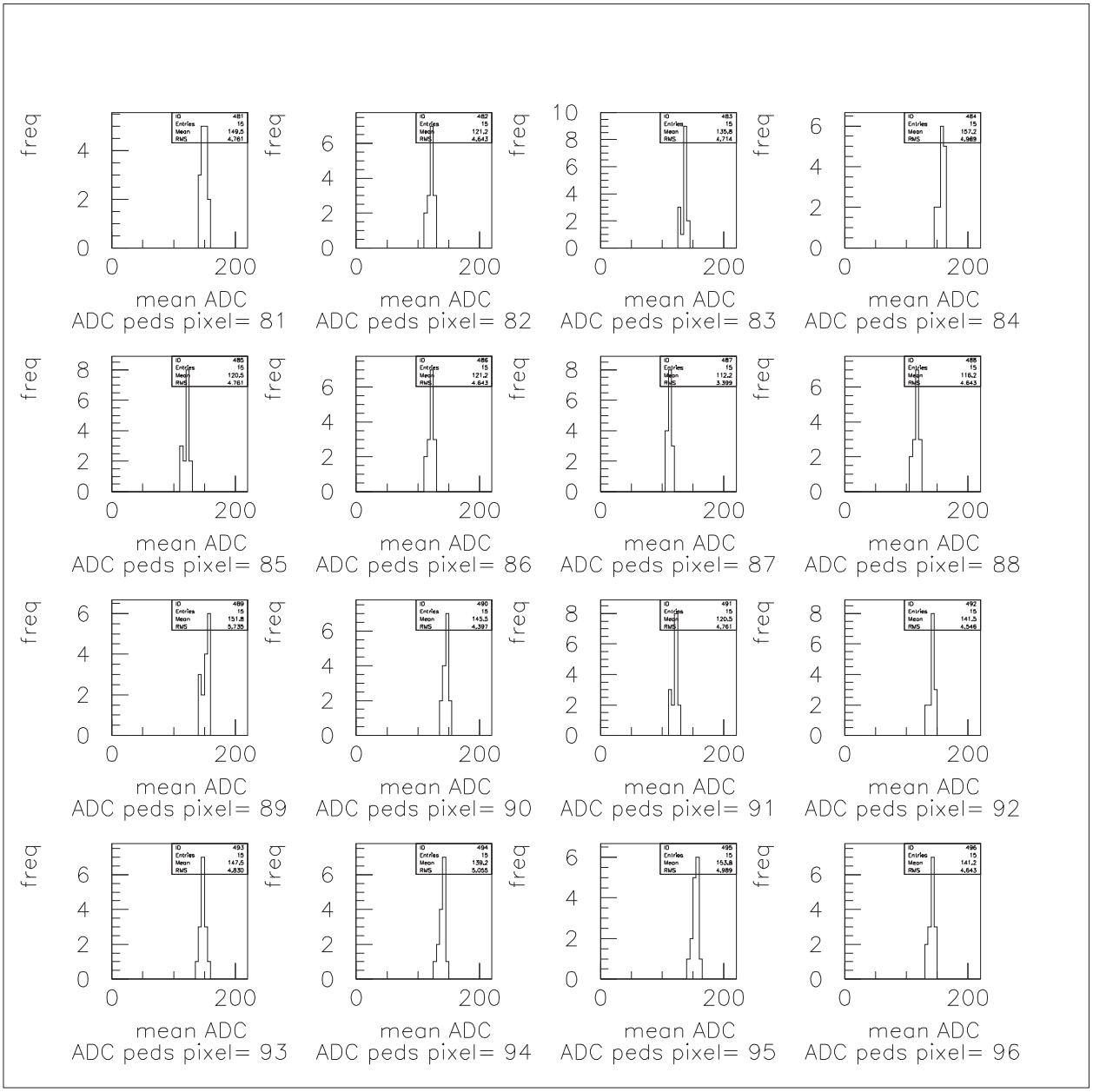

Figure C.6: Box 6. ADC pixel number is shown below each histogram.

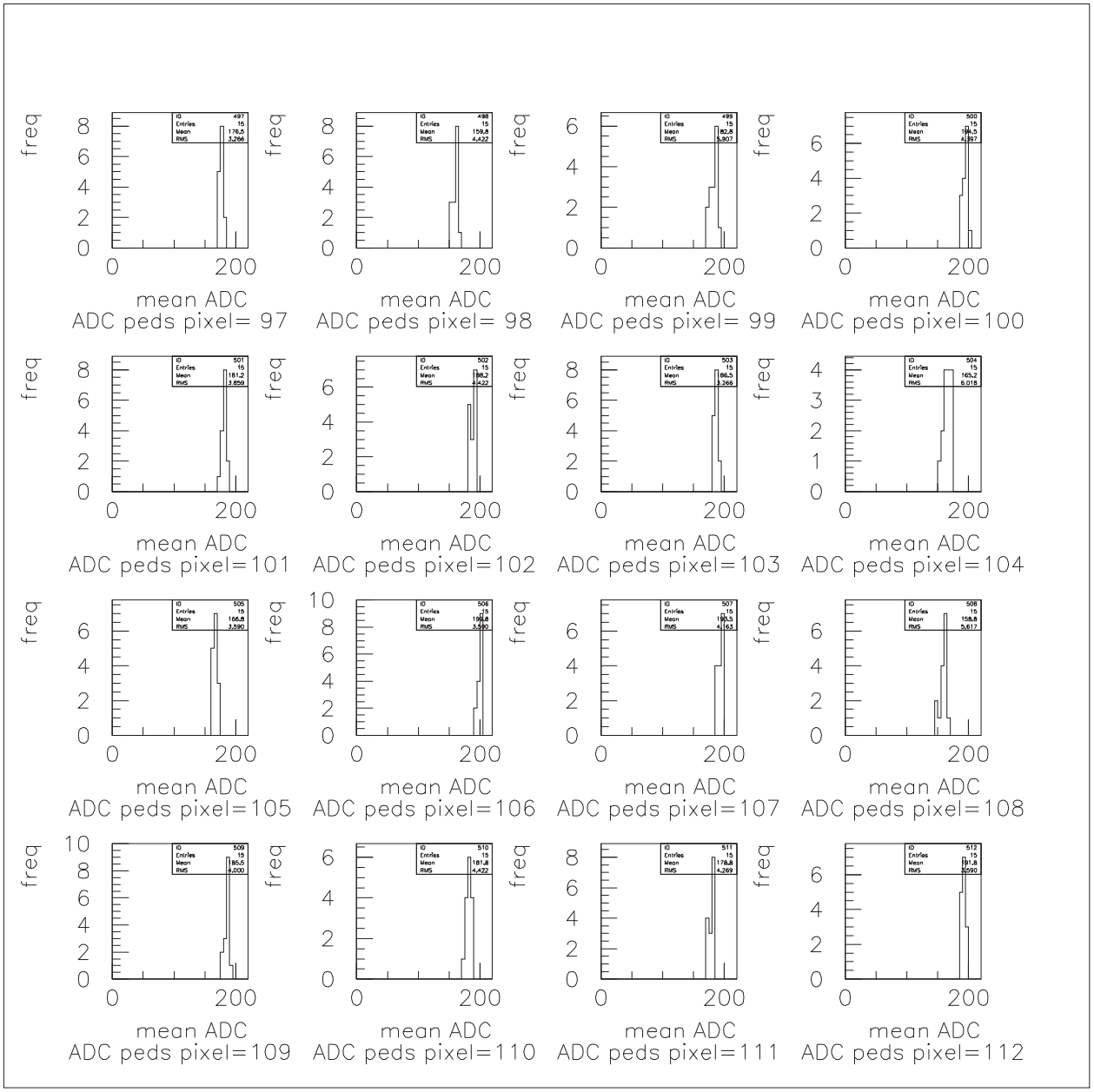

Figure C.7: Box 7. ADC pixel number is shown below each histogram.

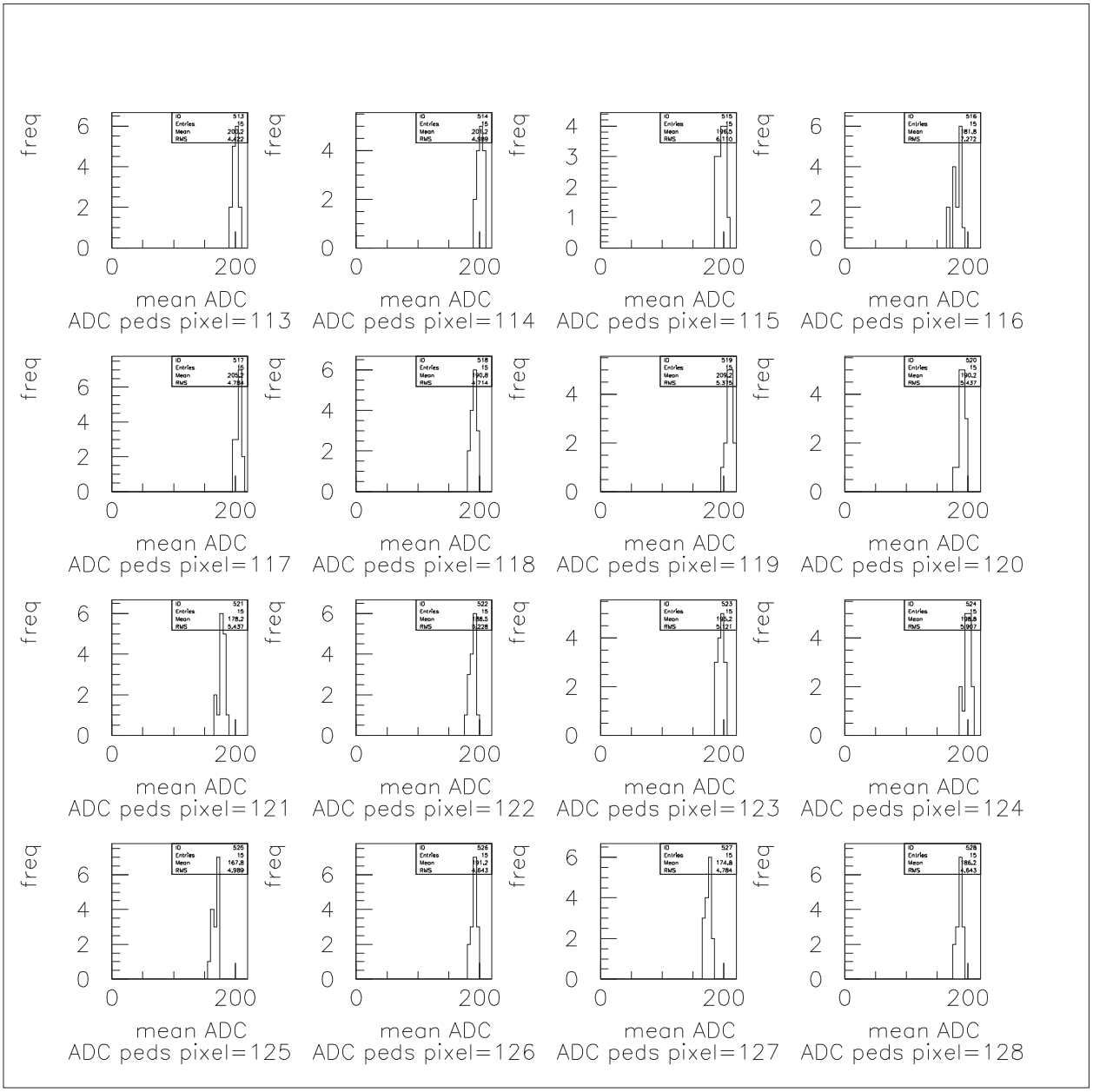

Figure C.8: Box 8. ADC pixel number is shown below each histogram.

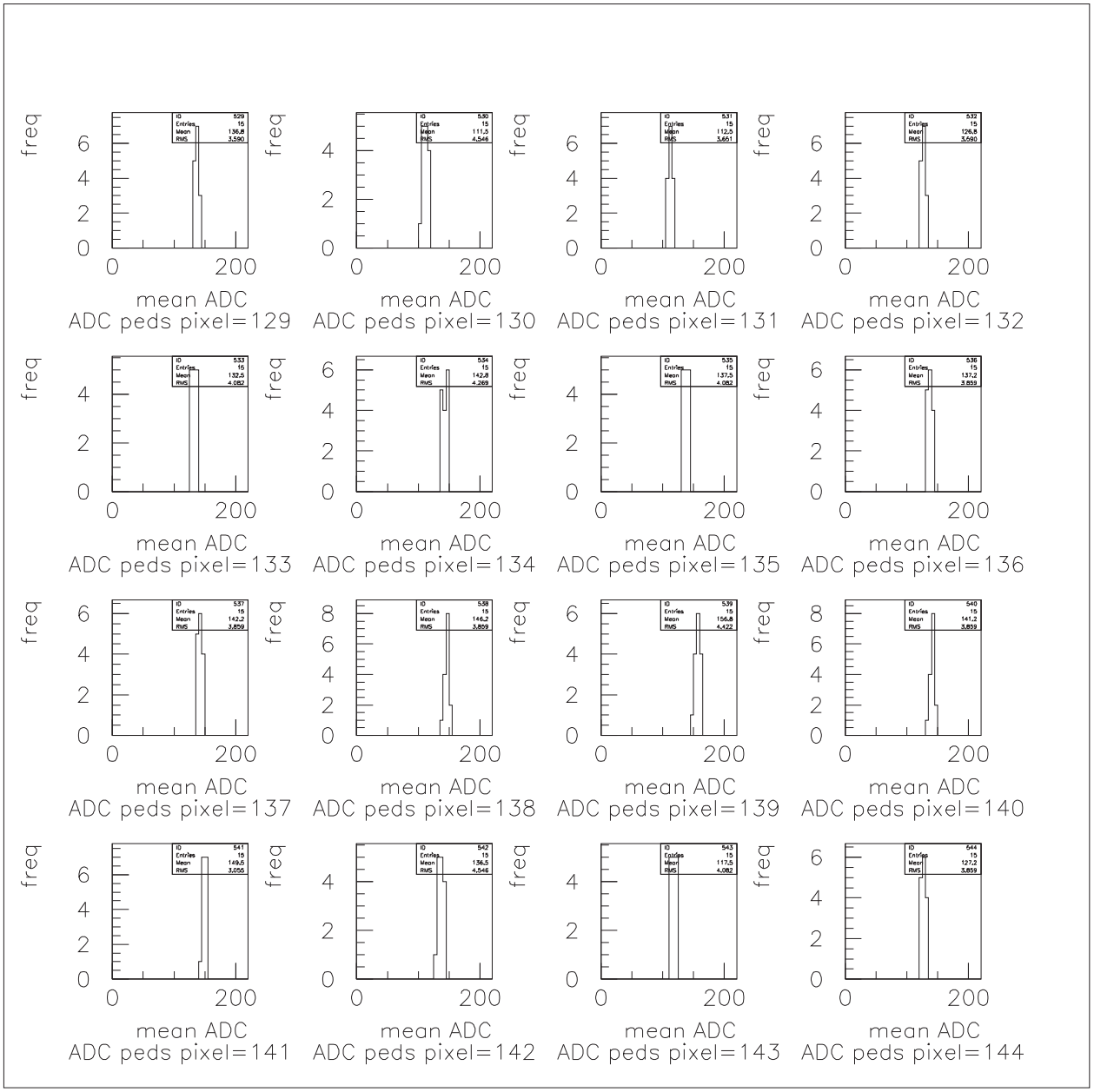

Figure C.9: Box 9. ADC pixel number is shown below each histogram.

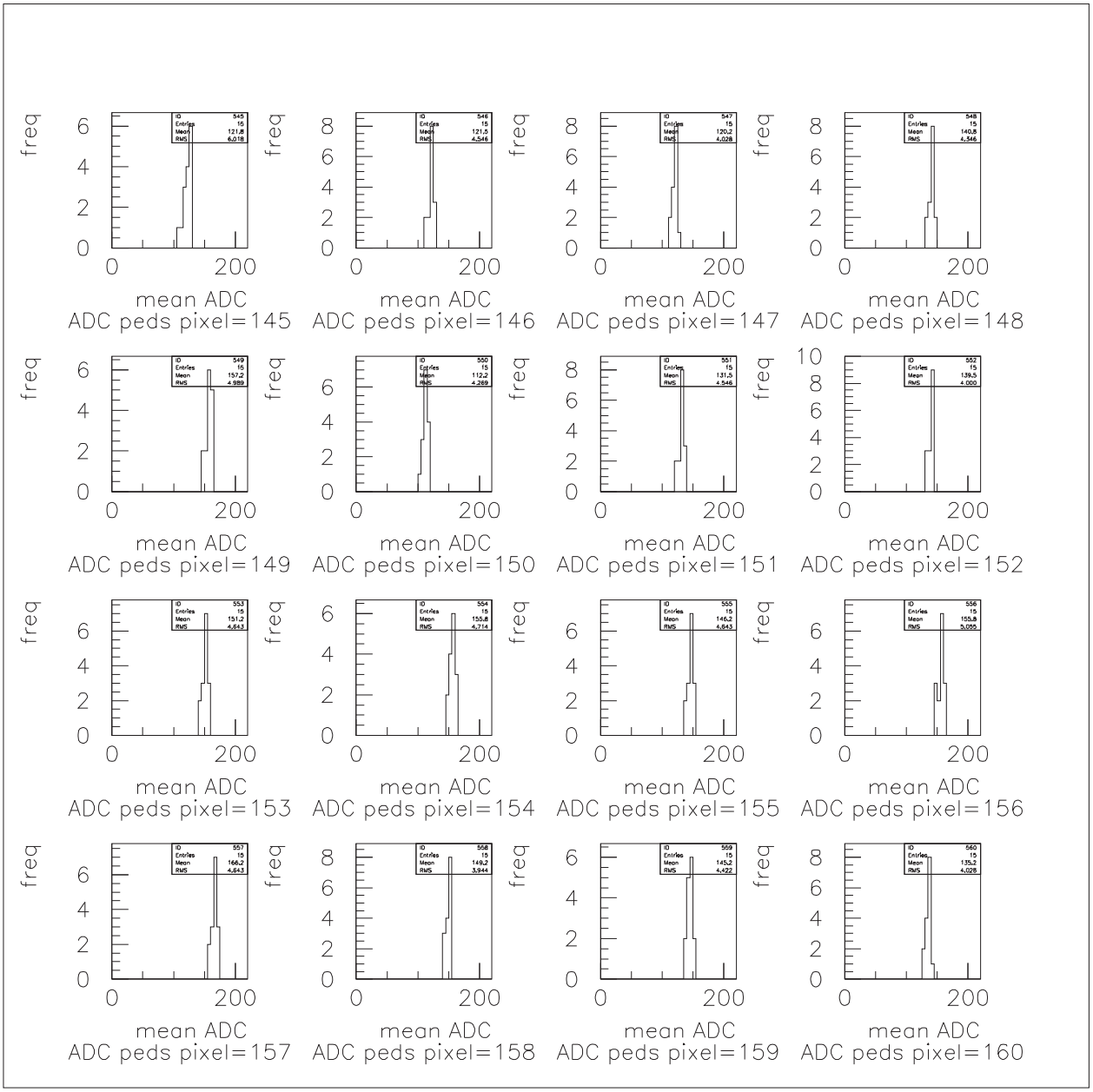

Figure C.10: Box 10. ADC pixel number is shown below each histogram.

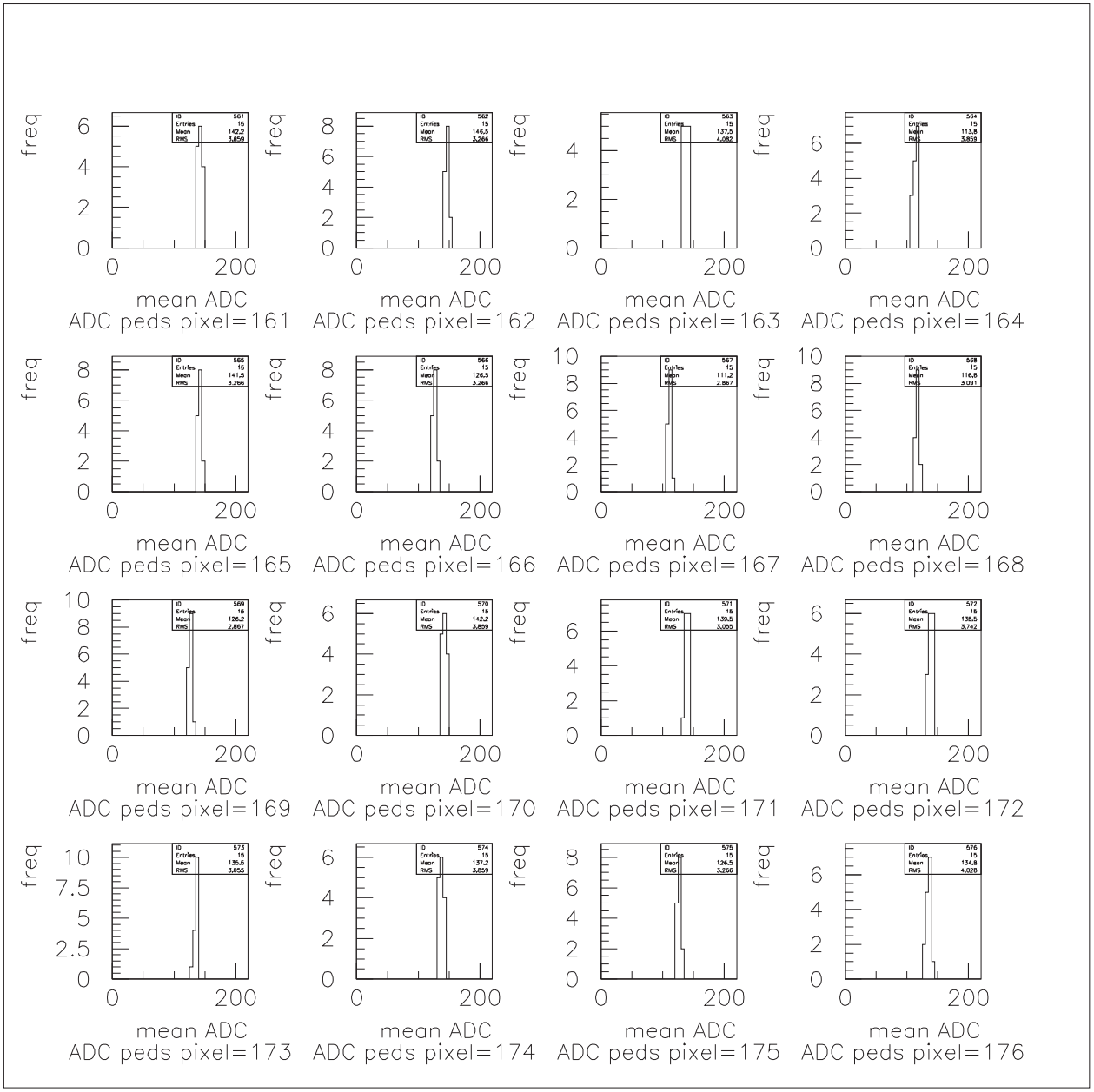

Figure C.11: Box 11. ADC pixel number is shown below each histogram.

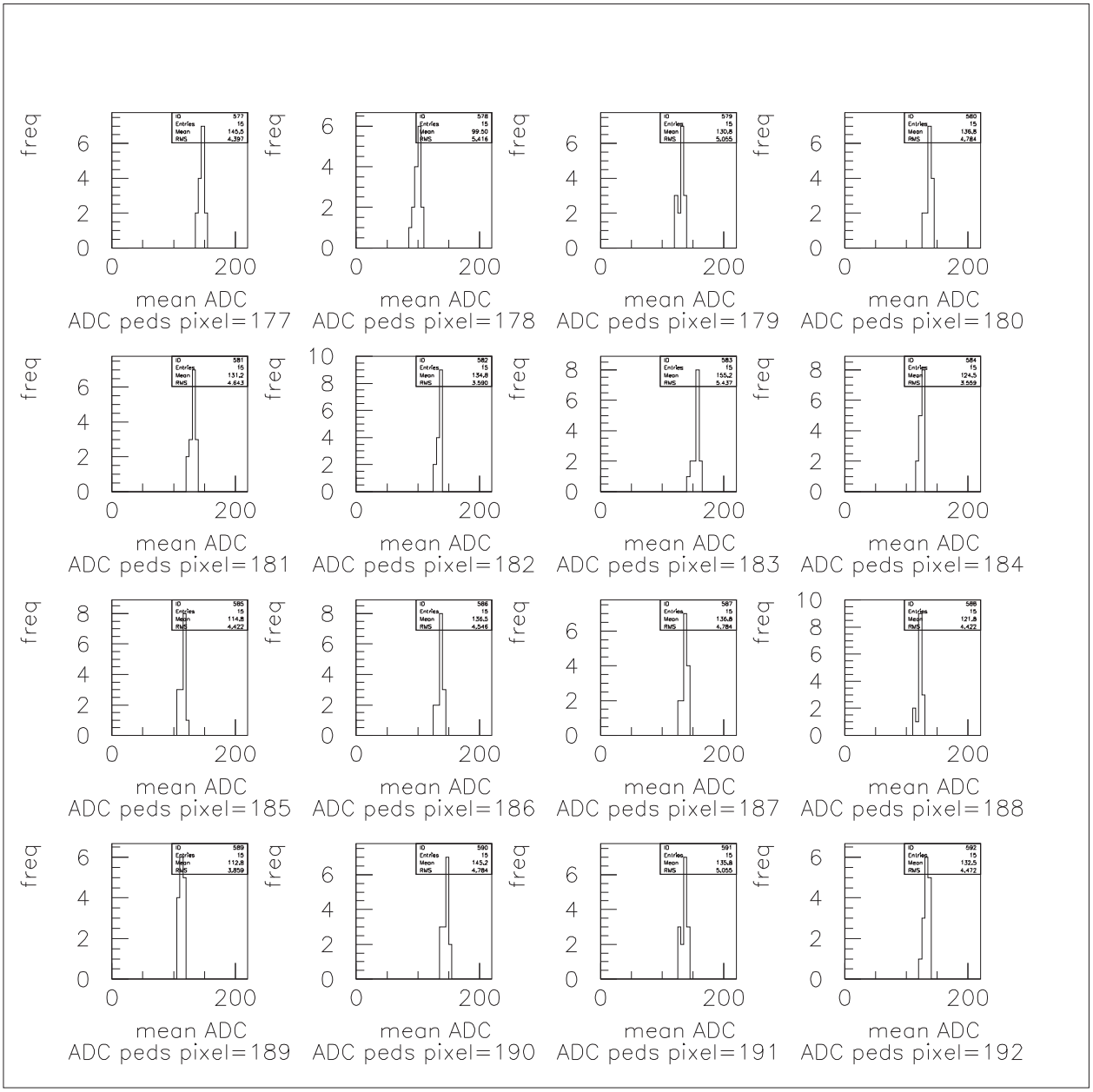

Figure C.12: Box 12. ADC pixel number is shown below each histogram.

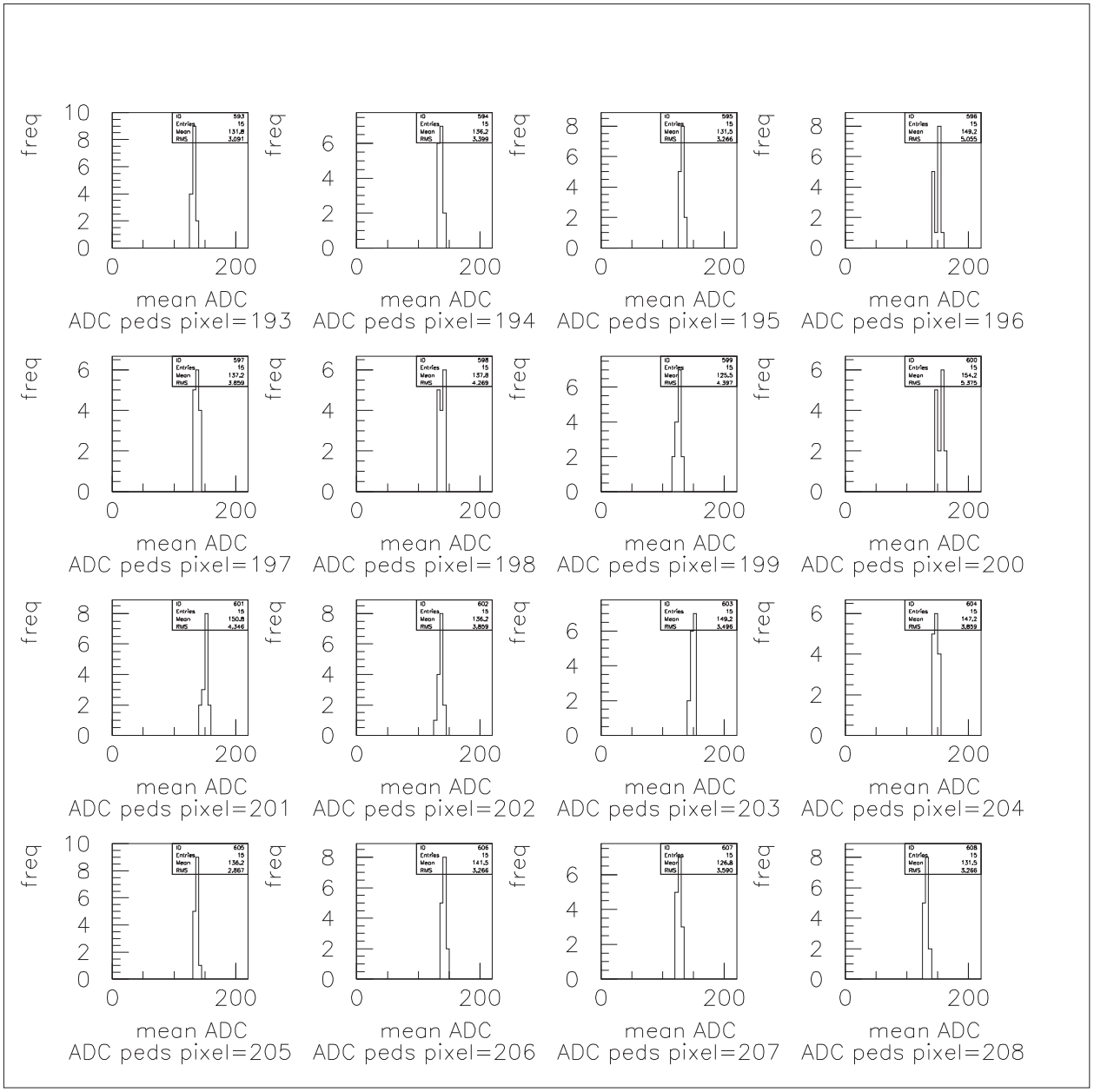

Figure C.13: Box 13. ADC pixel number is shown below each histogram.

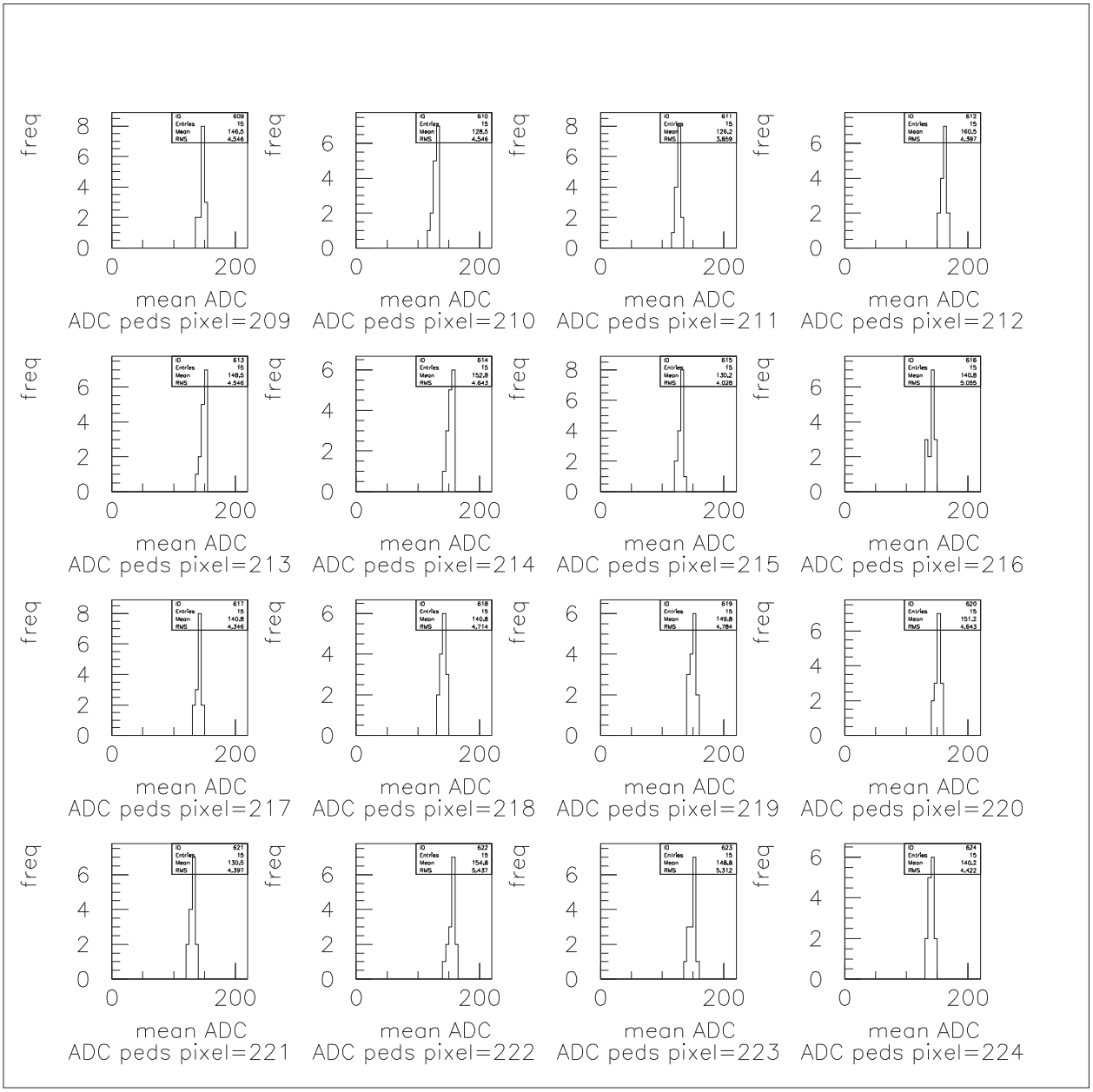

Figure C.14: Box 14. ADC pixel number is shown below each histogram.

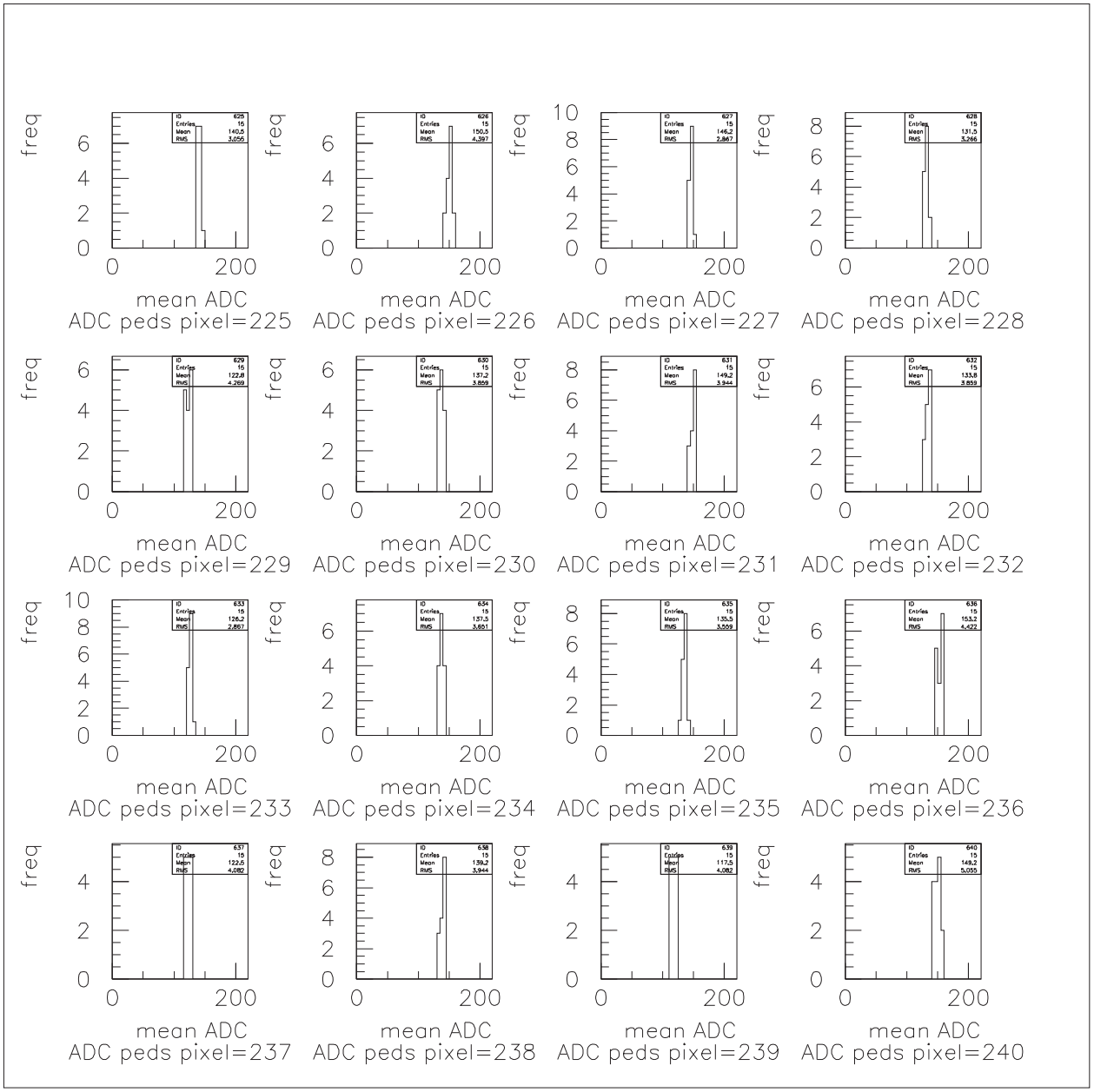

Figure C.15: Box 15. ADC pixel number is shown below each histogram.

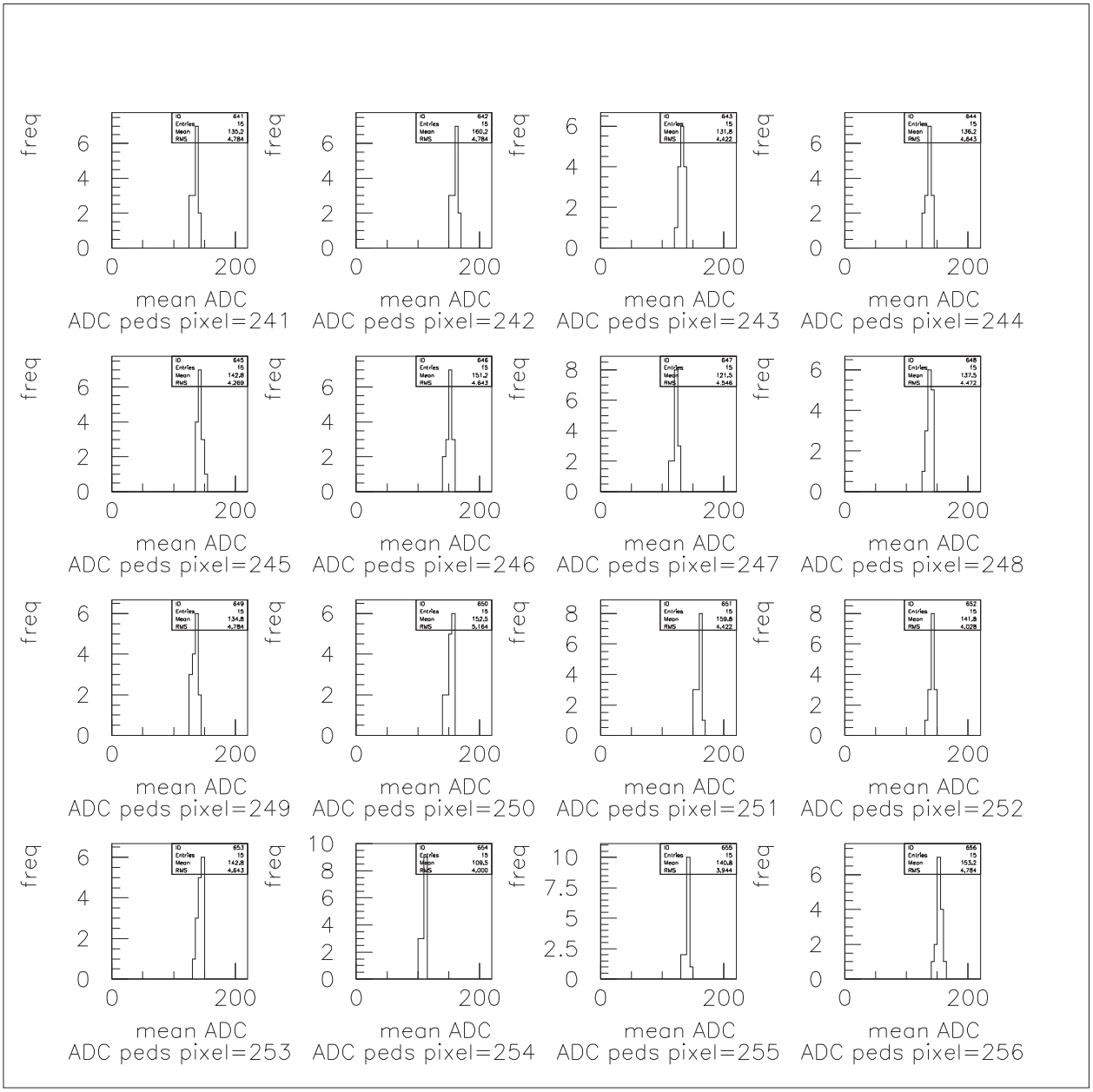

Figure C.16: Box 16. ADC pixel number is shown below each histogram.

Appendix D

T1 flasher calibration: Pedestal difference between the sample mean ADC and histogram calculated mean ADC

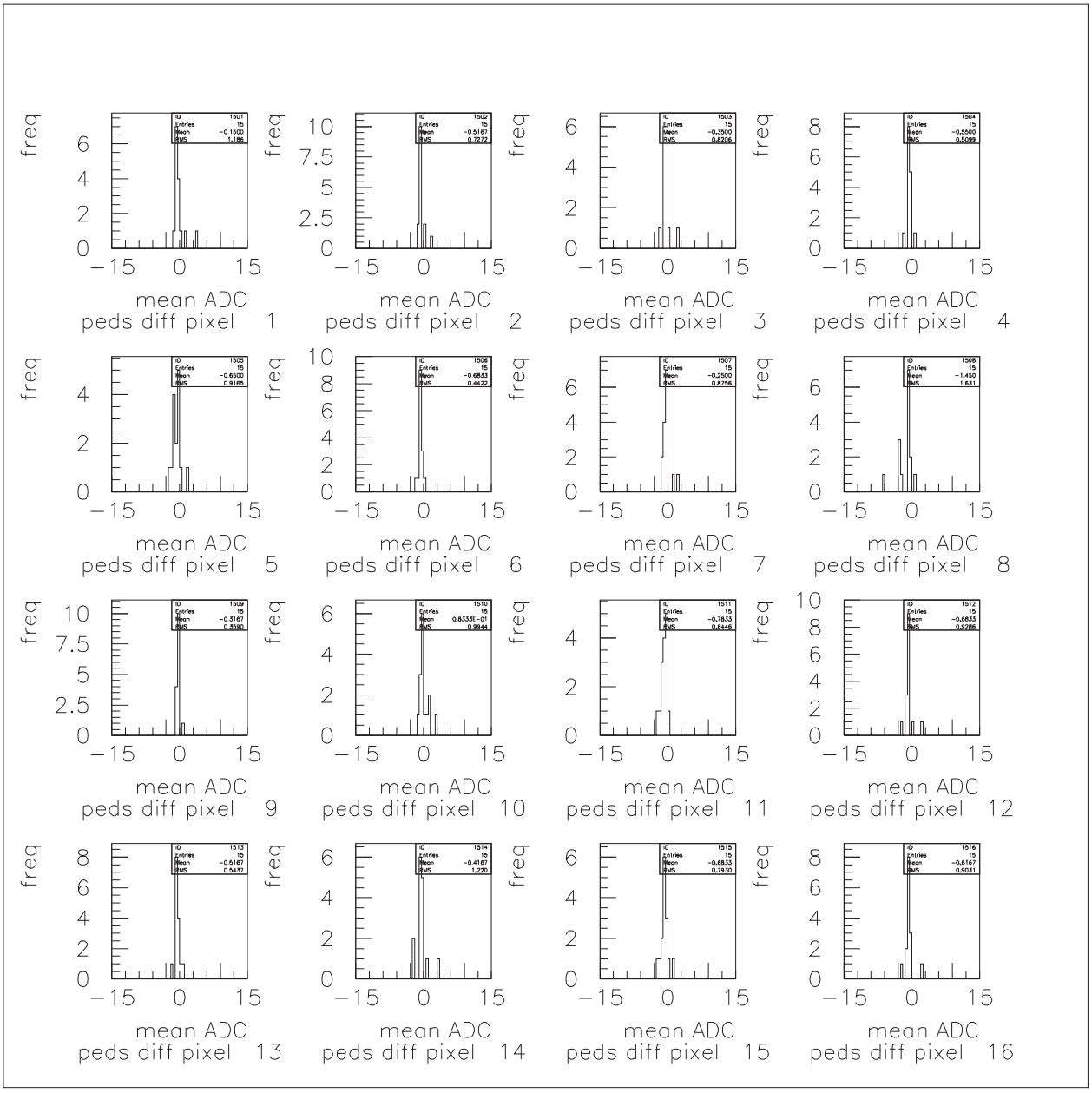

Figure D.1: ADC pedestals differences over 15 months. Box 1. Each figure shows a box of the T1 inner camera, (16 pixels per box). "Pedestal difference" is the difference between the sample mean ADC, see equation 5.4 (Section 5.1.6), and the mean ADC generated by *PAW*, from the ADC histogram.

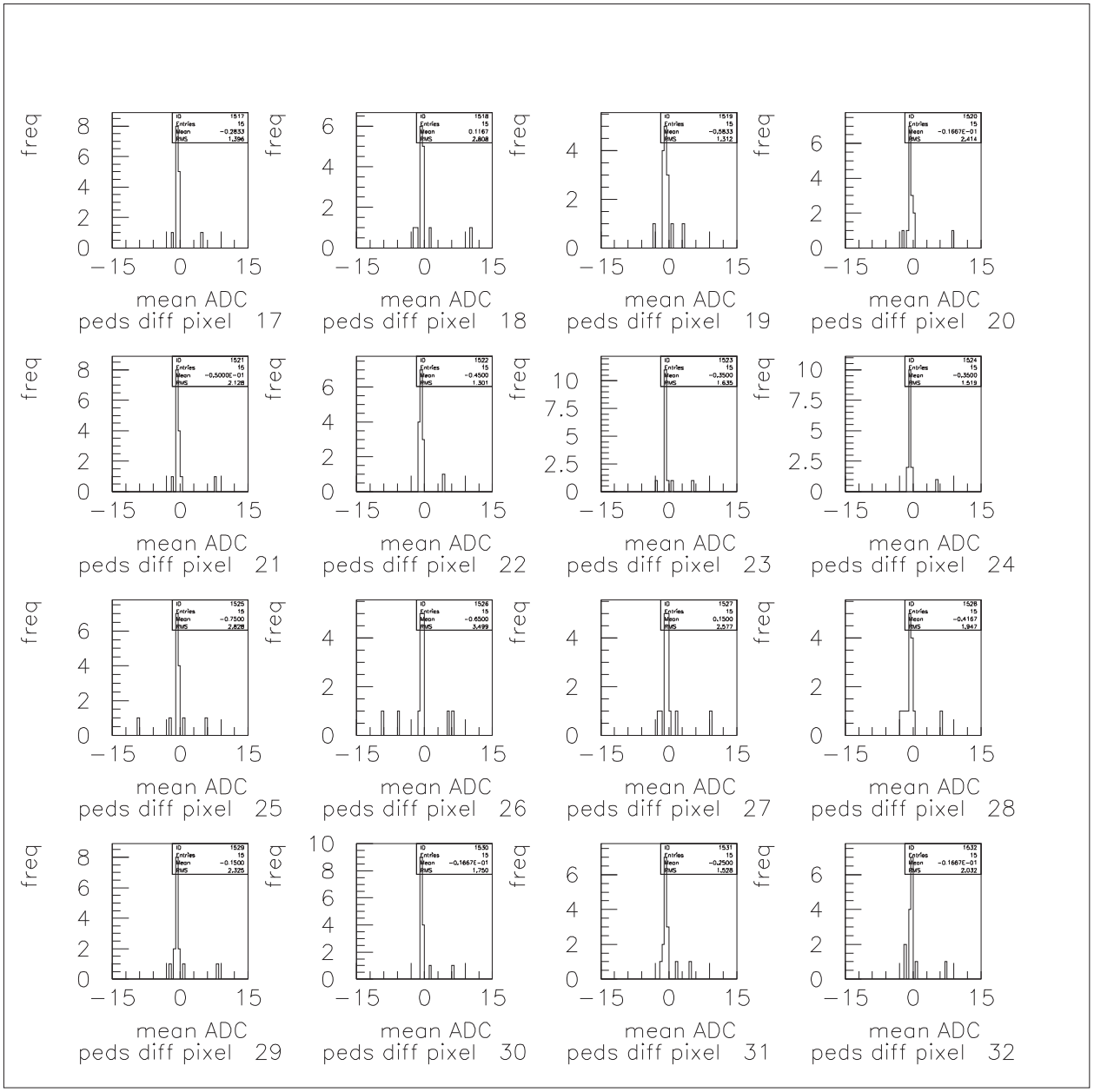

Figure D.2: Box 2. ADC pixel number is shown below each histogram.

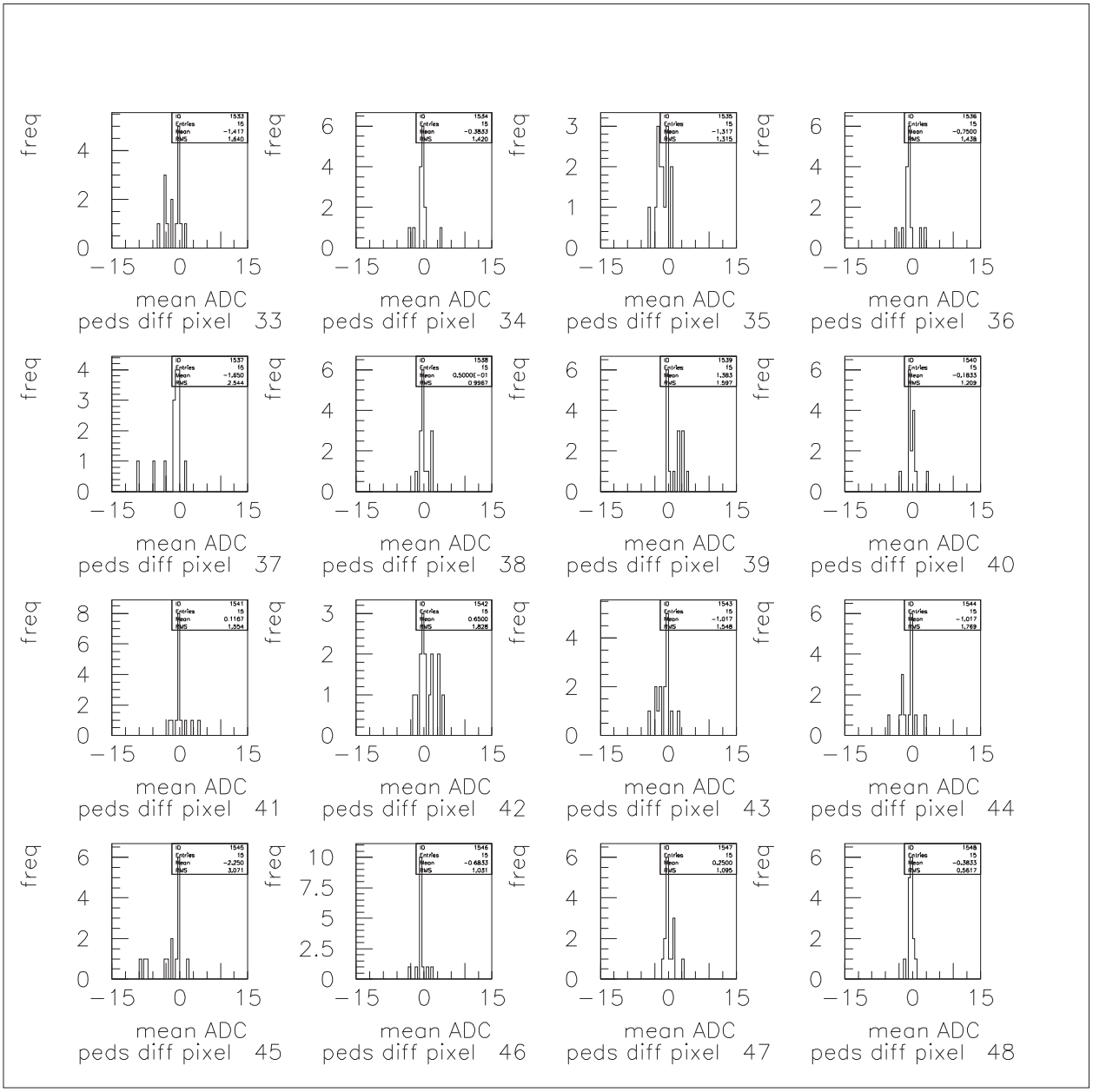

Figure D.3: Box 3. ADC pixel number is shown below each histogram.

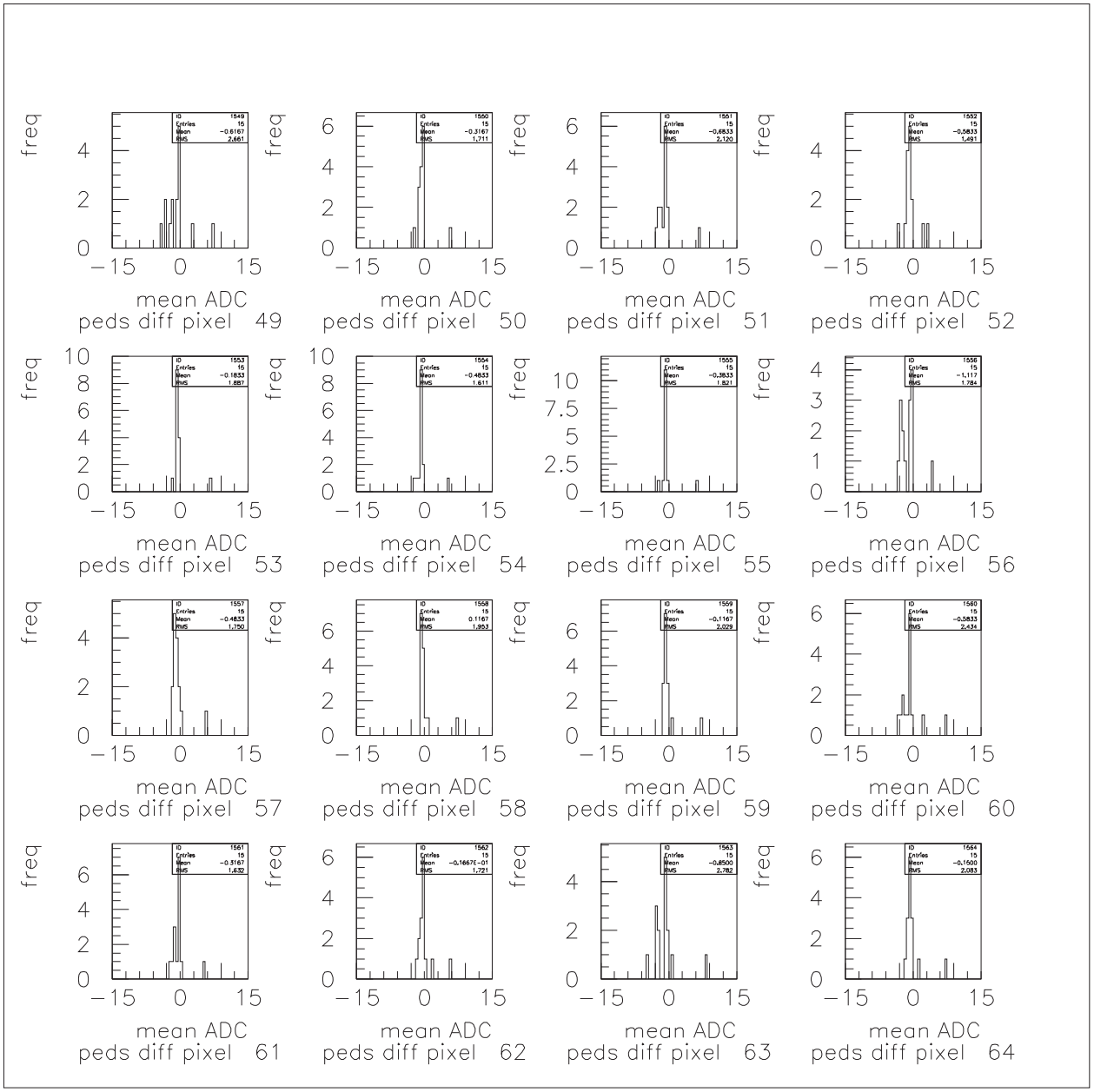

Figure D.4: Box 4. ADC pixel number is shown below each histogram.

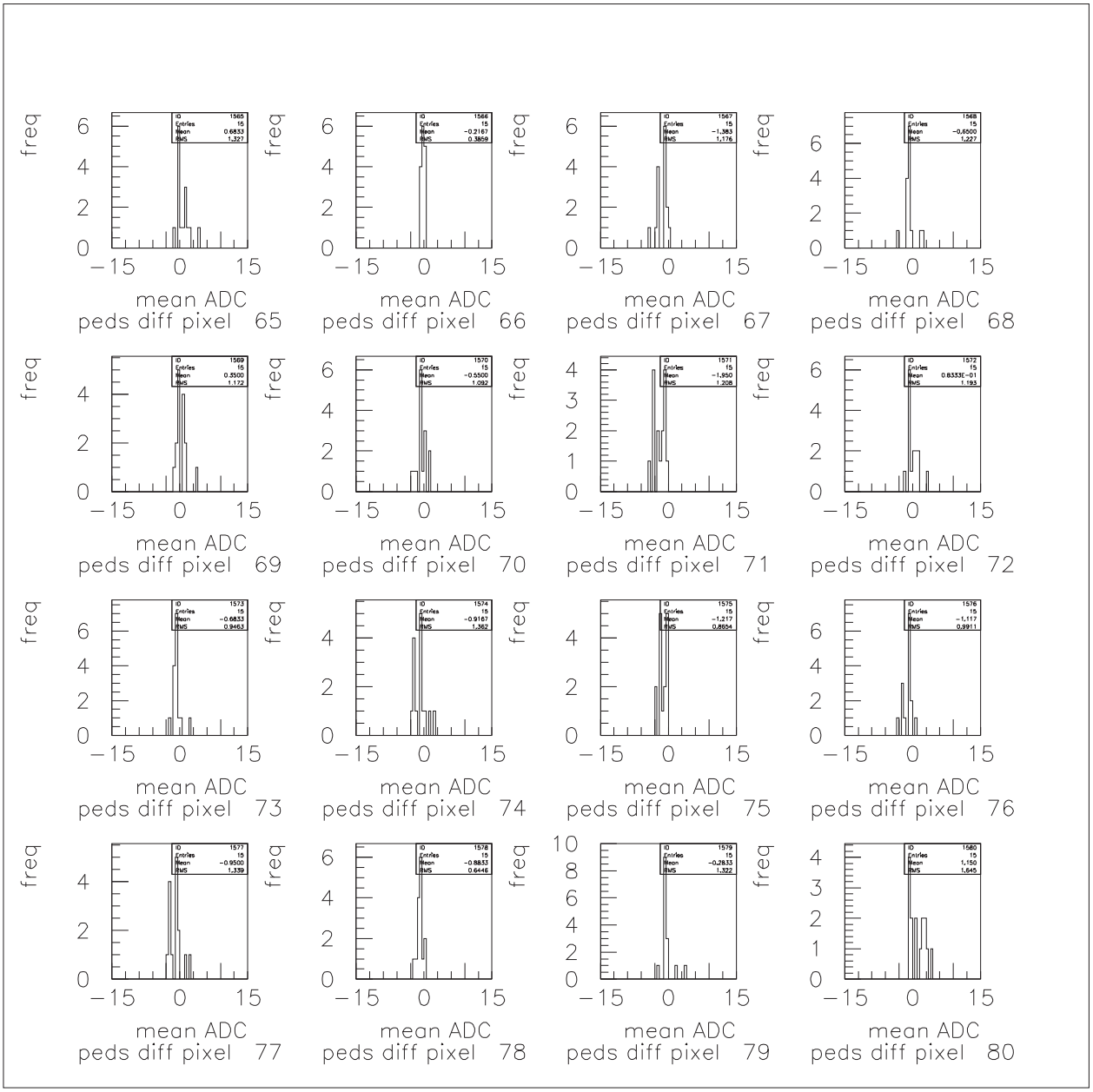

Figure D.5: Box 5. ADC pixel number is shown below each histogram.

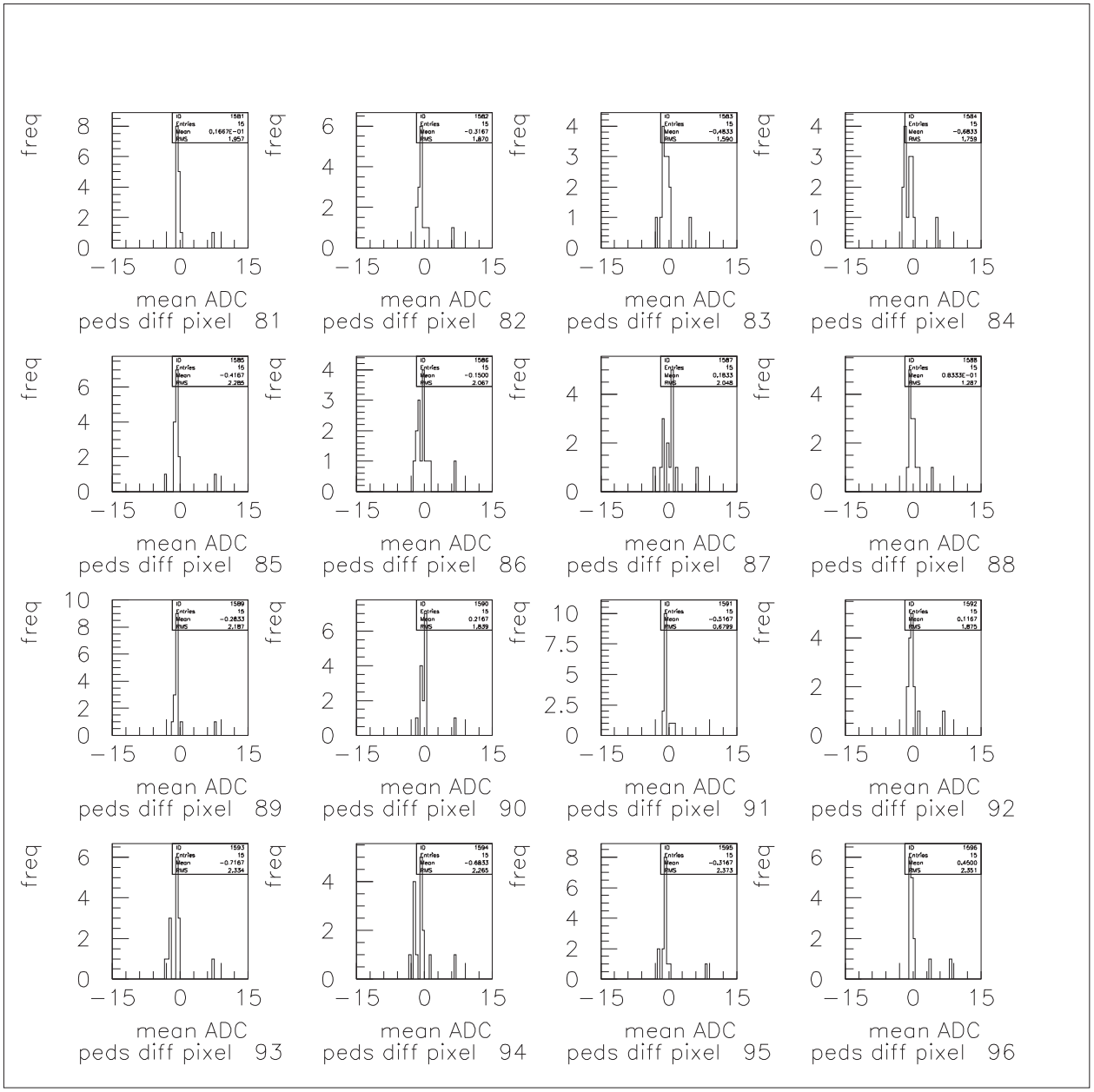

Figure D.6: Box 6. ADC pixel number is shown below each histogram.

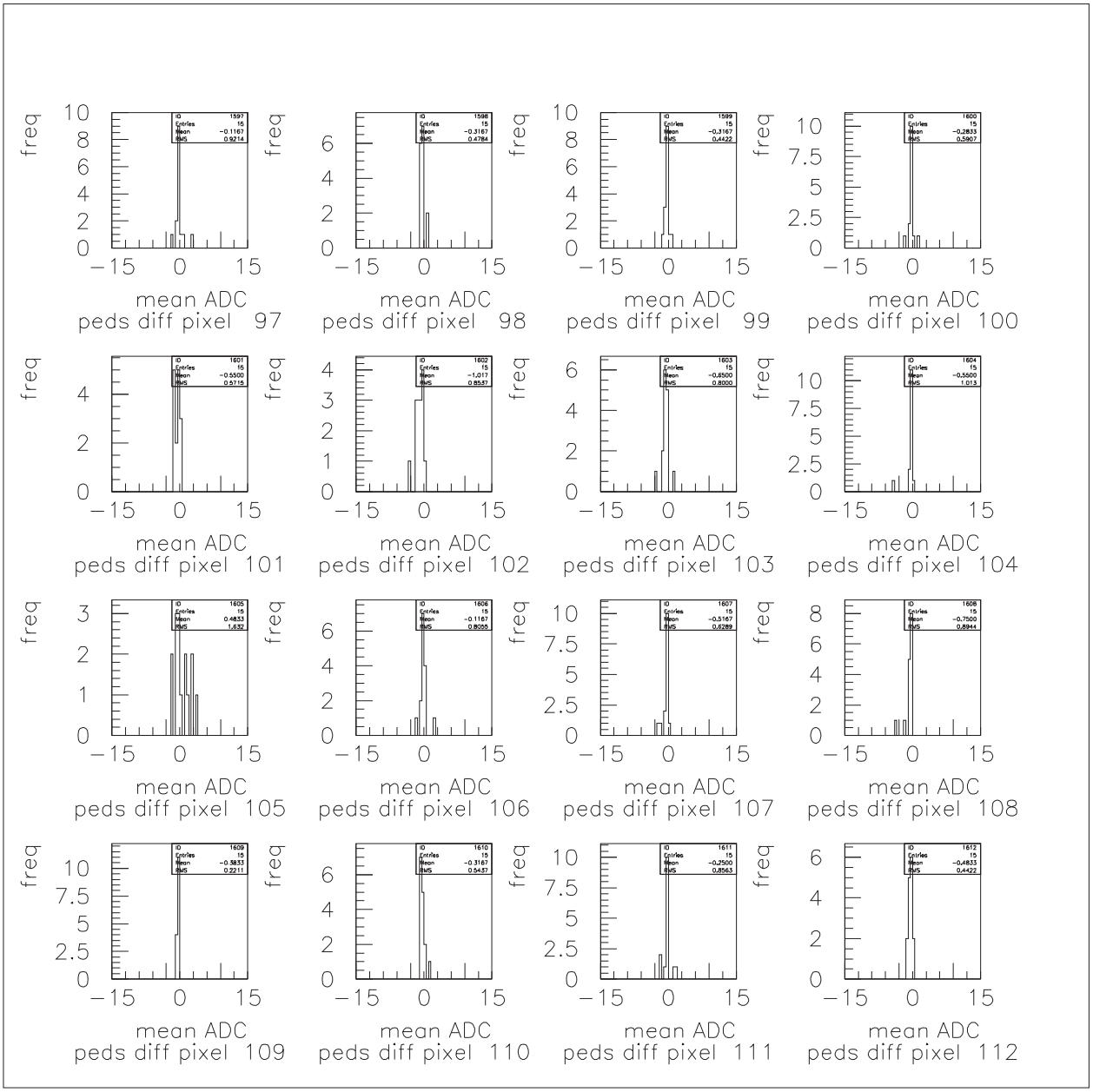

Figure D.7: Box 7. ADC pixel number is shown below each histogram.

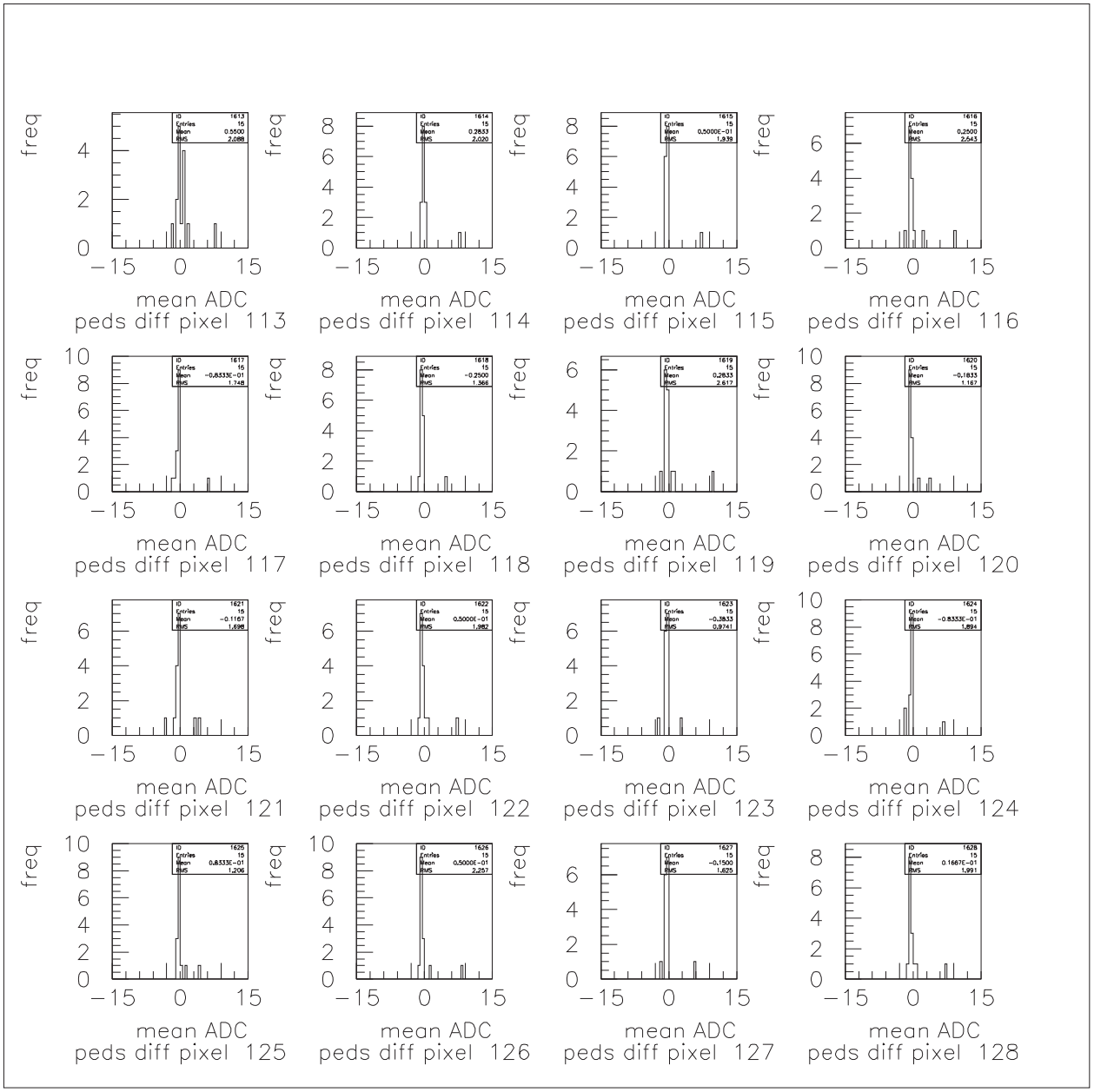

Figure D.8: Box 8. ADC pixel number is shown below each histogram.

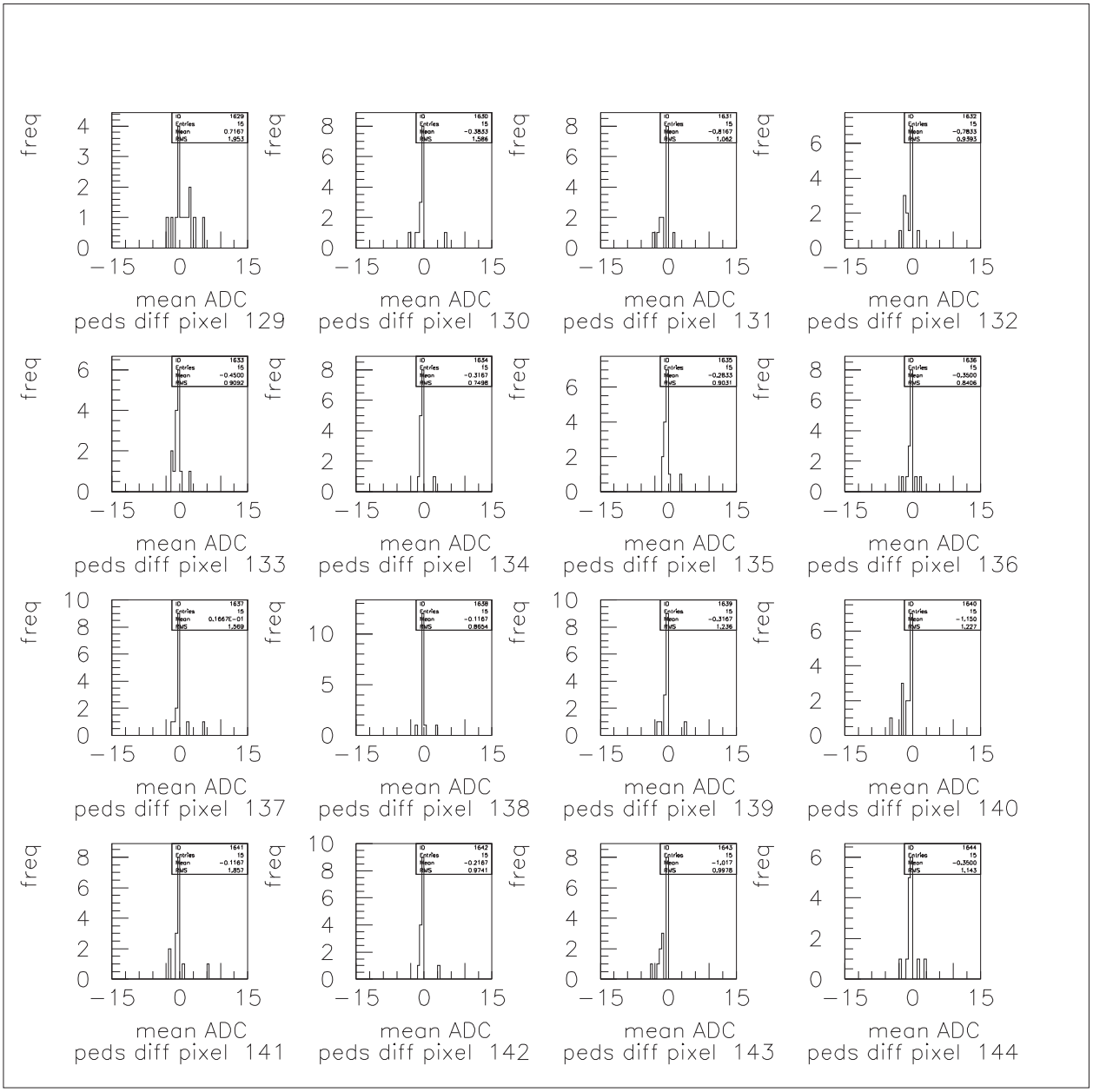

Figure D.9: Box 9. ADC pixel number is shown below each histogram.

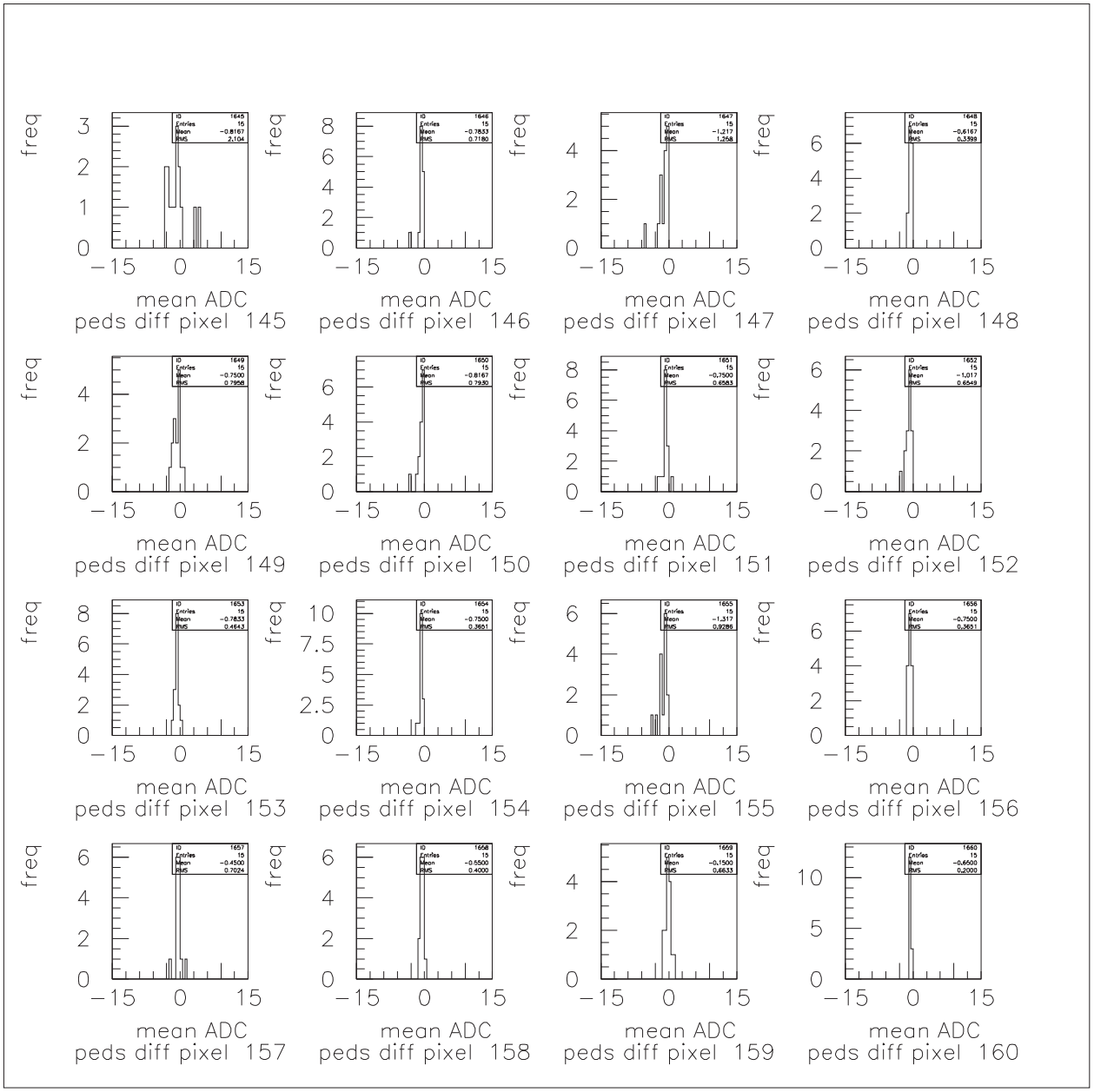

Figure D.10: Box 10. ADC pixel number is shown below each histogram.

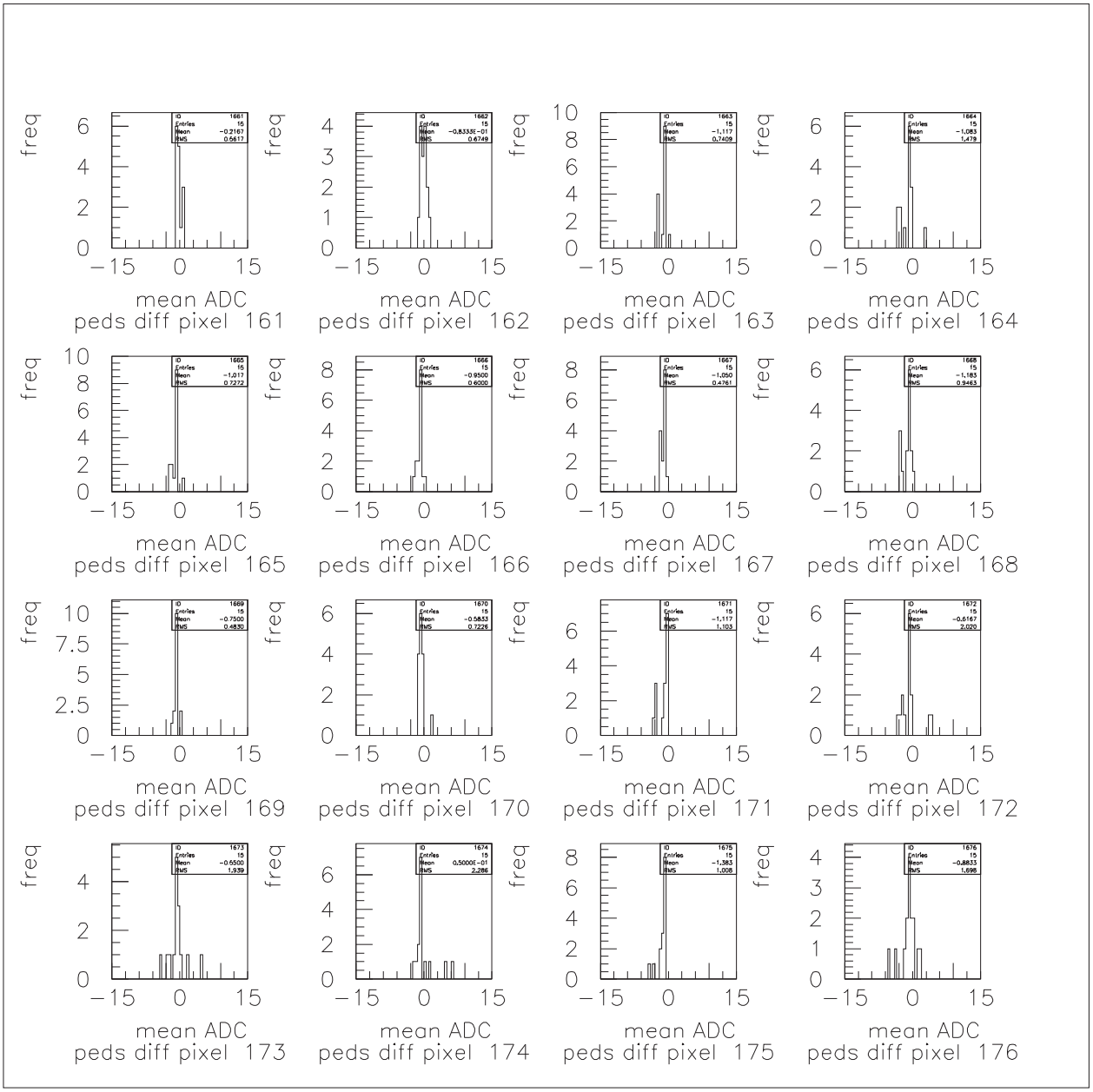

Figure D.11: Box 11. ADC pixel number is shown below each histogram.

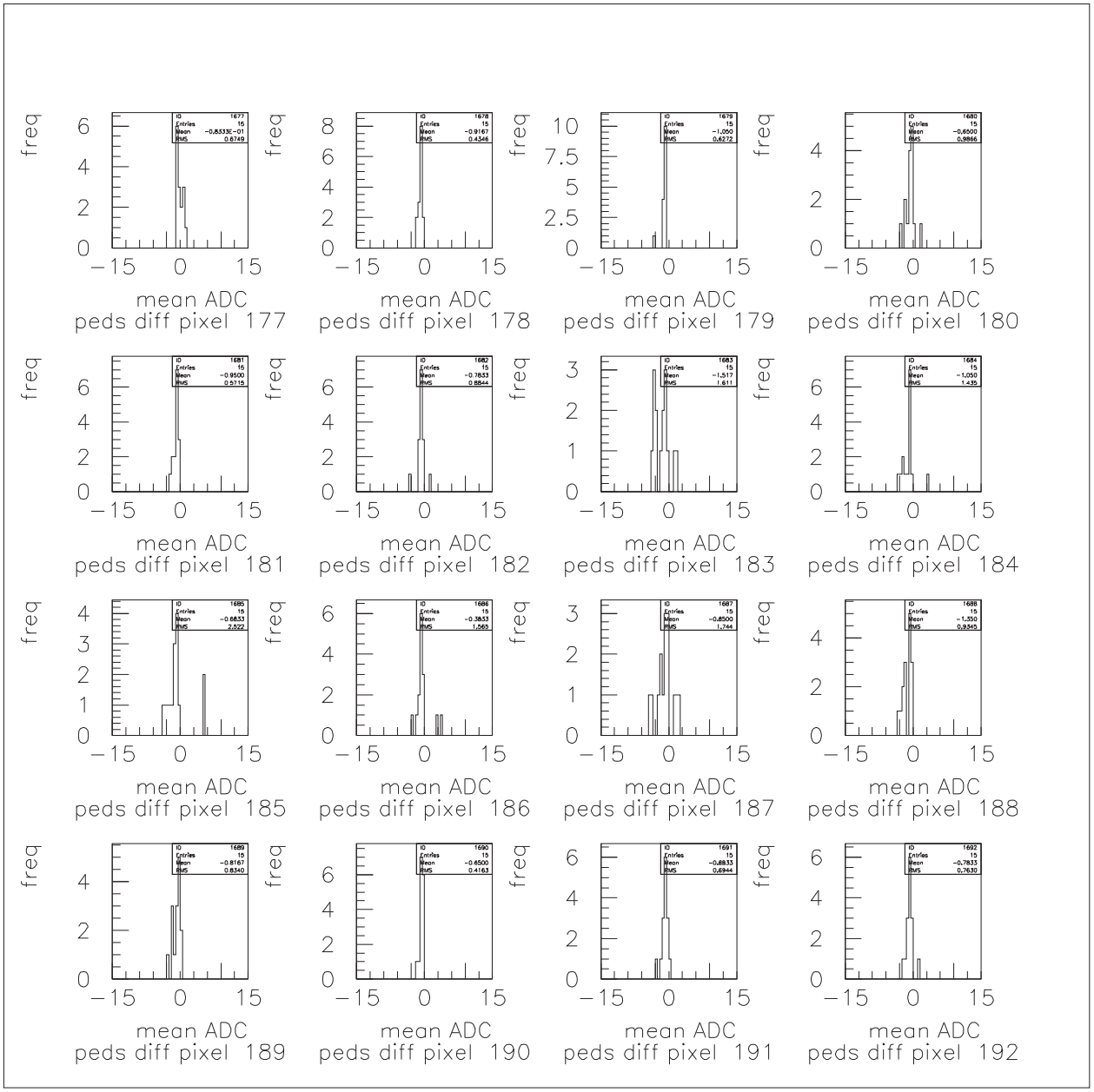

Figure D.12: Box 12. ADC pixel number is shown below each histogram.

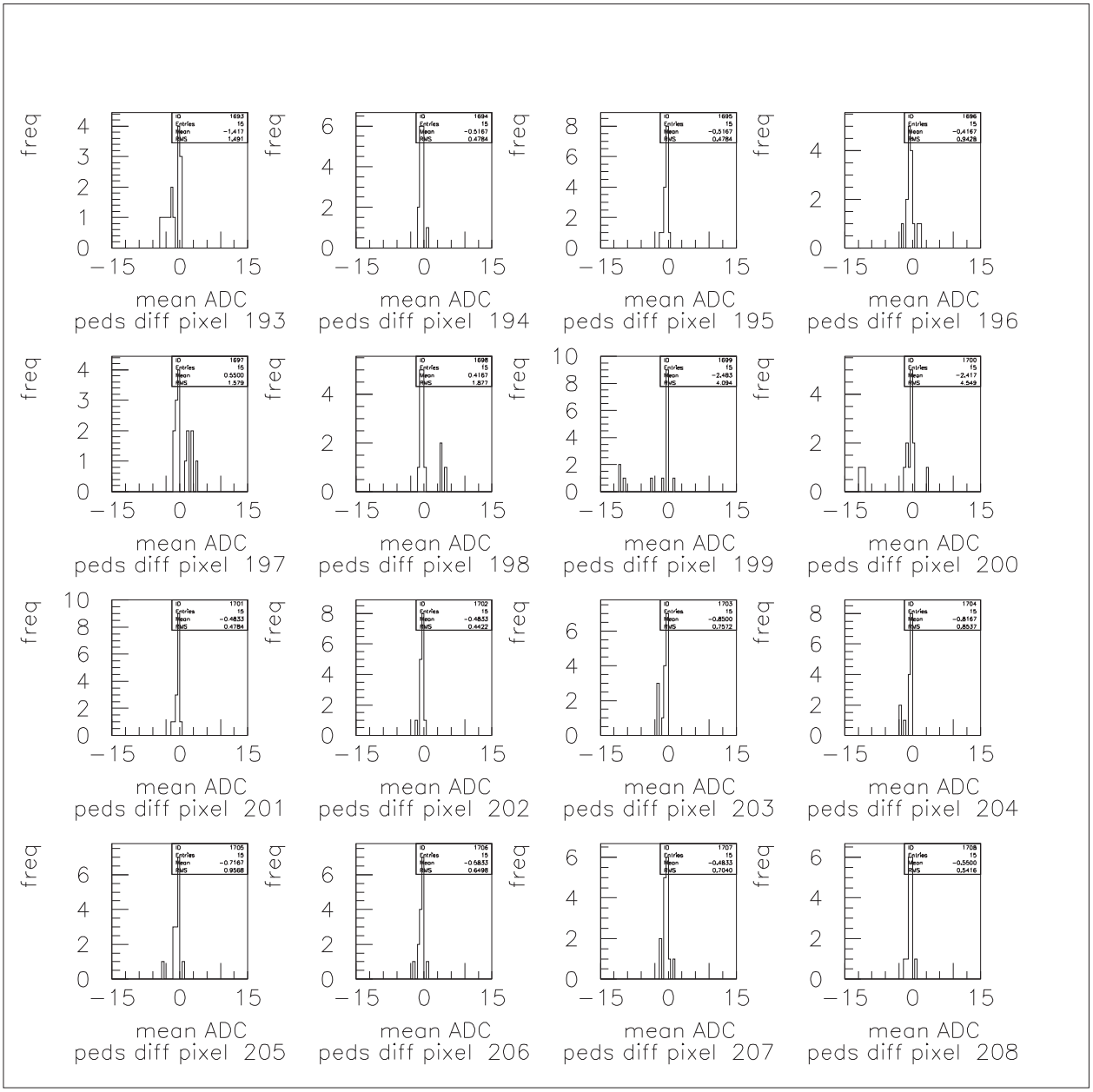

Figure D.13: Box 13. ADC pixel number is shown below each histogram.

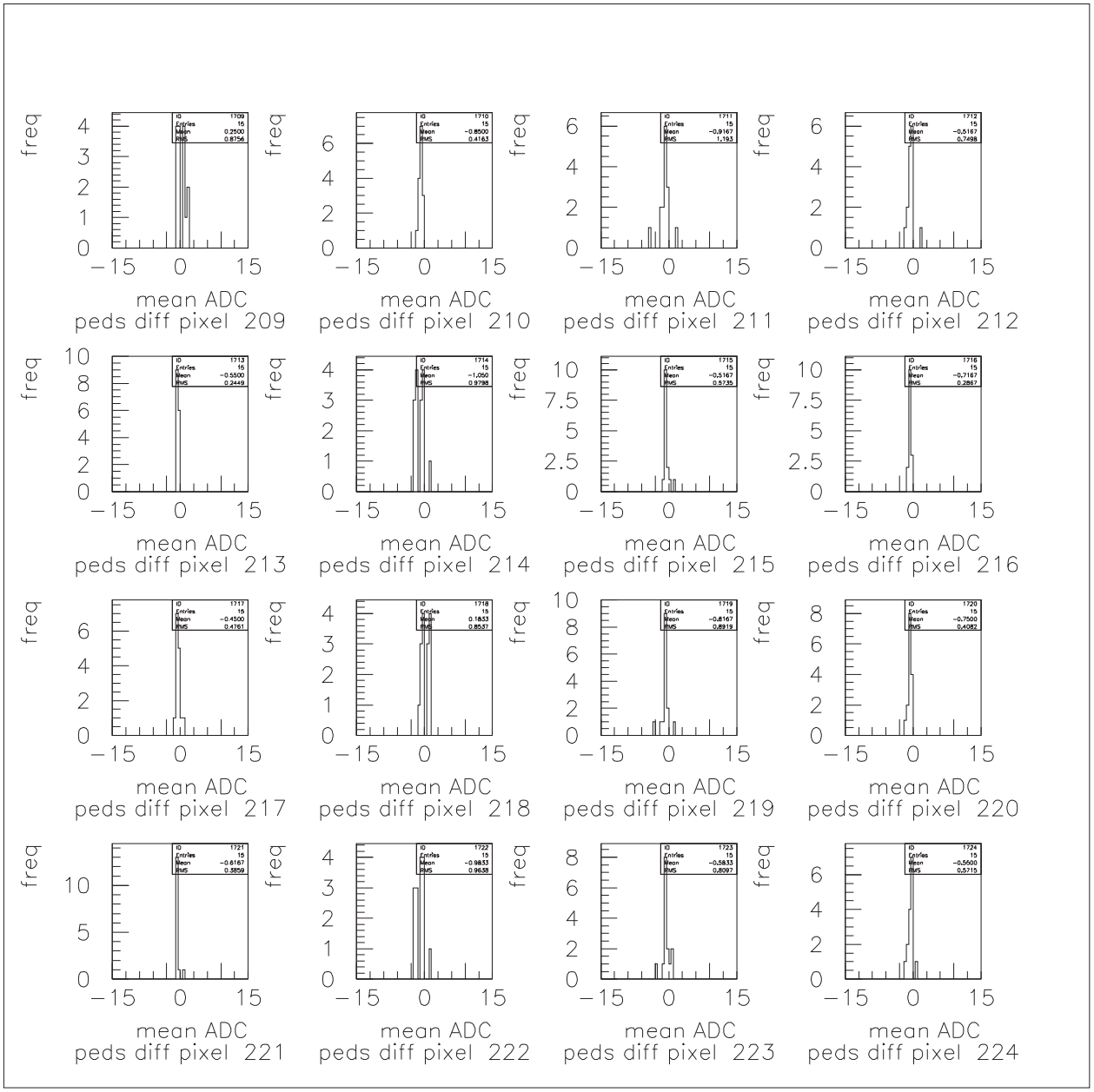

Figure D.14: Box 14. ADC pixel number is shown below each histogram.

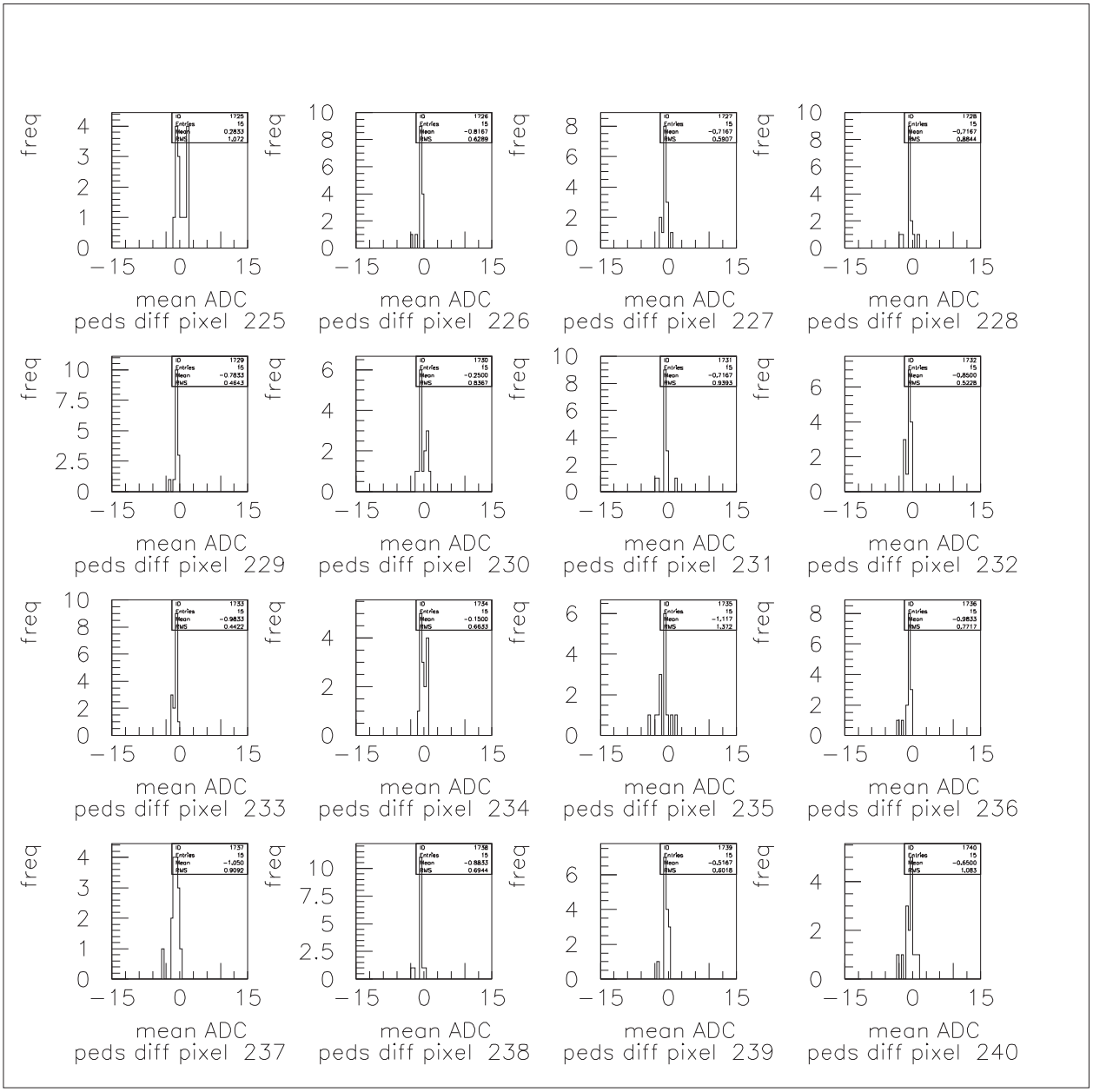

Figure D.15: Box 15. ADC pixel number is shown below each histogram.

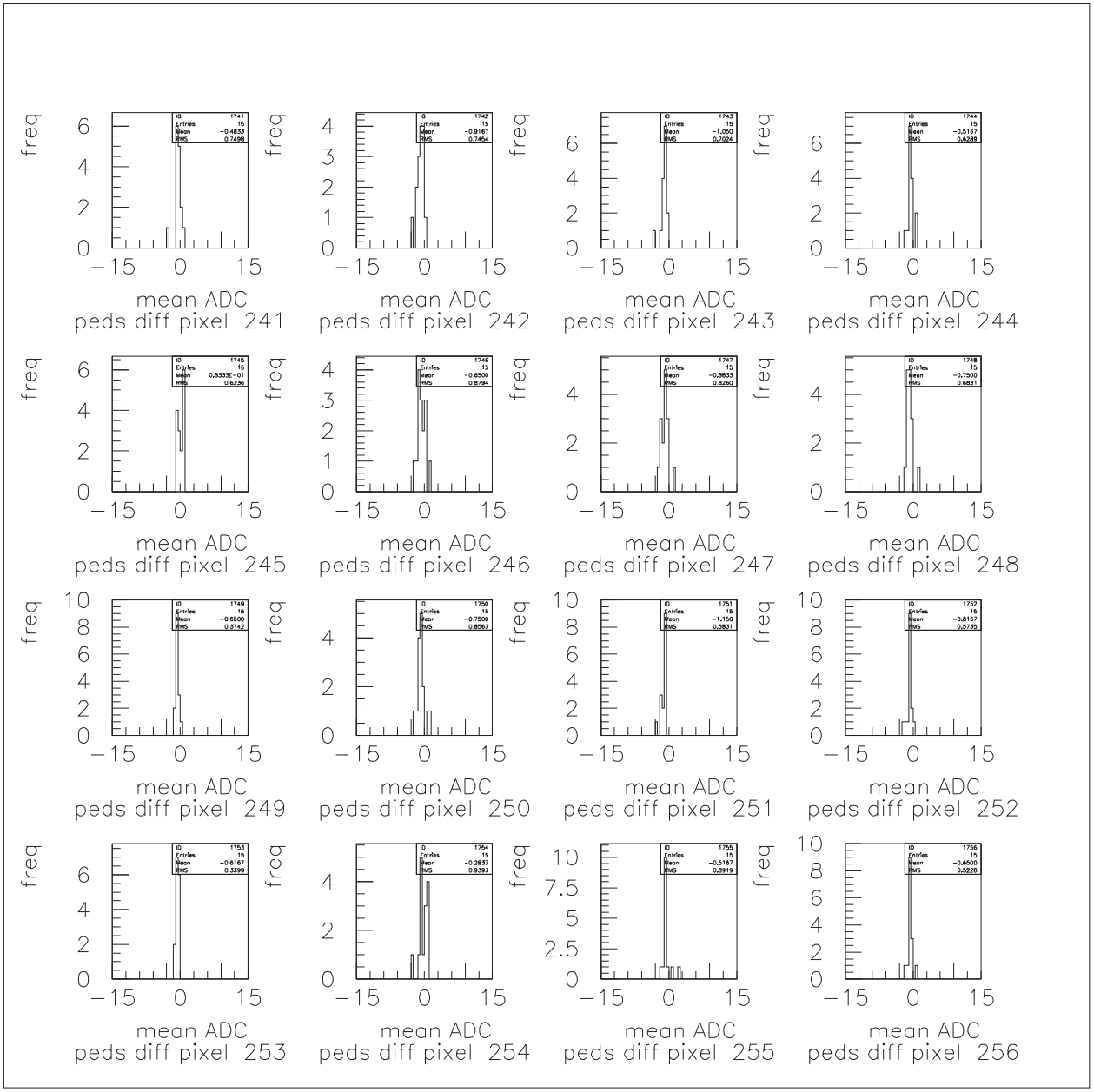

Figure D.16: Box 16. ADC pixel number is shown below each histogram.

Appendix E

Two-dimensional flasher calibration image results from T1 and T2's camera

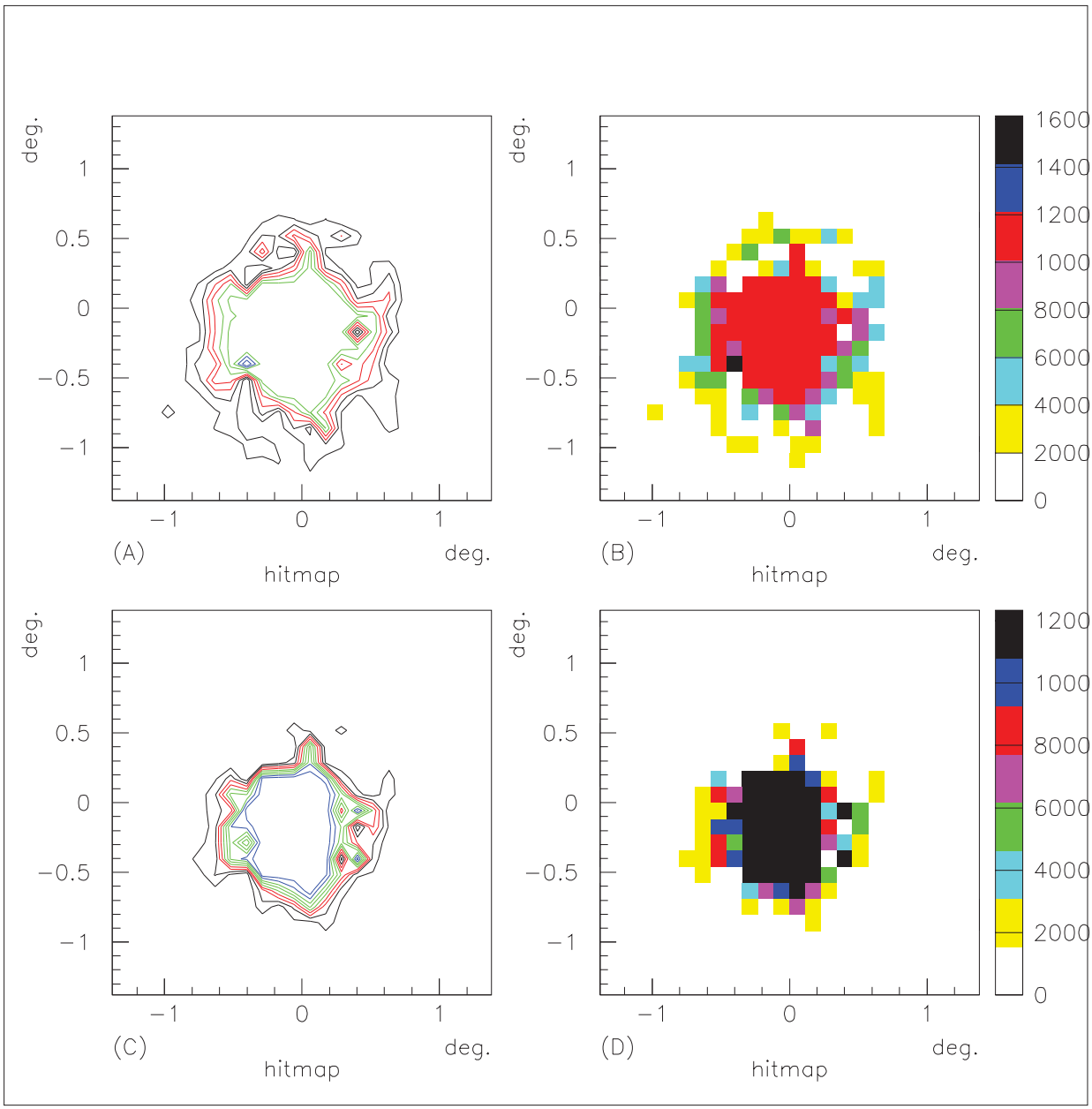

Figure E.1: Hit-map of T1 flasher images from Feb 7th 2002. This "hit-map" is a two dimensional image map (of the T1 camera), where any PMT pixel recorded a "hit" during the data acquisition run (see Section 3.2.6), hence hit pixels. The colour scale on the two right hand side slides (slides B and D) is hit pixel count where, e.g. yellow indicates a hit pixel count between 2000 to 3999. The number of equidistant contour lines are fixed at 10. Contour line colours are false and not set to any level. Contour line levels are determined from the maximum pixel value to zero. Slides A and B are unit 2 at 20ns. Slides C and D are unit 2 at 10 ns. The FOV of the camera shown in each slide is about 3 degrees by 3 degrees.

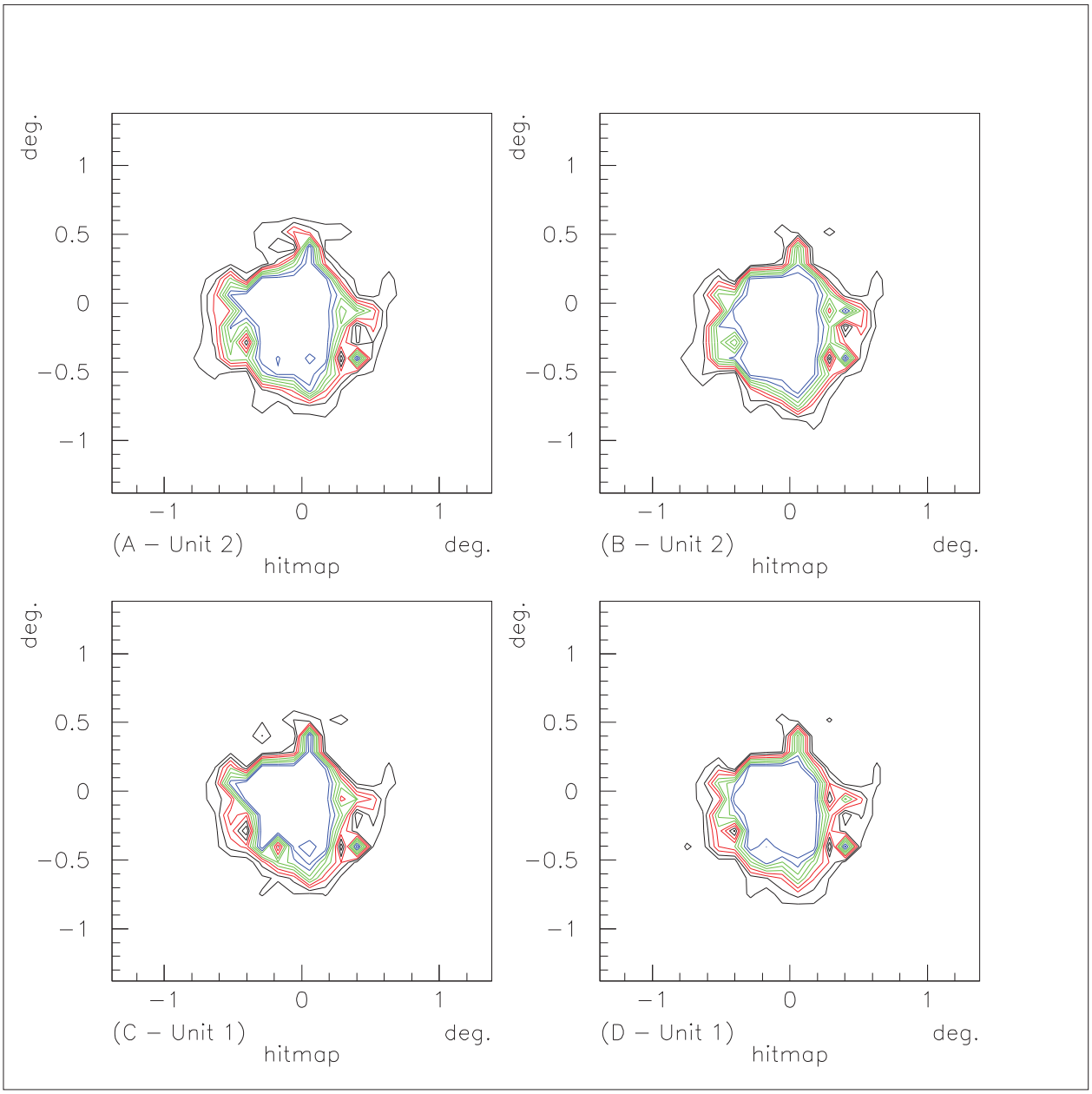

Figure E.2: Comparison of 10ns flasher T1 hit-map contour images with the calibration in Feb. 2002, compared to July 2001. The number of equidistant contour lines are fixed at 10. Contour colours are false and not set to any level. Contour levels are determined from the maximum pixel value to zero. Slide A is July 2001 (unit 2), slide B is Feb. 2002 (unit 2), slide C is July 2001 (unit 1), slide D is Feb. 2002 (unit 1).

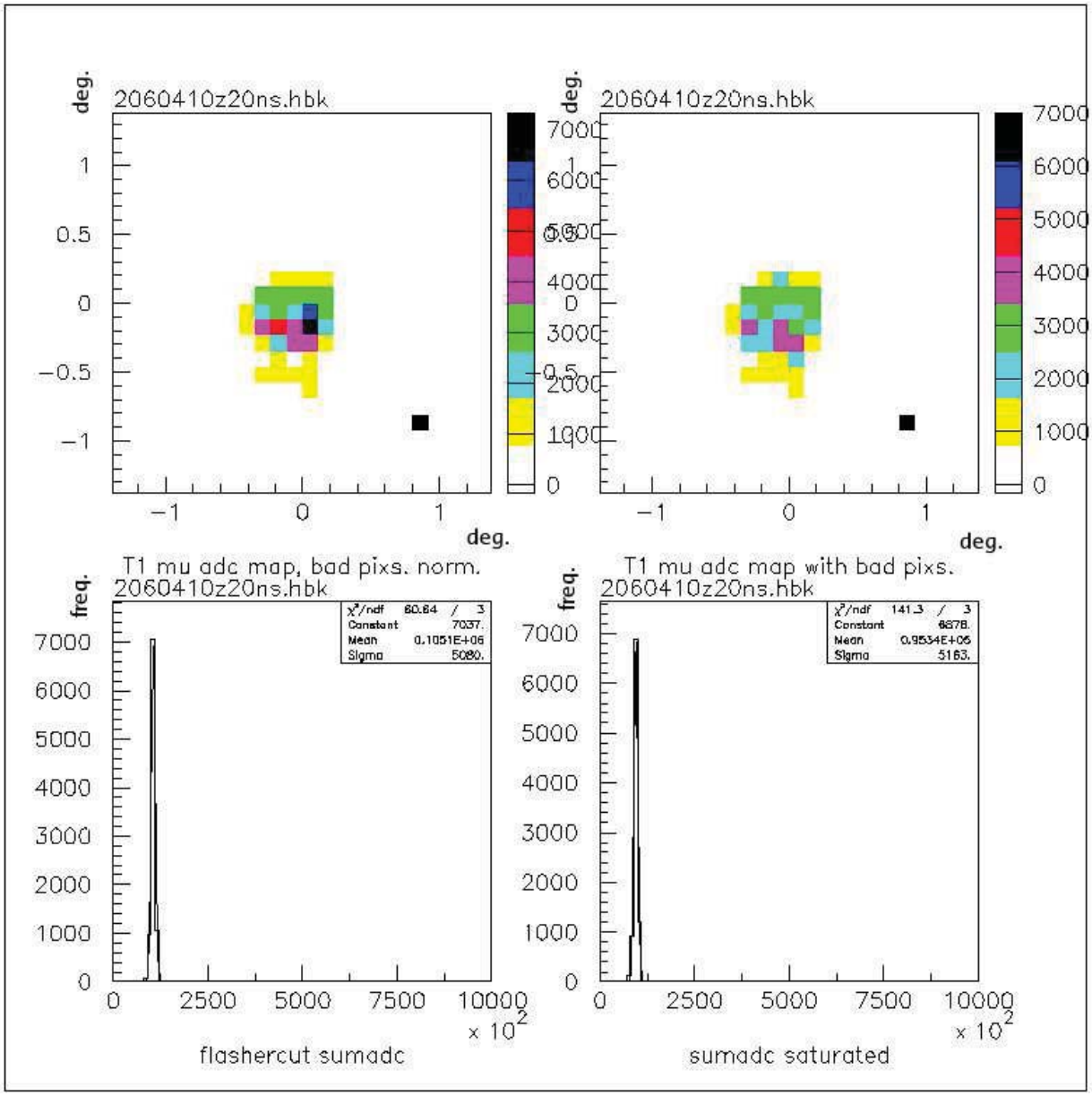

Figure E.3: T1 flasher mean ADC two dimensional pixel map (top two slides), and mean sum ADC (bottom two histograms). The data for all four figures is 20ns (no ND filters) from T1 in June 2003. The colour scale on the right hand side of the top slides is mean ADC count where, e.g. yellow indicates a mean ADC pixel count between 1000 to 1999. The isolated bright (> 7000 mean ADC counts) pixel in the lower right hand corner of the pixel maps is a scaling reference pixel only, and is not a real data point. "Flashercut" and "saturated" were an early attempt at pixel correction, where "saturated" are uncorrected pixels, see Section 5.2.5.

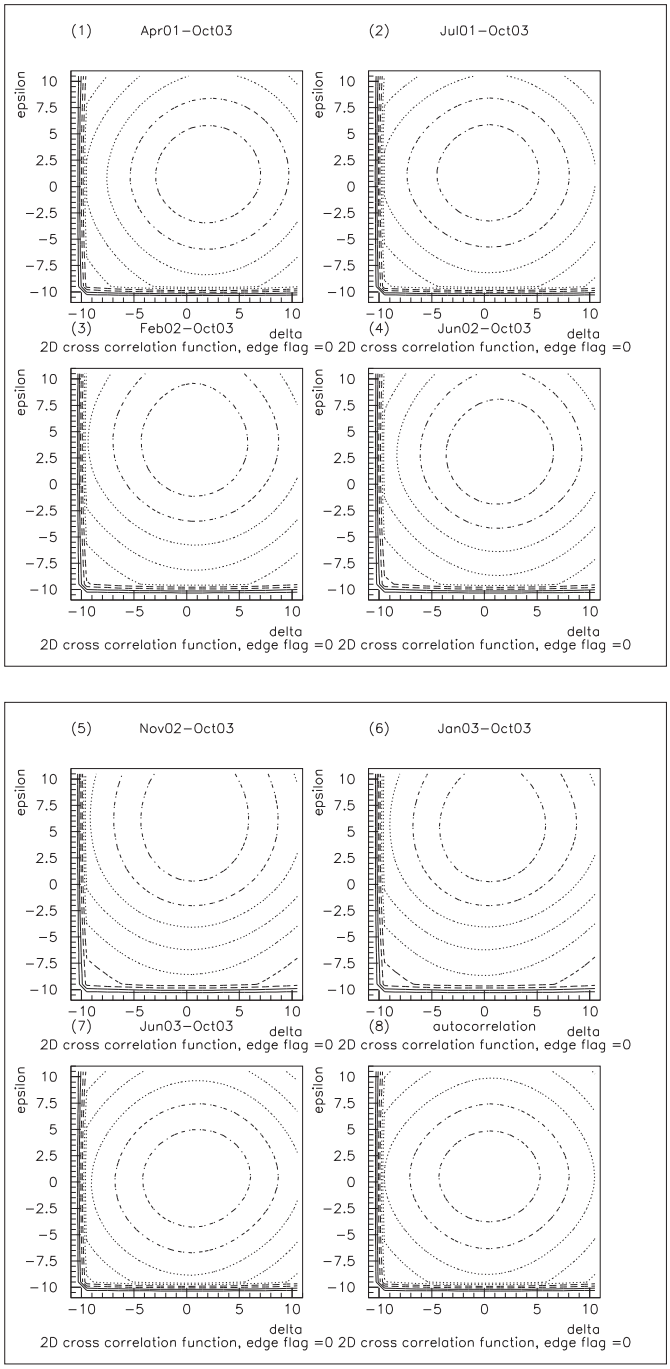

Figure E.4: Two dimensional cross-correlation results for the T1 flasher calibration by the calibration month, shown in the cross-correlation transform space of x-shift (delta, δ), y-shift (epsilon, ϵ). The flasher calibration month is shown as the first month above each slide with the slide number on the top left, e.g. slide no. 1 is the April 2001 calibration. The centre of the concentric rings in these slides (numbers 1 to 8), is the position of the cross-correlation maximum. This maximum position is shown in δ and ϵ, in Table 5.4. Slide no. 8 shows the autocorrelation function, (cross-correlating October 2003 with itself).

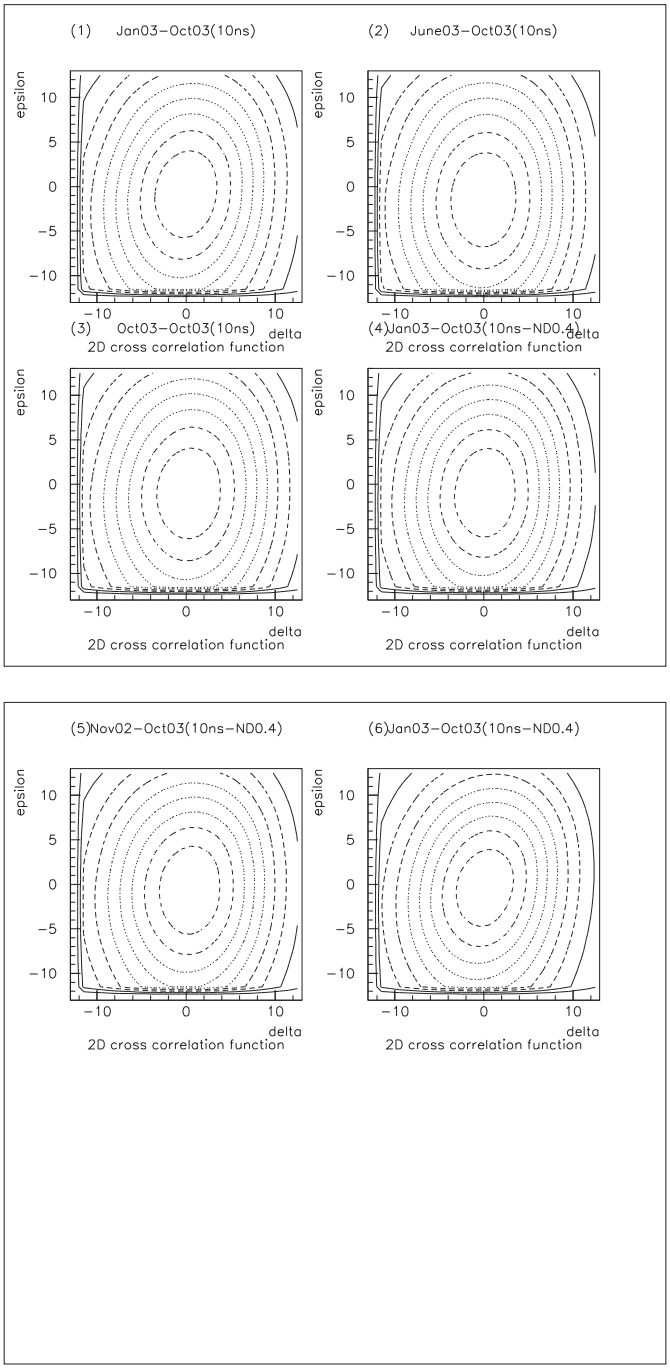

Figure E.5: Two dimensional cross-correlation results for the T2 flasher calibration by calibration month, shown in the cross-correlation transform space of x-shift (delta, δ), y-shift (epsilon, ϵ). The centre of the concentric rings in these slides (numbers 1 to 6), is the position of the cross-correlation maximum. This maximum position is shown in δ and ϵ, in Table 5.7. Slides 1 to 3 are the 10 ns flasher setting and slides 4 to 6 are 10 ns ND 0.4 flasher setting. The cross-correlation months (shown above each slide) as January and June 2003 with slides 3 and 6 showing the autocorrelation function, (cross-correlating October 2003 with itself).

Appendix F

T1 and T2 flasher calibration results & weather station data

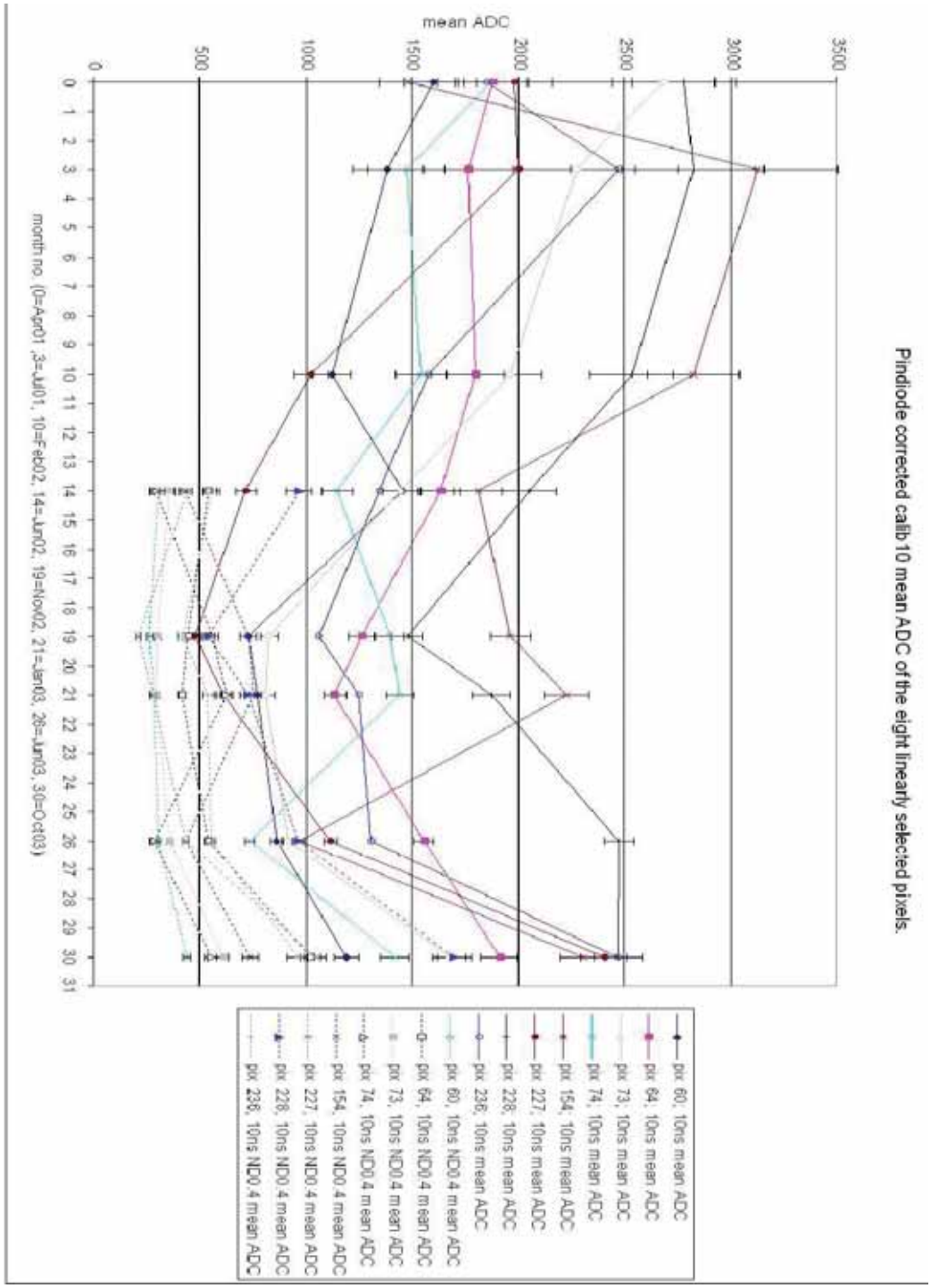

Figure F.1: Mean ADC over all calibration months, per pixel (rotated 90° to fit page). The eight selected inner camera linear pixels used are (by ADC ID-number); 60, 64, 73, 74, 154, 227, 228, 236. Flasher settings are 10ns (solid lines), and 10ns ND 0.4 filter (dotted lines), recorded in **calib10a** data format. Each point and line, pertinent to its particular pixel, is indicated by the table on the right of the graph. Each monthly mean ADC value is corrected using the PDM derived ratio values, shown in Table 4.3.

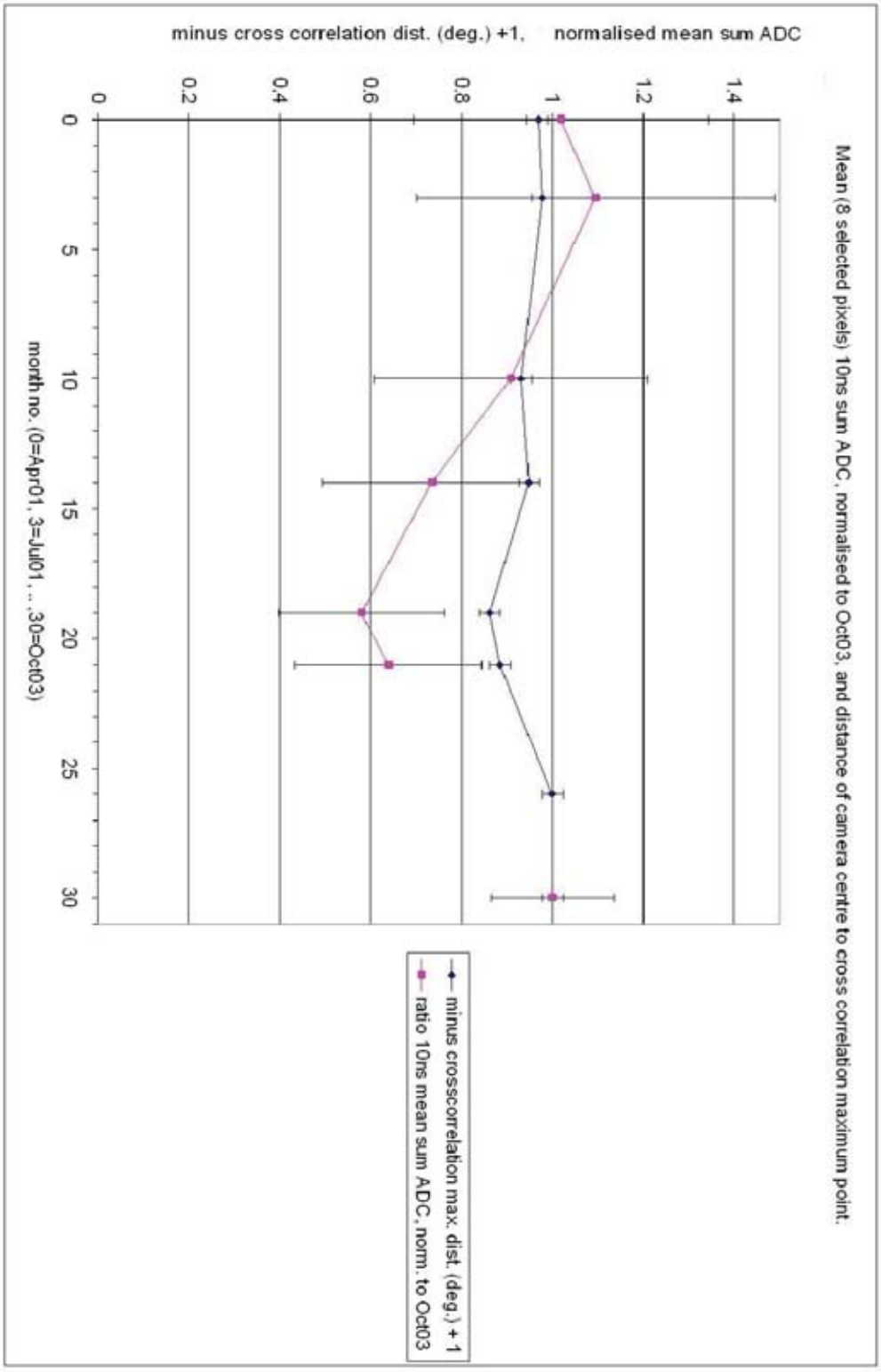

Figure F.2: Normalized ratio of average mean ADC of the eight selected T1 camera pixels over all calibration months for the 10ns setting with T1 cross-correlation maximum position distance (where 1.0 indicates the camera centre position and a lower value, further away from it). Both these quantities plotted together are unit-less. The average mean ADC datum point from June 2003 has been left out due to mirror dewing.

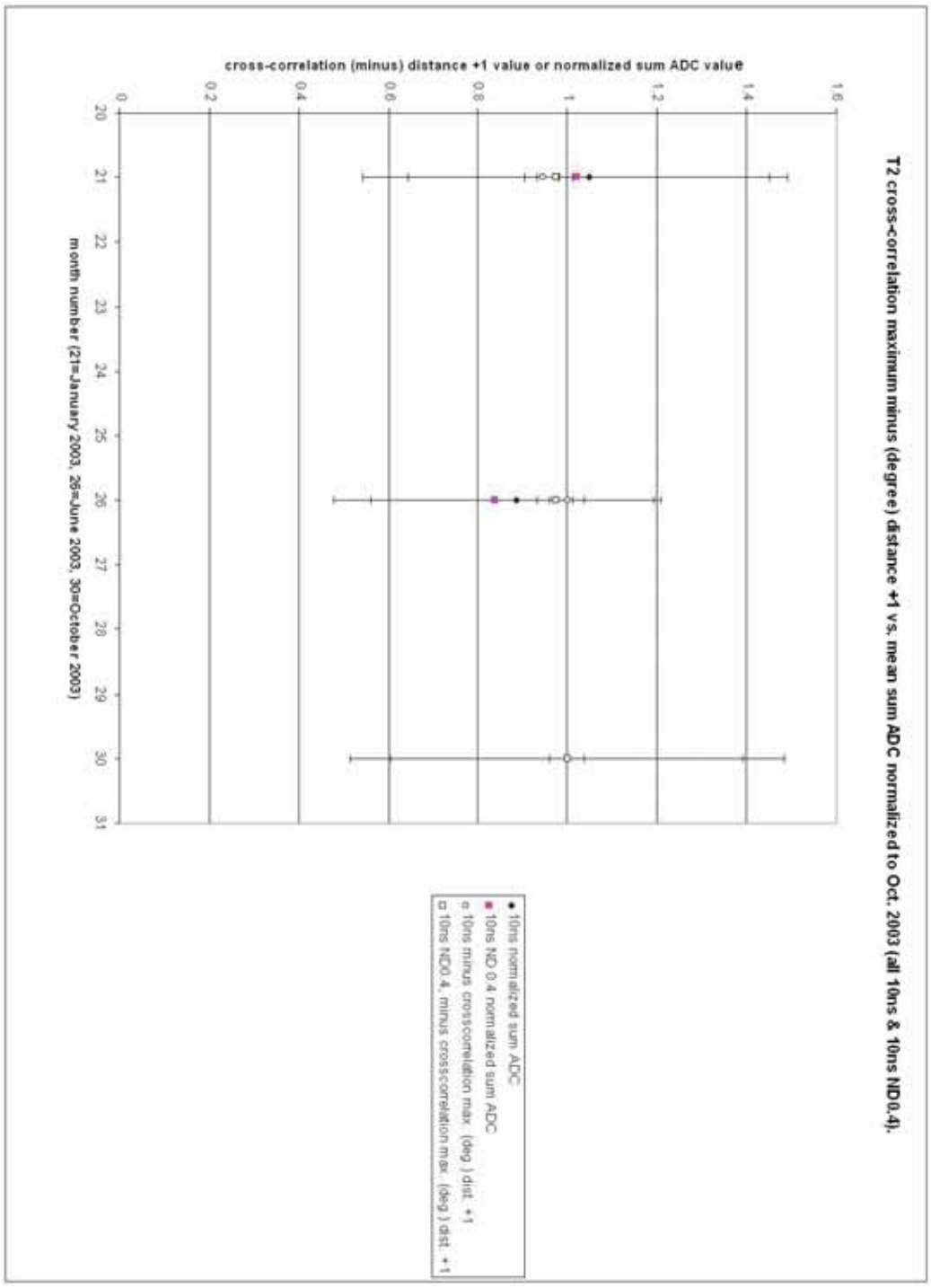

Figure F.3: (Rotated to fit page). Showing: 1. Normalized ratio of average mean ADC of the 192 inner T2 camera pixels for the calibration months, January, June & October 2003, for 10 ns & 10 ns settings. 2. Normalized T2 cross-correlation maximum position distance from 1.0, for 10 ns & 10 ns ND 0.4 settings. All results from other months are normalized to the sum ADC and cross-correlation maximum values from October 2003.

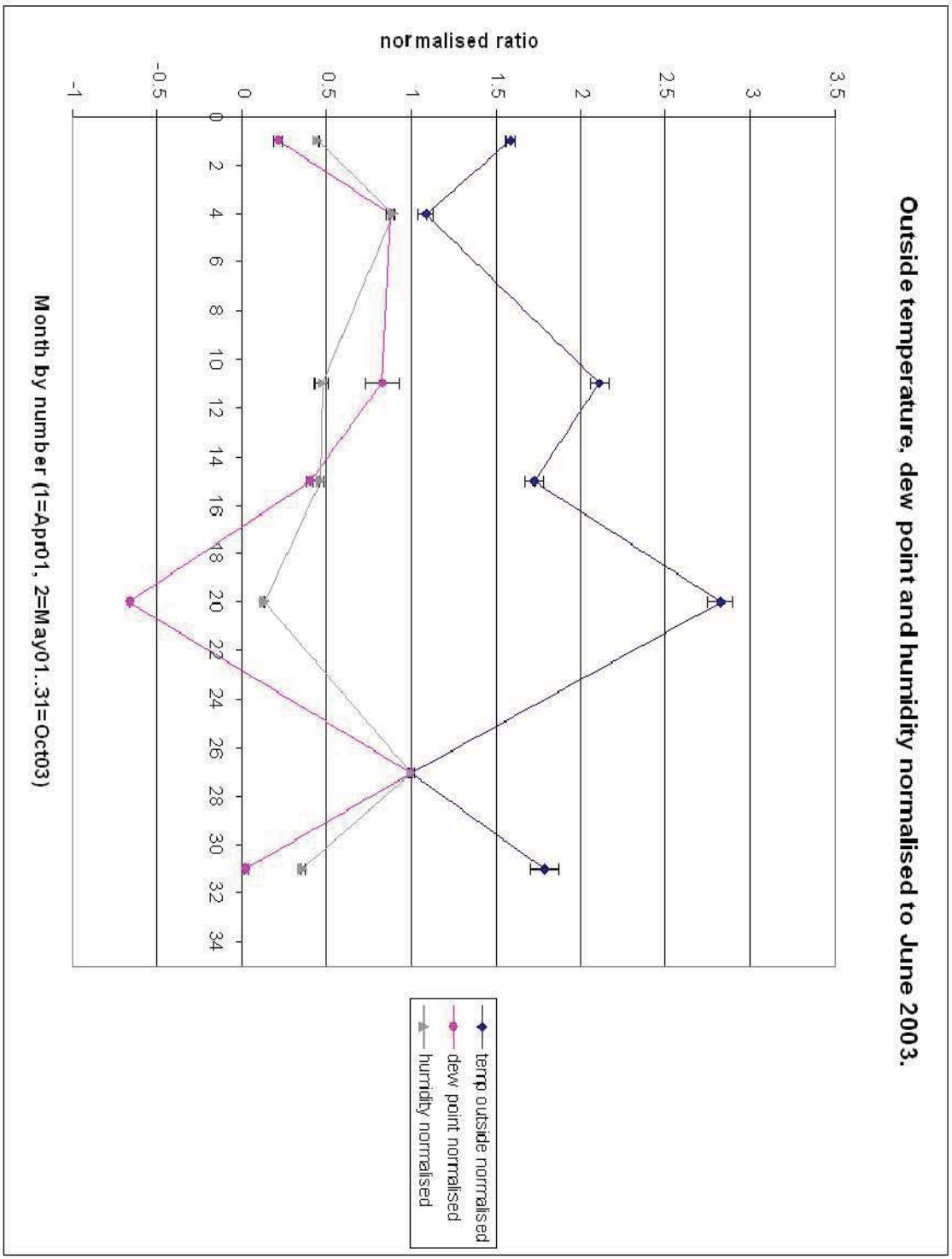

Figure F.4: (Rotated to fit page). Monthly data of Outside Temperature, Dew Point and Humidity from the Davis Weather Station at the T1 telescope.

Appendix G

Logbook data from 24/2/01, 25/2/01 and 2/1/01 flasher calibrations, supporting "square structure"

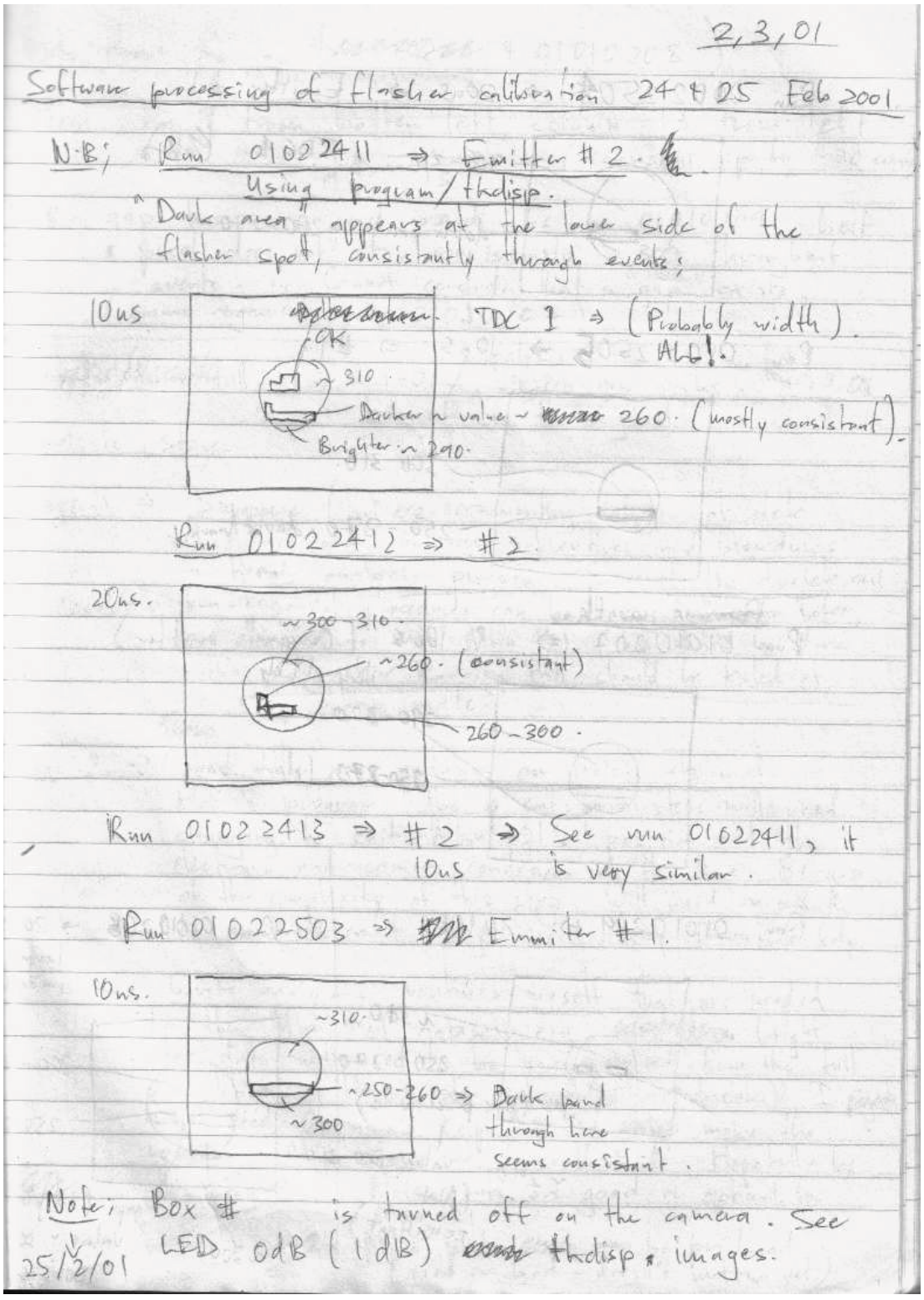

Figure G.1: **Page 1** logbook entry detailing flasher image analysis from 24/2/01 and 25/2/01 showing consistent dark bands through different flasher data files

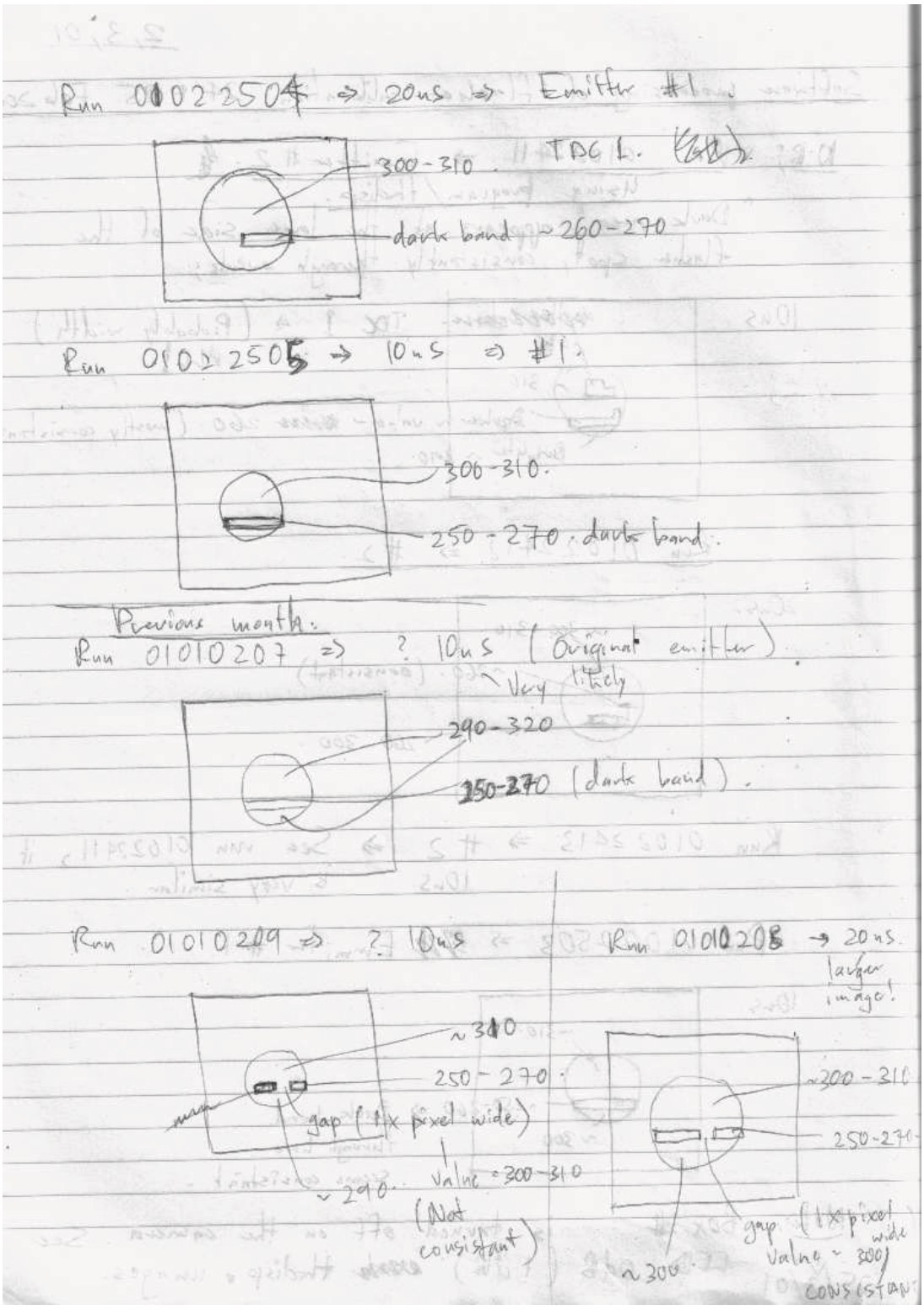

Figure G.2: **Page 2** logbook entry, detailing flasher image analysis from 25/2/01 (and previous month's data on the 2nd January 2001), showing consistent dark bands through different flasher data files.

Appendix H

CANGAROO-II (T1) TeV blazar observation summary: Data files

Run number	on/off	no. events	exposure (min)	weather	faults
01012405	off	53519	61	fine	
01012408	on	34819	29	fine	DA trouble
01012409	on	49496	35	fine	DA trouble
01012410	on	8842	9	fine	DA trouble
01012413	on	41367	20	fine	DA trouble
01012609	off	136586	62	thin cloud	
01012619	on	437460	84	fine	
01012703	off	92607	105	fine	
01012713	on	151726	110	fine	
01012803	off	54303	55	fine to cloudy	
01012809	on	23093	41	fine to cloudy	
01013003	off	32151	37	fine	ground lights
01013004	off	139594	110	fine	
01013007	on	100210	12	fine	ground lights
01013008	on	144604	144	fine	
01013113	off	10603	19	fine	ground lights
01013114	off	53716	98	fine	
01013117	on	19029	31	fine	ground lights
01013118	on	69132	103	fine	
01013121	off	15300	17	fine	
01020120	off	30359	27	fine	ground lights
01020121	off	131290	62	fine	
01020124	on	23653	32	fine	ground lights
01020125	on	165424	92	fine	
01020128	off	55694	25	fine	
01030107	on	103460	60	fine	
01030110	off	124457	52	fine	
01030206	on	135353	76	fine	
01030209	off	141595	68	fine	
01030303	on	47344	125	?	
01030306	off	112214	139	?	
01030403	on	56831	101	?	
01030409	off	28692	99	?	
TOTAL	**on**	1611843	1104		
TOTAL	**off**	1212680	1036		

Table H.1: Markarian 421 T1 observation results for data collection in January, February and March 2001. The data file number is shown as the run number. The on/off indicates the long on and long off source exposure, with the exposure time for that run in minutes. Weather and run time faults reports on the data taking night are sometimes included, (question mark indicates that the weather was not reported for the night). The total indicates the sum of on or off source number of triggered events and exposure times for Markarian 421 in 2001.

Run number	on/off	no. events	exposure (min)	weather	faults
02021604	off	28462	123.8	fine	
02021608	on	197634	201.9	fine	
02021612	off	40788	58.7	fine	
02021704	off	12120	97.9	thin cloud	ADC trouble
02021709	on	14894	96.2	fine	HV box out, dish elev.
02021710	on	20607	76.7	fine	
02021717	off	37457	65.9	fine	
02021804	off	4195	79.9	cloudy	ADC trouble
02021810	on	14005	165.8	thin cloud	
02021814	off	14320	82.2	cloudy	
02021906	off	2442	34	cloudy	
02021910	on	38069	160.3	thin cloud	
02021914	off	70238	96	cloudy	
02022004	on	66424	149.9	fine	
02022008	off	121291	109.4	fine	
03010808	off	257762	62	?	
03010809	on	178024	63.7	?	
03010919	on	130141	57.3	?	
03011012	off	91540	55.5	?	
03011016	on	94516	63.9	?	
03011204	off	35603	81.2	?	
03011205	on	116932	96.2	?	
03011209	off	24063	78	?	
03011212	on	85373	78	?	
TOTAL	**on**	956619	1209.9		
TOTAL	**off**	740281	1024.5		

Table H.2: Markarian 421 T1 observation results for data collection in February 2002 and January 2003. The total is inclusive of the sum of exposure times and events of the Markarian 421 data in 2002 and 2003 above.

Run number	on/off	no. events	exposure (min)	weather	faults
02110307	off	135928	168	cloudy	
02110310	on	161175	208	?	
02110403	off	69373	218	clear	
02110407	on	177751	217	clear	
02110511	off	118180	172	clear	
02110514	on	184407	158	clear	
02110603	off	54750	216	cloudy	
02110606	on	156973	213	cloudy	
02110716	off	67462	118	cloudy	
02110719	on	65818	110	cloudy	
02110803	off	59877	147	clear	
02110806	on	205853	144	clear	
02110906	off	52230	95	clear	
02110909	on	105013	95	clear	
02111003	off	47045	92	clear	
02111006	on	66811	91	clear	
02111204	off	23459	19	clear	
02111208	on	104693	51	clear	
02122612	on	59134	50.9	?	
02122714	off	70735	38.6	?	
02122717	on	170571	96.5	?	
02122909	on	55278	106.7	?	
02122913	off	45527	49	?	
02123108	on	452846	179.1	?	
02123111	off	215681	118.4	?	
03010204	off	50145	36.6	?	
03010207	on	288503	194.7	?	
03010210	off	157107	129.3	?	
03010304	off	46317	34.9	?	
03010306	on	397950	186.7	?	
03010310	off	302917	141.5	?	
03010404	off	34477	34.9	?	
03010406	on	343044	198.4	?	
03010409	off	387349	152.4	?	
TOTAL	**on**	1767326	1013		
TOTAL	**off**	1310255	786.5		

Table H.3: The BL Lac. blazar; EXO 055625-3838.6 observation results for data collection in November and December 2002, and in January 2003 from the T1 telescope. The data file number is shown as the run number. The on/off indicates the long on and off source exposure, with the exposure time for that run in minutes. The total indicates the sum of total on or off source number of triggered events and exposure times, and is the sum of the data files shown in this table for this source observation.

Appendix I

T1 Monte Carlo simulation results: Proton showers

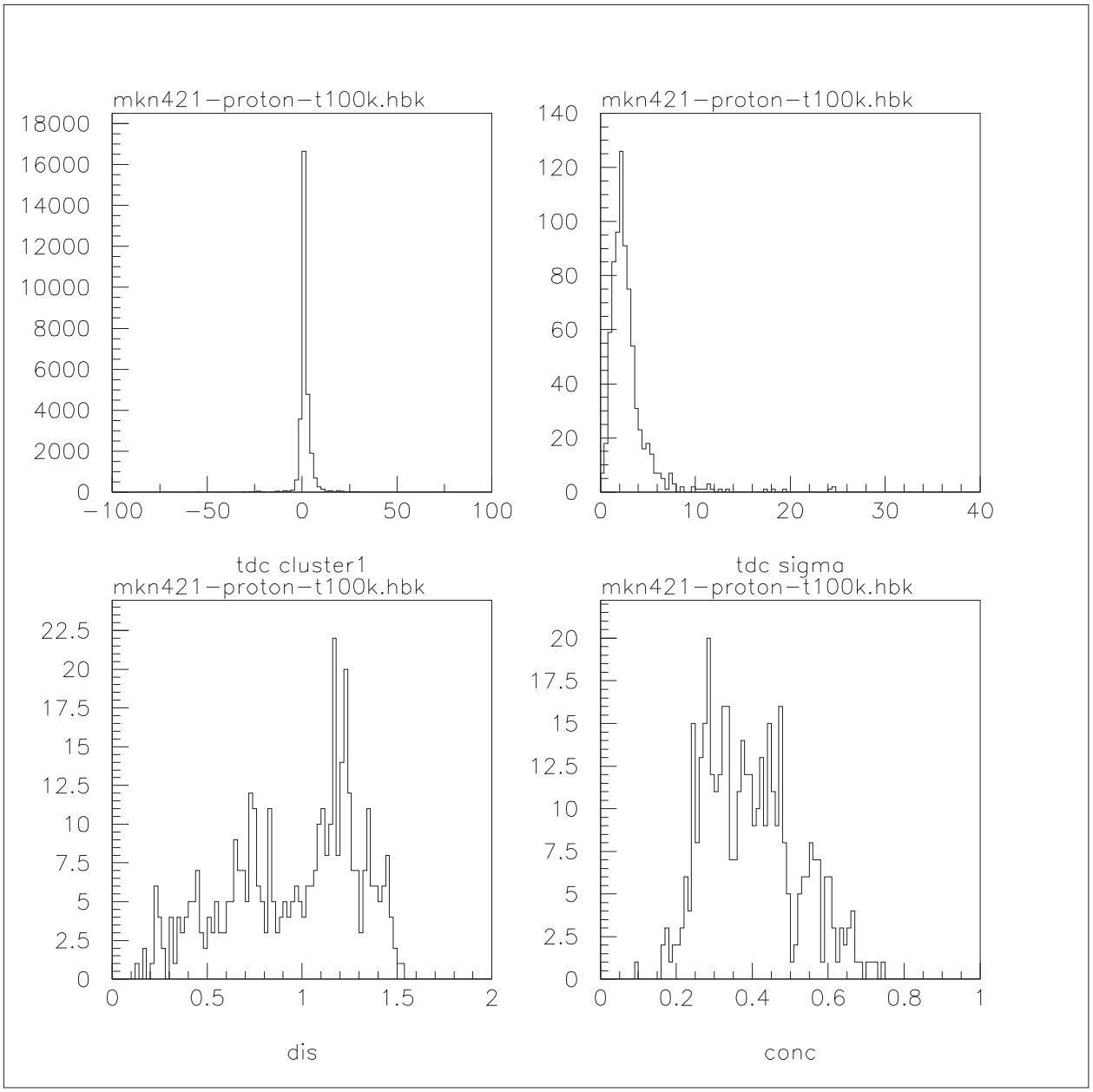

Figure I.1: Histograms of primary proton EAS Monte Carlo *GEANT 3.21* simulation results for Markarian 421: Showing the Hillas Parameter *distance* (*dis*), amongst other results. The spectral index for this source is 2.7, the zenith angle is 70° and the number of events simulated are 1×10^5.

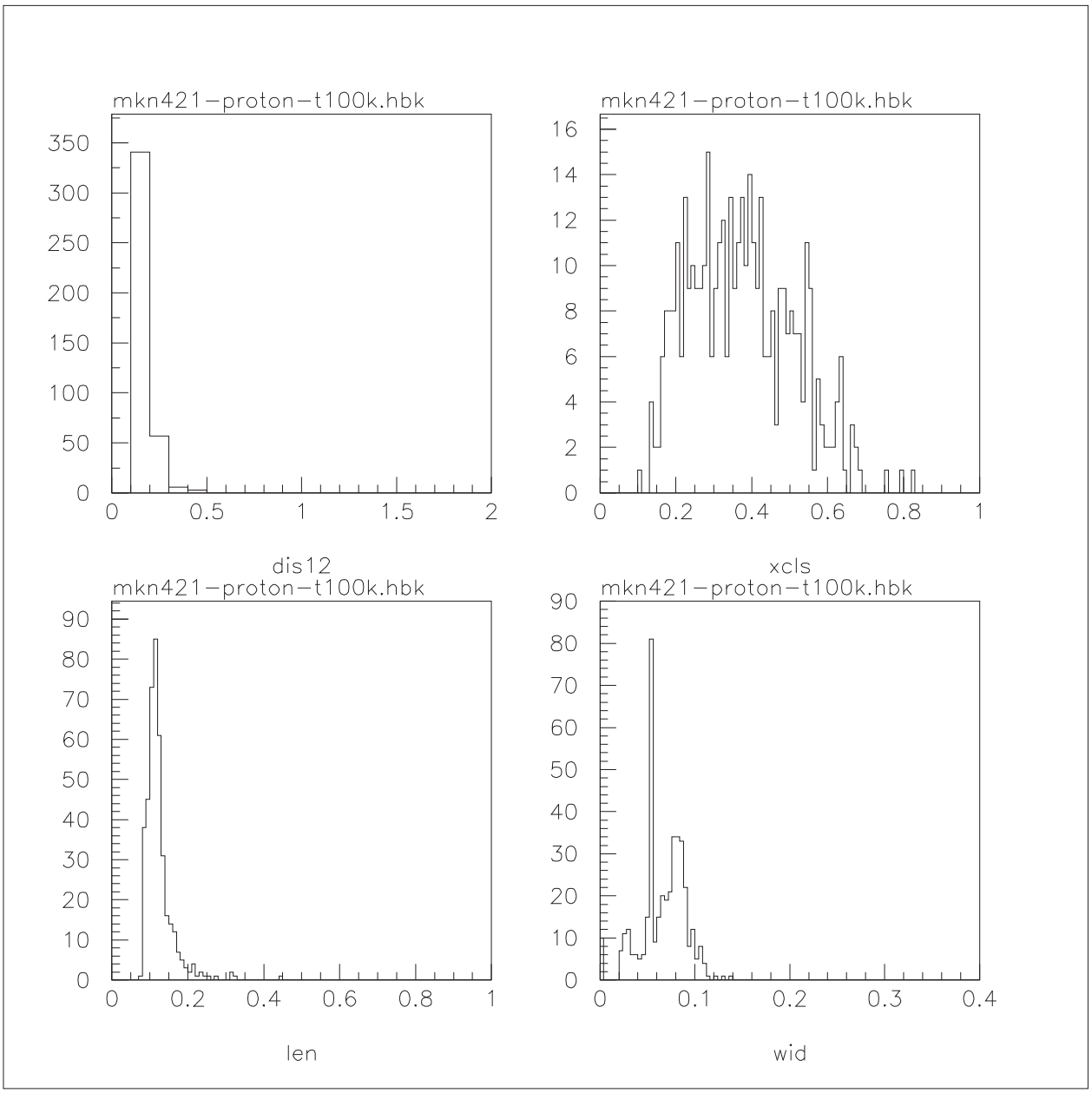

Figure I.2: Histograms of primary proton EAS Monte Carlo *GEANT 3.21* simulation results for Markarian 421: Showing the Hillas Parameter *length* (*len*) and *width* (*wid*), amongst other results. The spectral index for this source is 2.7, the zenith angle is 70° and the number of events simulated are 1×10^5.

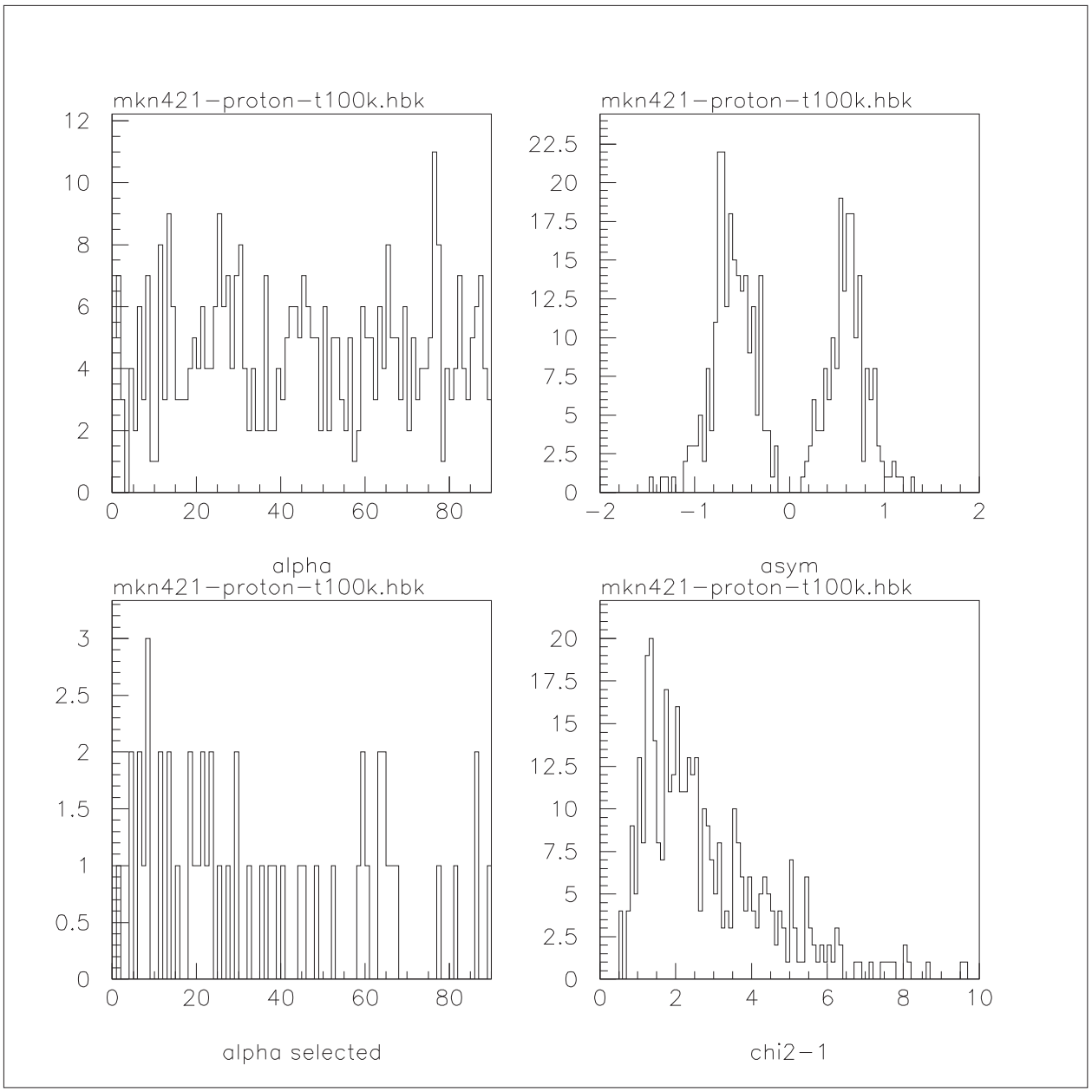

Figure I.3: Histograms of primary proton EAS Monte Carlo *GEANT 3.21* simulation results for Markarian 421: Showing the Hillas Parameter *alpha* (top left histogram), amongst other results. The spectral index for this source is 2.7, the zenith angle is 70° and the number of events simulated are 1×10^5.

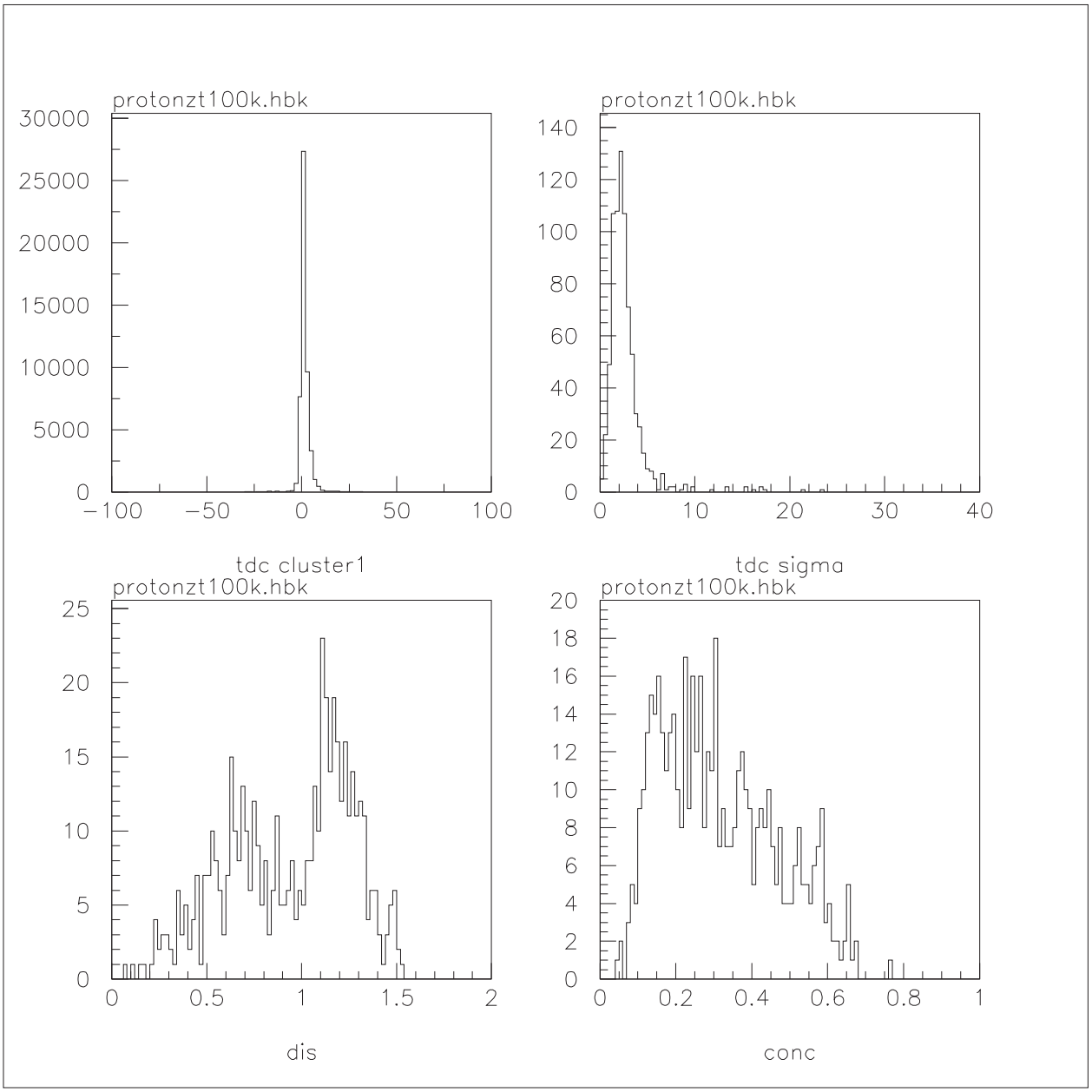

Figure I.4: Histograms of primary proton EAS Monte Carlo *GEANT 3.21* simulation results for EXO 055625-3838.6: Showing the Hillas Parameter *distance* (*dis*), amongst other results. The spectral index for this source is 2.7, the zenith angle is 10° and the number of events simulated are 1×10^5.

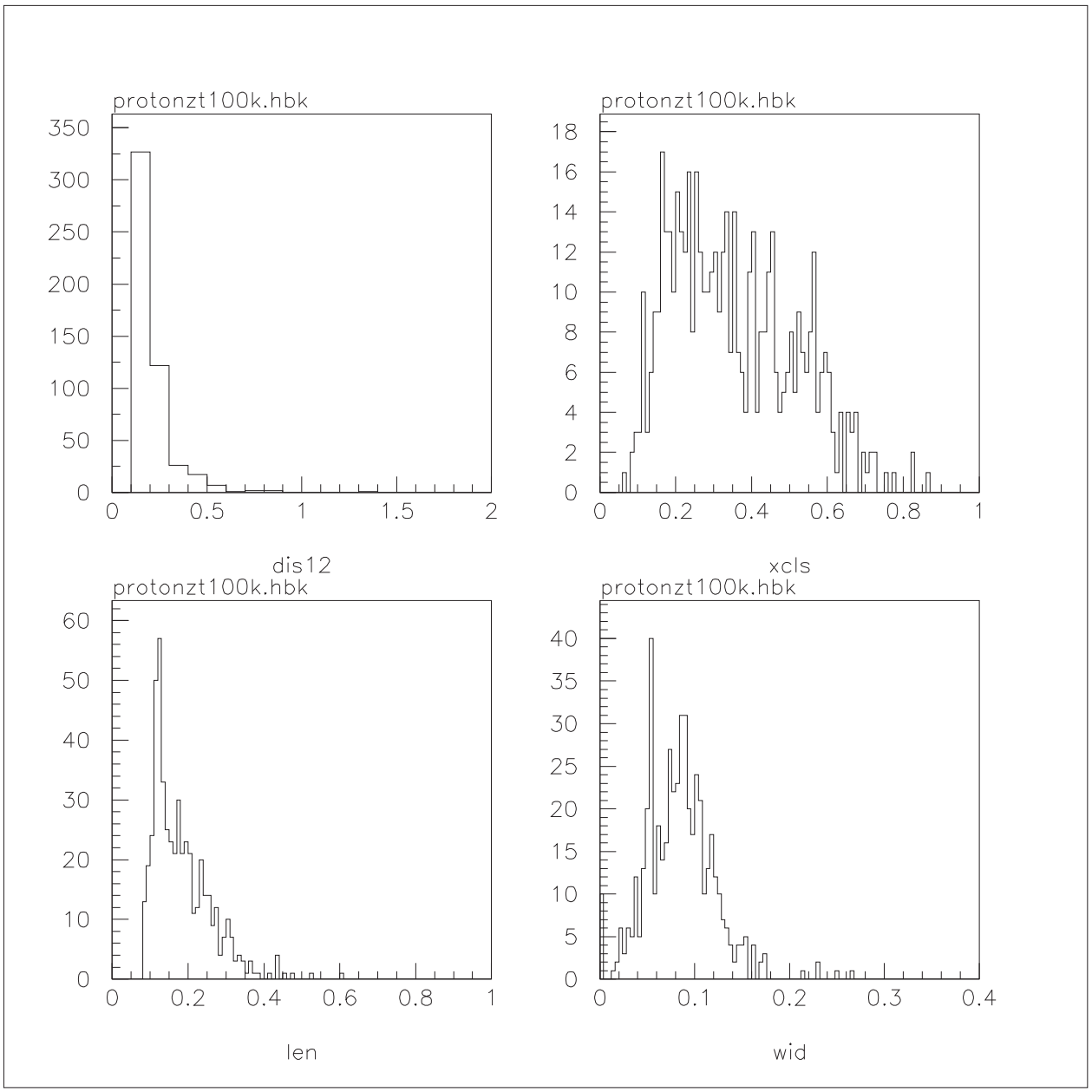

Figure I.5: Histograms of primary proton EAS Monte Carlo *GEANT 3.21* simulation results for EXO 055625-3838.6: Showing the Hillas Parameter *length* (*len*) and *width* (*wid*), amongst other results. The spectral index for this source is 2.7, the zenith angle is 10° and the number of events simulated are 1×10^5.

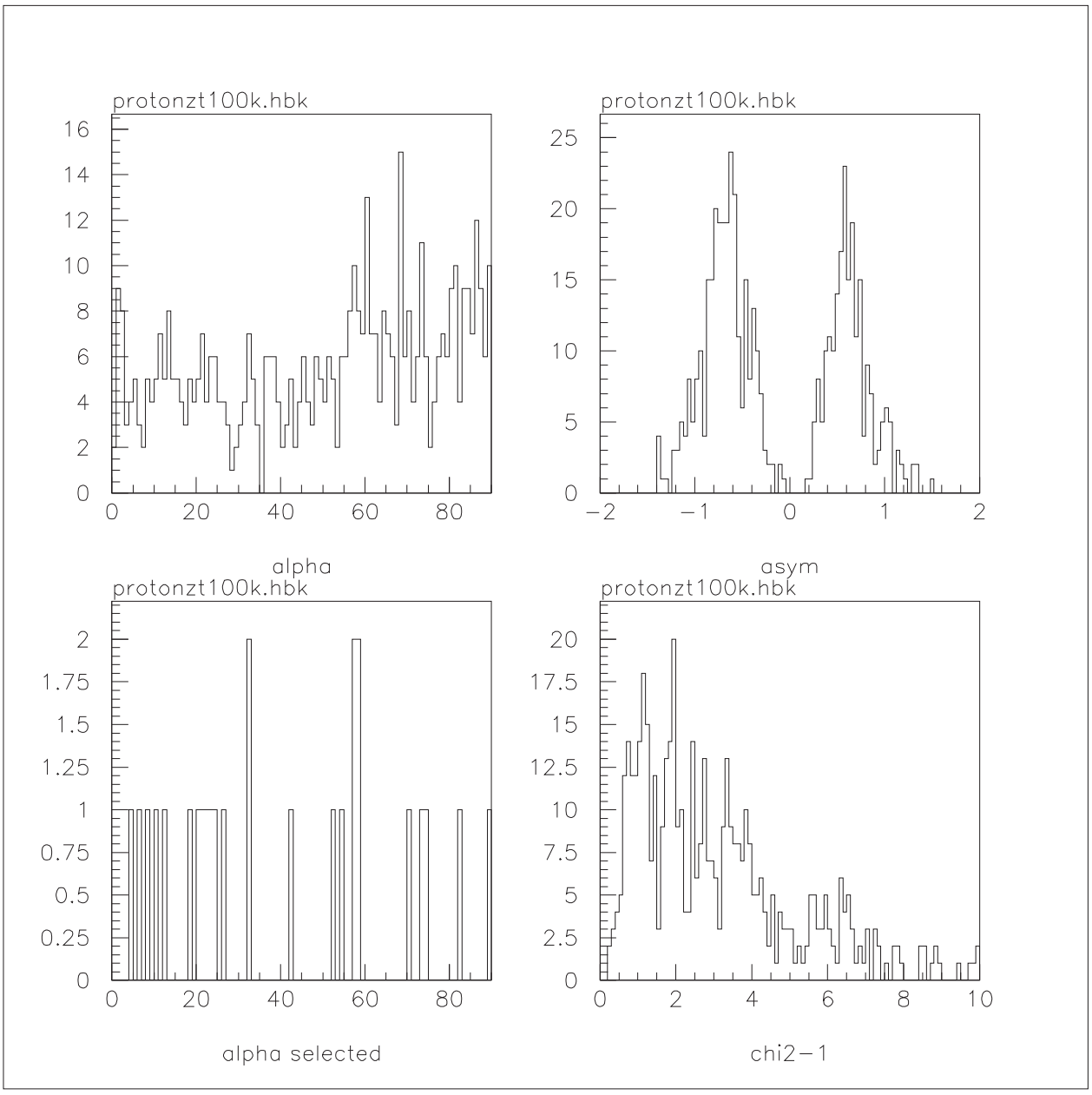

Figure I.6: Histograms of primary proton EAS Monte Carlo *GEANT 3.21* simulation results for EXO 055625-3838.6: Showing the Hillas Parameter *alpha* (top left histogram), amongst other results. The spectral index for this source is 2.7, the zenith angle is 10° and the number of events simulated are 1×10^5.

Appendix J

Markarian 421 and EXO 055625-3838.6 *alpha* plot results from T1

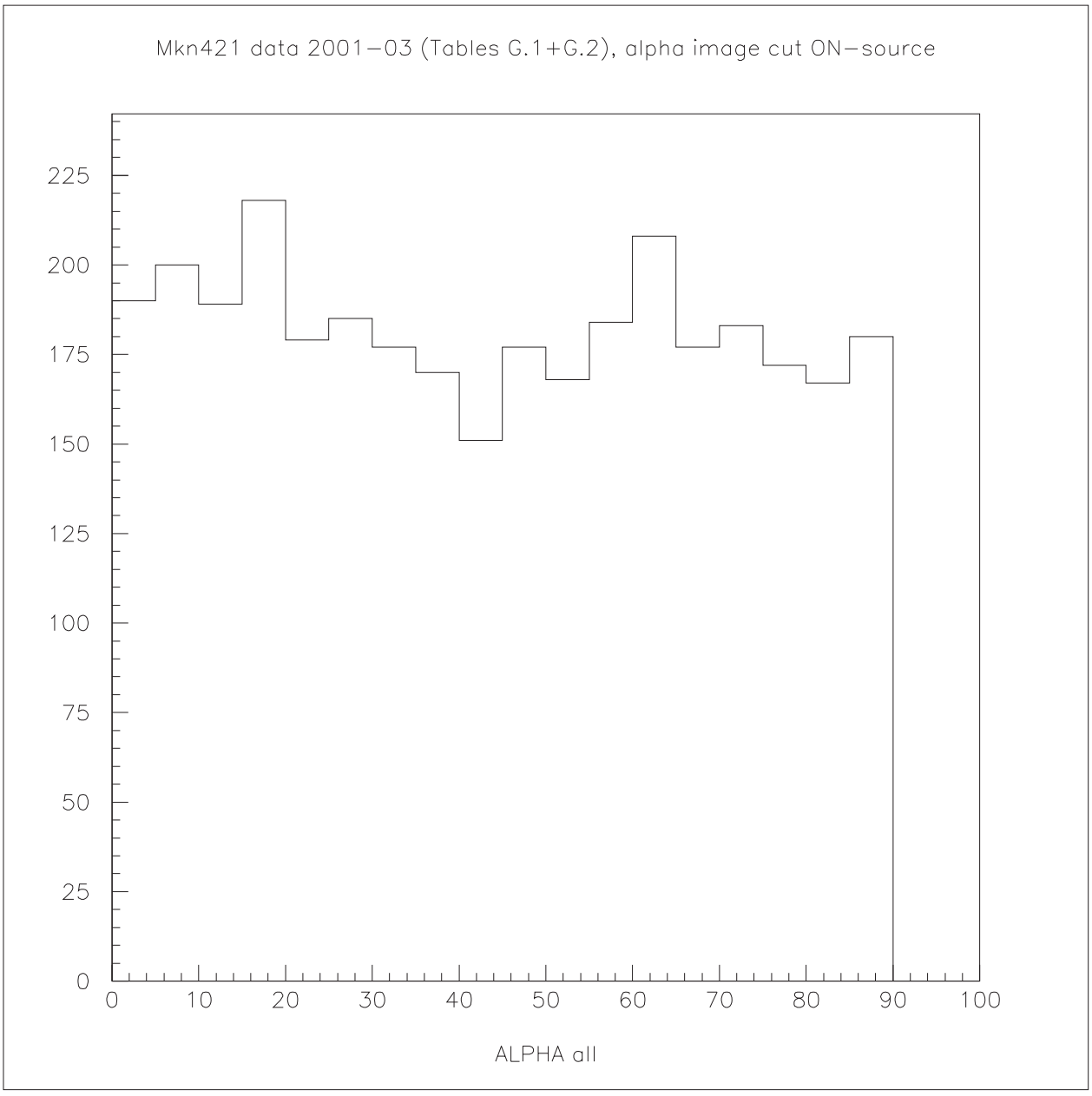

Figure J.1: The *alpha* image plot for all Markarian 421 T1 observation data from 2001 to 2003 (data files; see Tables H.1 and H.2, Appendix H). On-source *alpha* plot only. See Figure 7.7 for comparison.

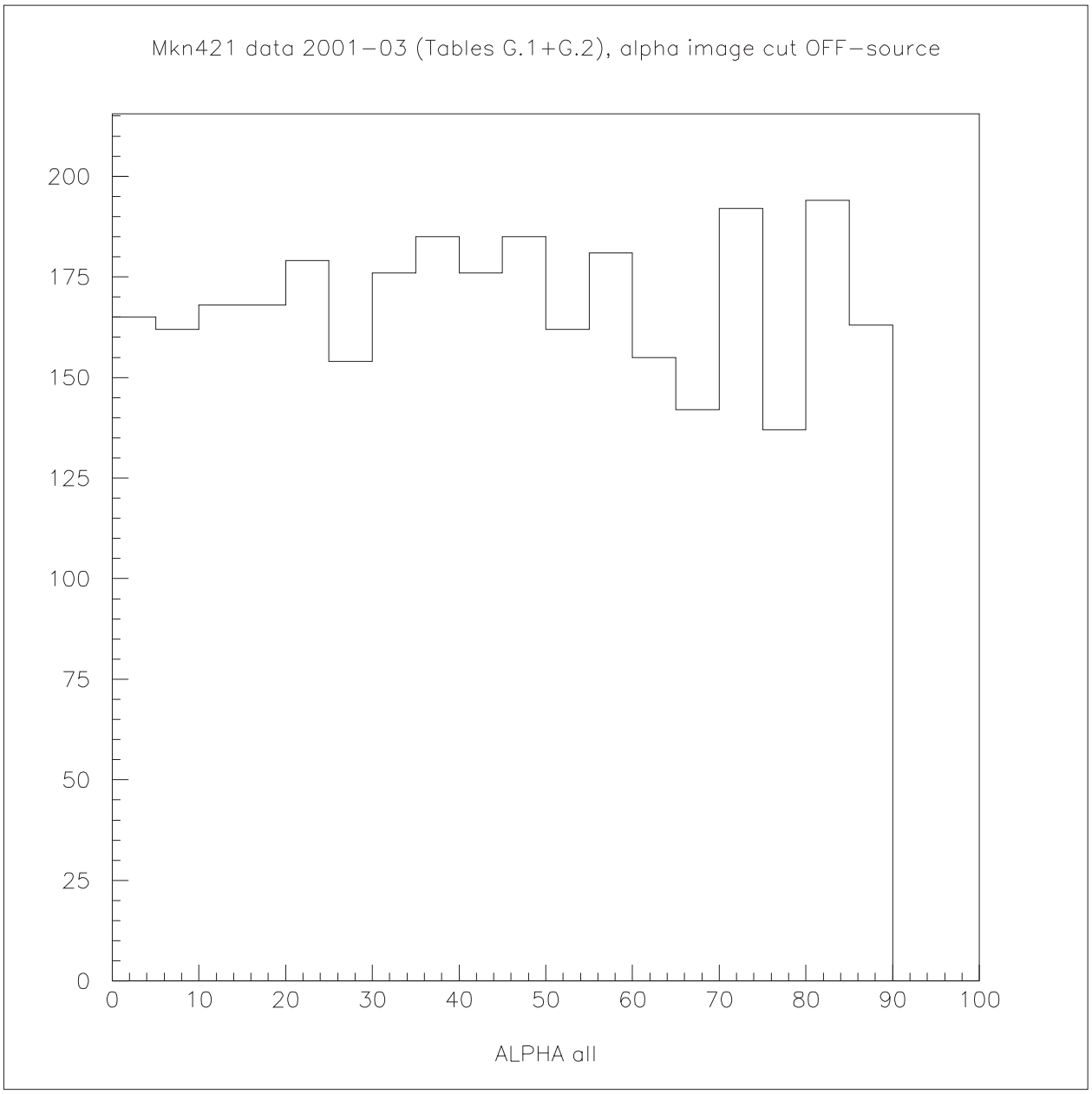

Figure J.2: The *alpha* image plot for all Markarian 421 T1 observation data from 2001 to 2003 (data files; see Tables H.1 and H.2, Appendix H). Off-source *alpha* plot only. See Figure 7.7 for comparison.

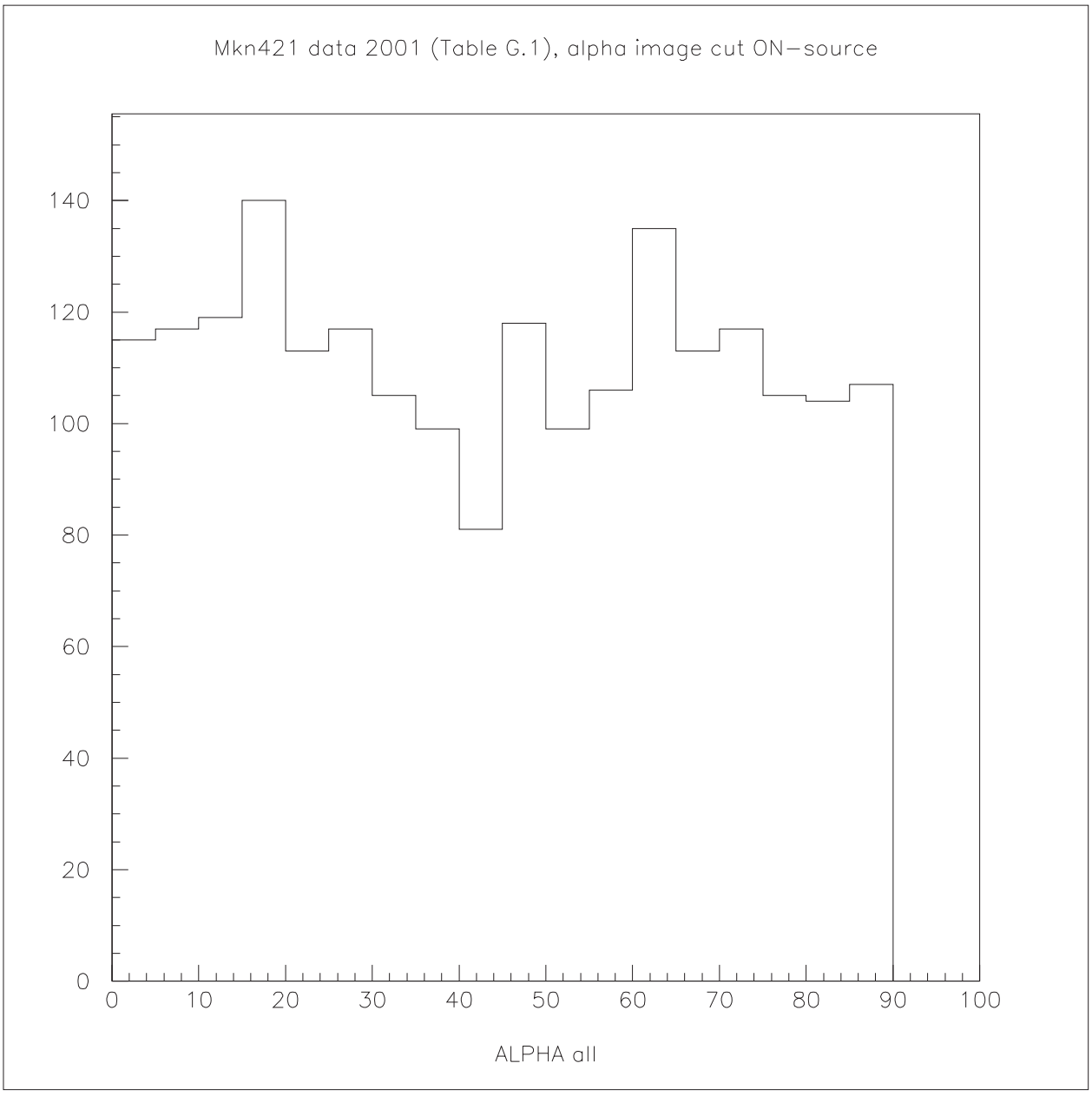

Figure J.3: The *alpha* image plot for Markarian 421 T1 observation data from 2001 (data files; see Table H.1, Appendix H). On-source *alpha* plot only. See Figure 7.8 for comparison.

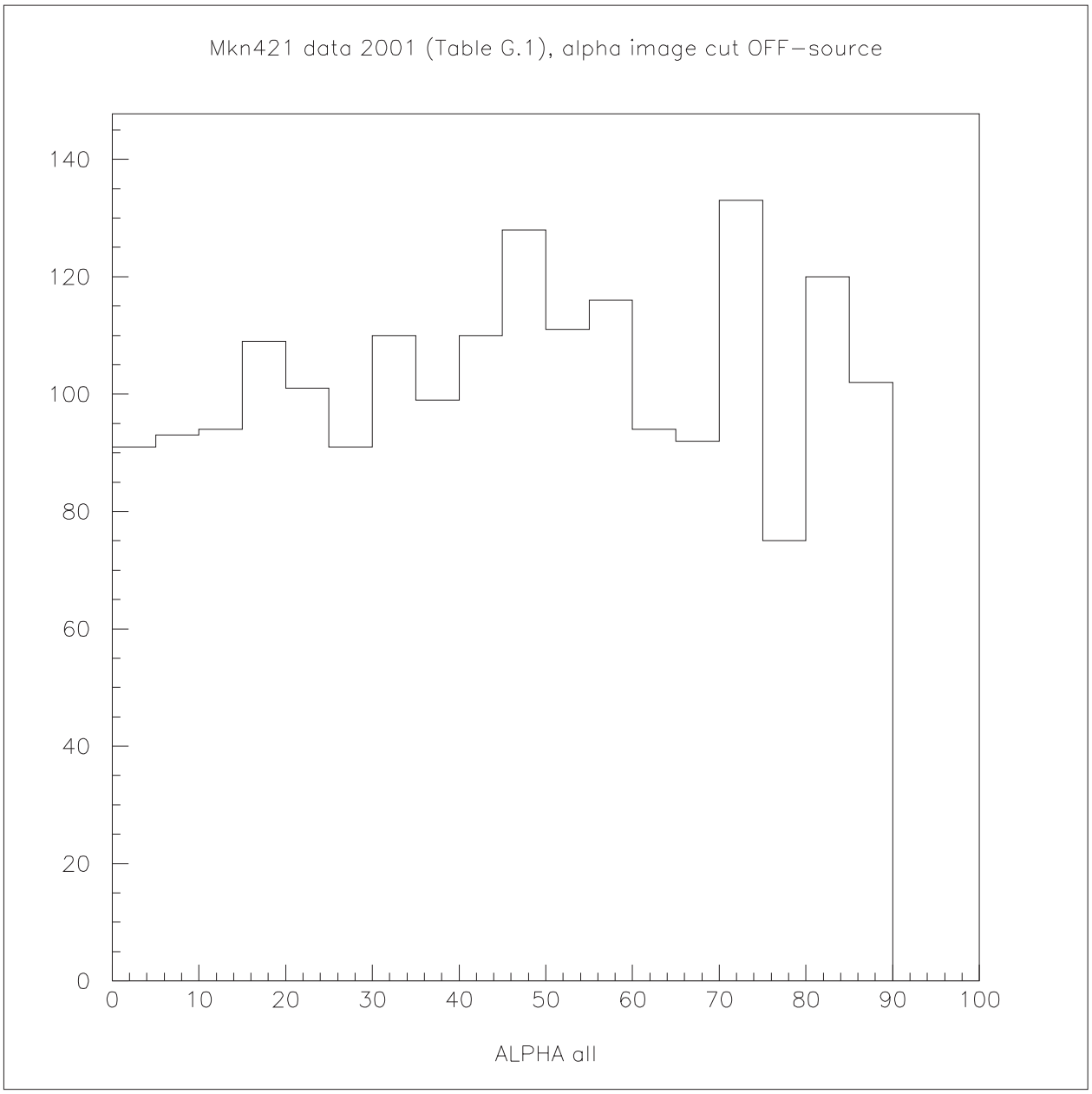

Figure J.4: The *alpha* image plot for Markarian 421 T1 observation data from 2001 (data files; see Table H.1, Appendix H). Off-source *alpha* plot only. See Figure 7.8 for comparison.

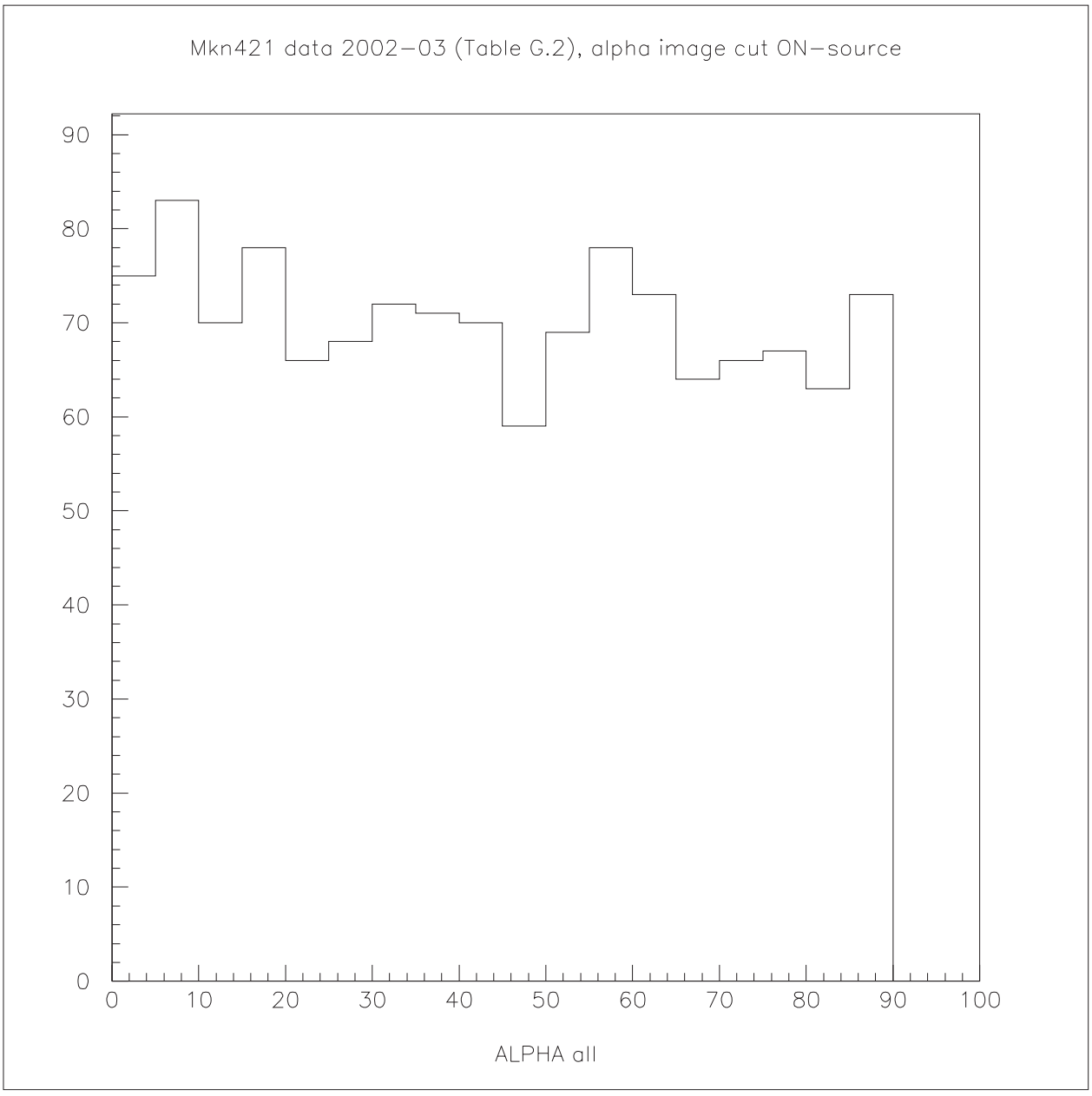

Figure J.5: The *alpha* image plot for Markarian 421 T1 observation data from 2002 to 2003 (data files; see Table H.2, Appendix H). On-source *alpha* plot only. See Figure 7.9 for comparison.

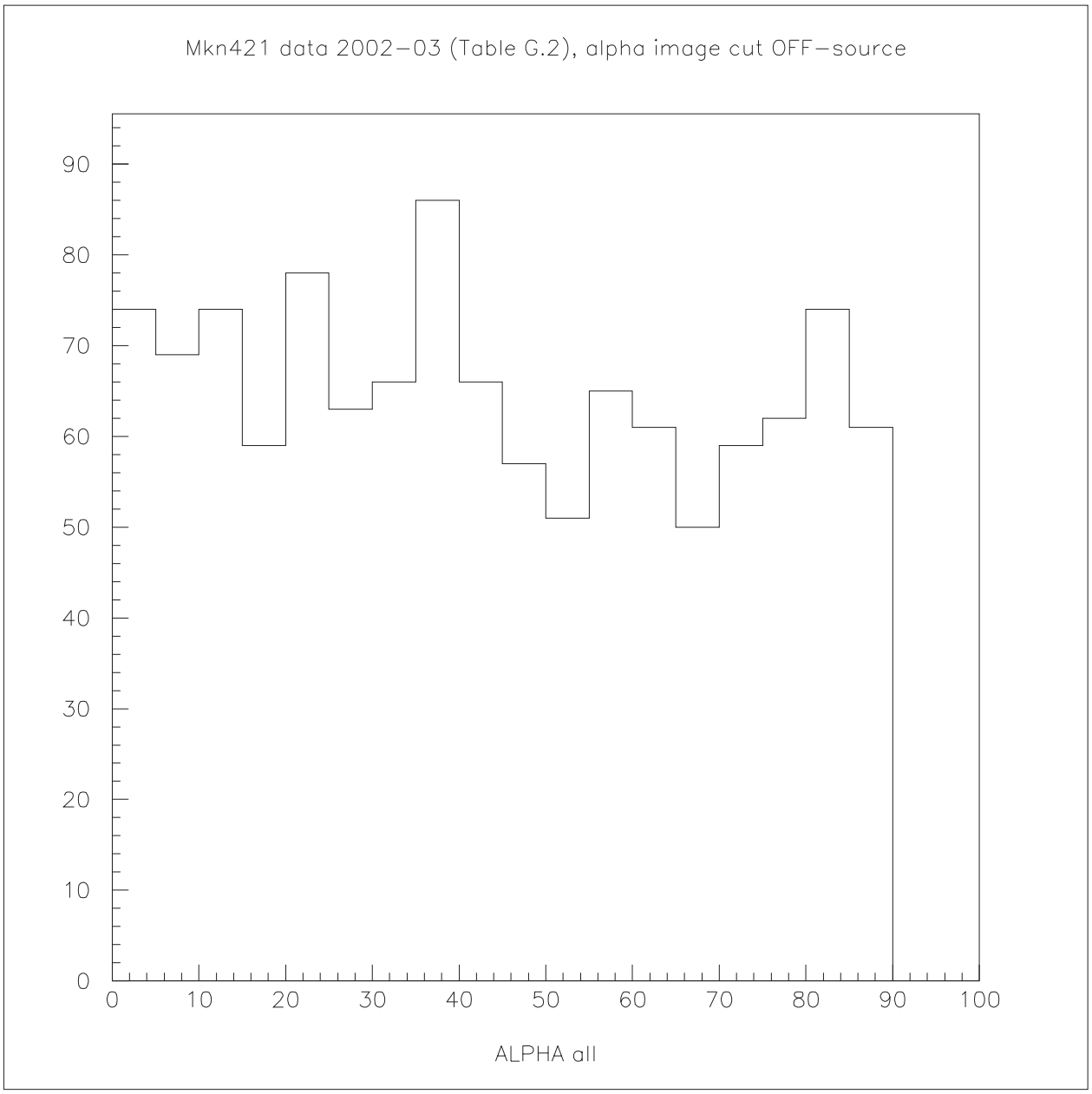

Figure J.6: The *alpha* image plot for Markarian 421 T1 observation data from 2002 to 2003 (data files; see Table H.2, Appendix H). Off-source *alpha* plot only. See Figure 7.9 for comparison.

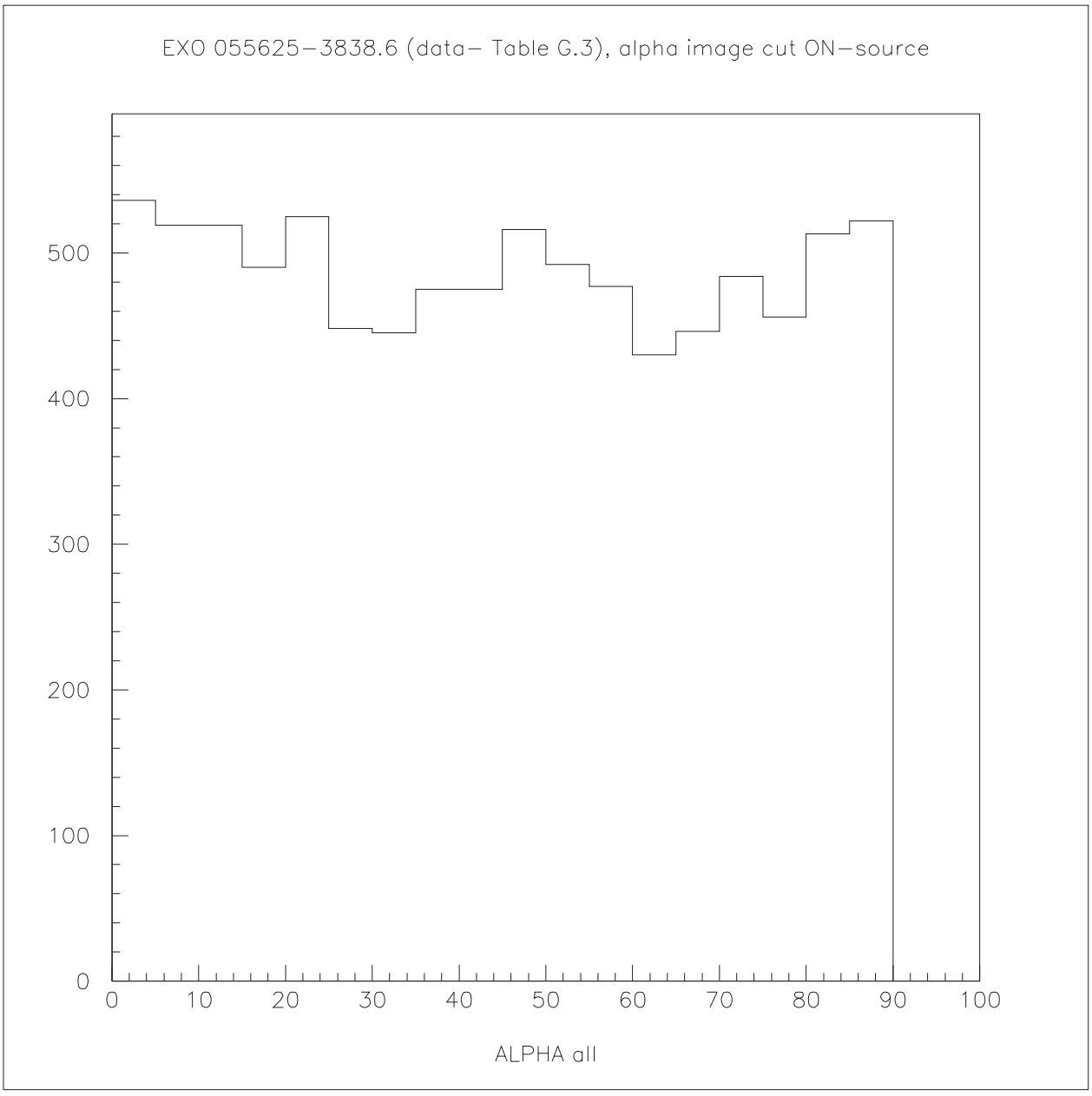

Figure J.7: The *alpha* image plot for EXO 055625-3838.6, T1 observation data from 2002-2003 (data files; see Table H.3, Appendix H). On-source *alpha* plot only. See Figure 7.14 for comparison.

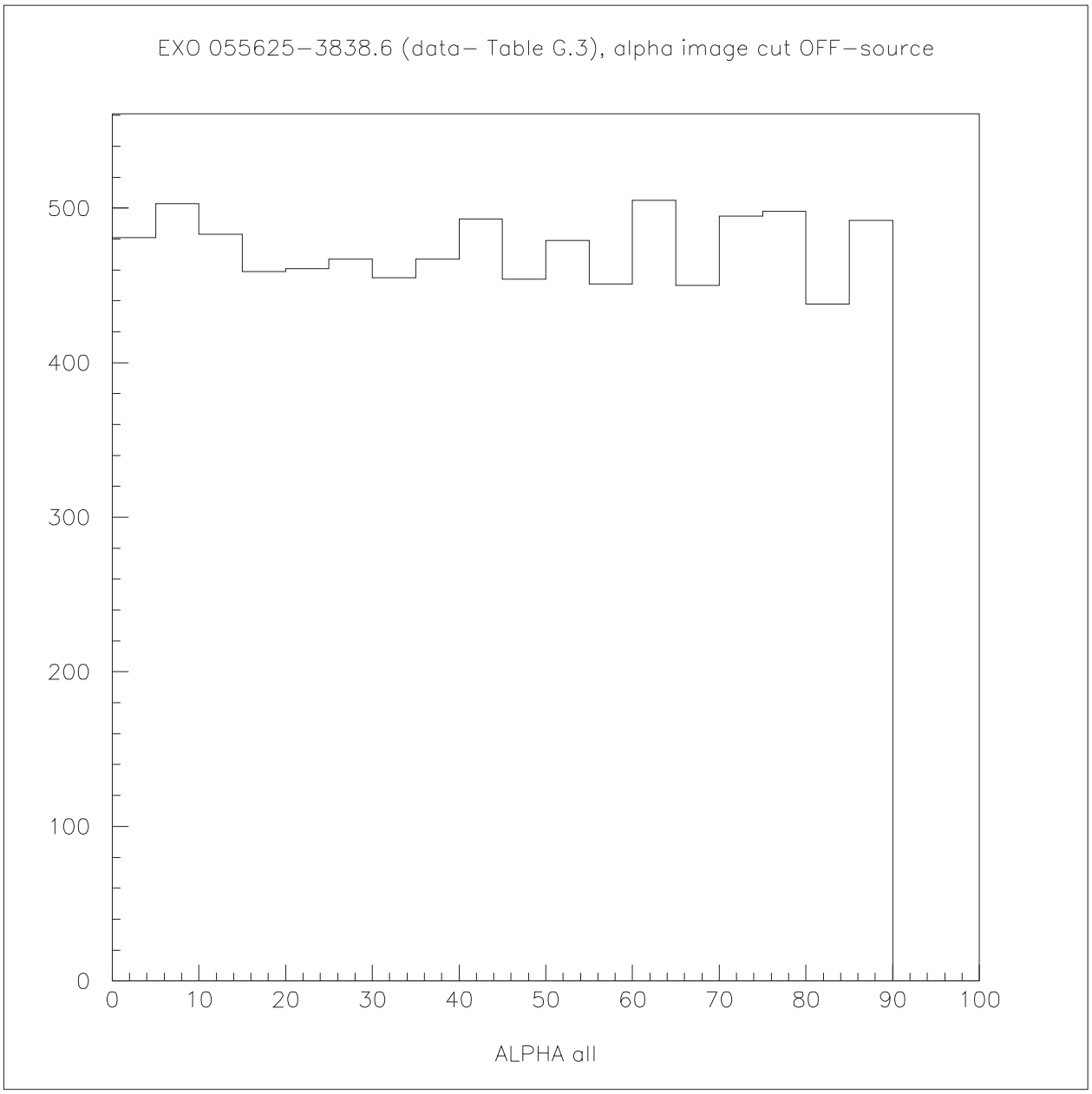

Figure J.8: The *alpha* image plot for EXO 055625-3838.6, T1 observation data from 2002-2003 (data files; see Table H.3, Appendix H). Off-source *alpha* plot only. See Figure 7.14 for comparison.

Appendix K

Incremental significance (S, Li & Ma (1983)) plotted against 5° $alpha$ distributions from Tables 7.2 and 7.3

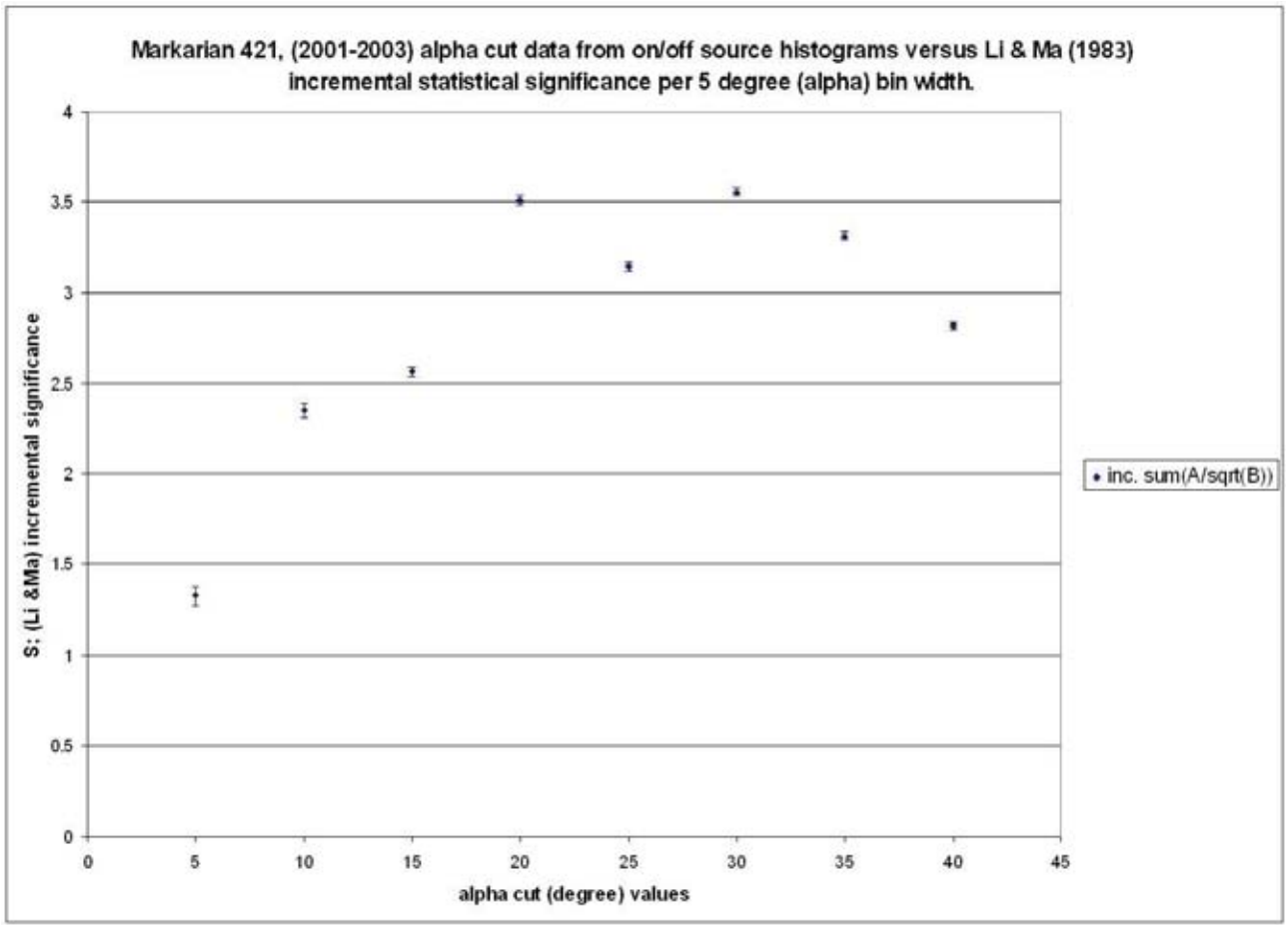

Figure K.1: Data taken directly from Table 7.2: Plot of Mkn 421 2001-2003 incremental significance calculated using equation 7.3 (Li & Ma (1983), [111]) against each 5° (bin width) angle in Figure 7.7 *alpha* cut histogram. The size of the error bars (uncertainty) in this figure are explained in Section 7.1.4 and in Table 7.2 caption.

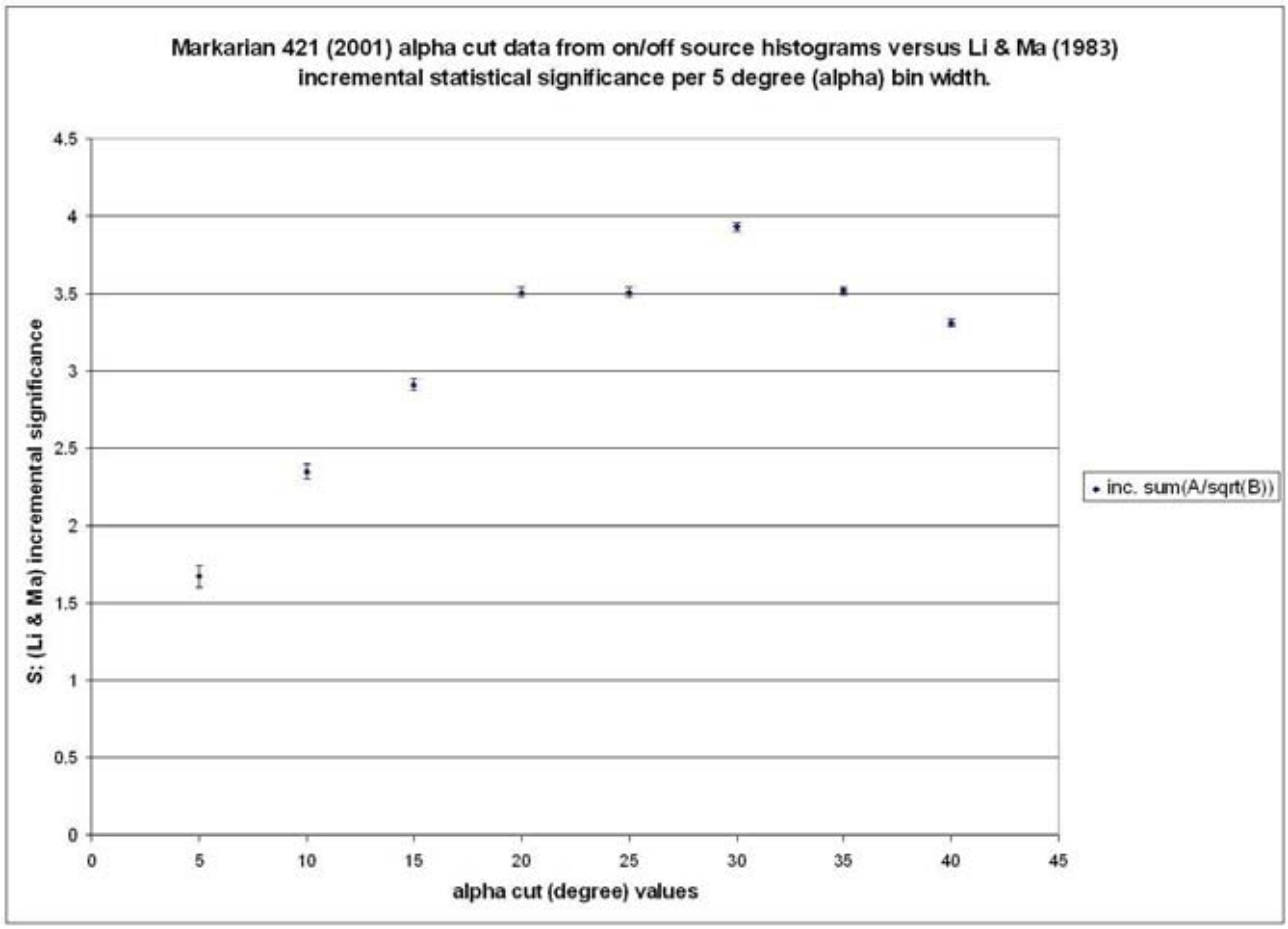

Figure K.2: Data taken directly from Table 7.2: Plot of Mkn 421 2001 incremental significance calculated using equation 7.3 (Li & Ma (1983), [111]) against each 5° (bin width) angle in Figure 7.8 *alpha* cut histogram. The size of the error bars (uncertainty) in this figure are explained in Section 7.1.4 and in Table 7.2 caption.

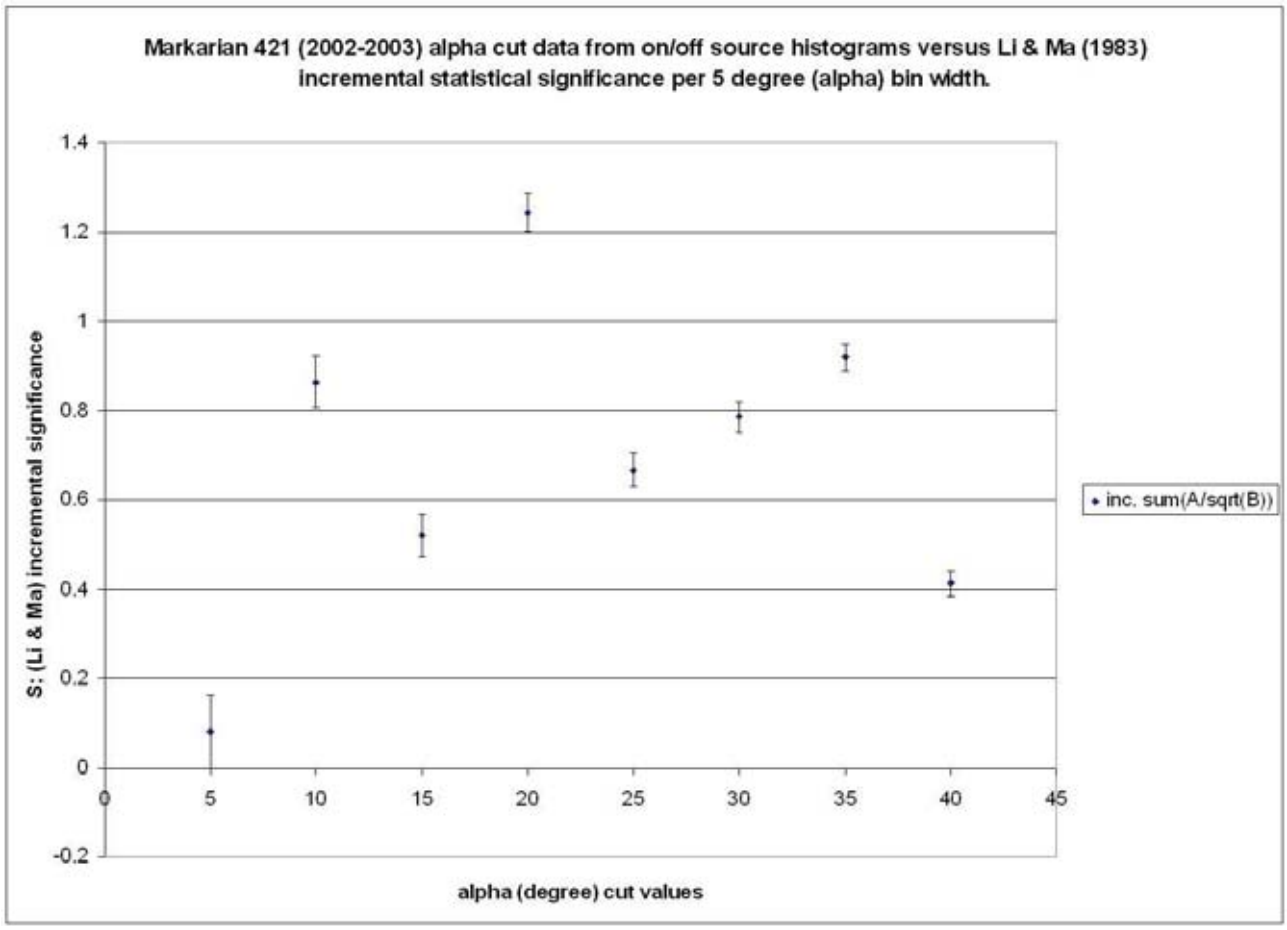

Figure K.3: Data taken directly from Table 7.2: Plot of Mkn 421 2002-2003 incremental significance calculated using equation 7.3 (Li & Ma (1983), [111]) against each 5° (bin width) angle in Figure 7.9 *alpha* cut histogram. The size of the error bars (uncertainty) in this figure are explained in Section 7.1.4 and in Table 7.2 caption.

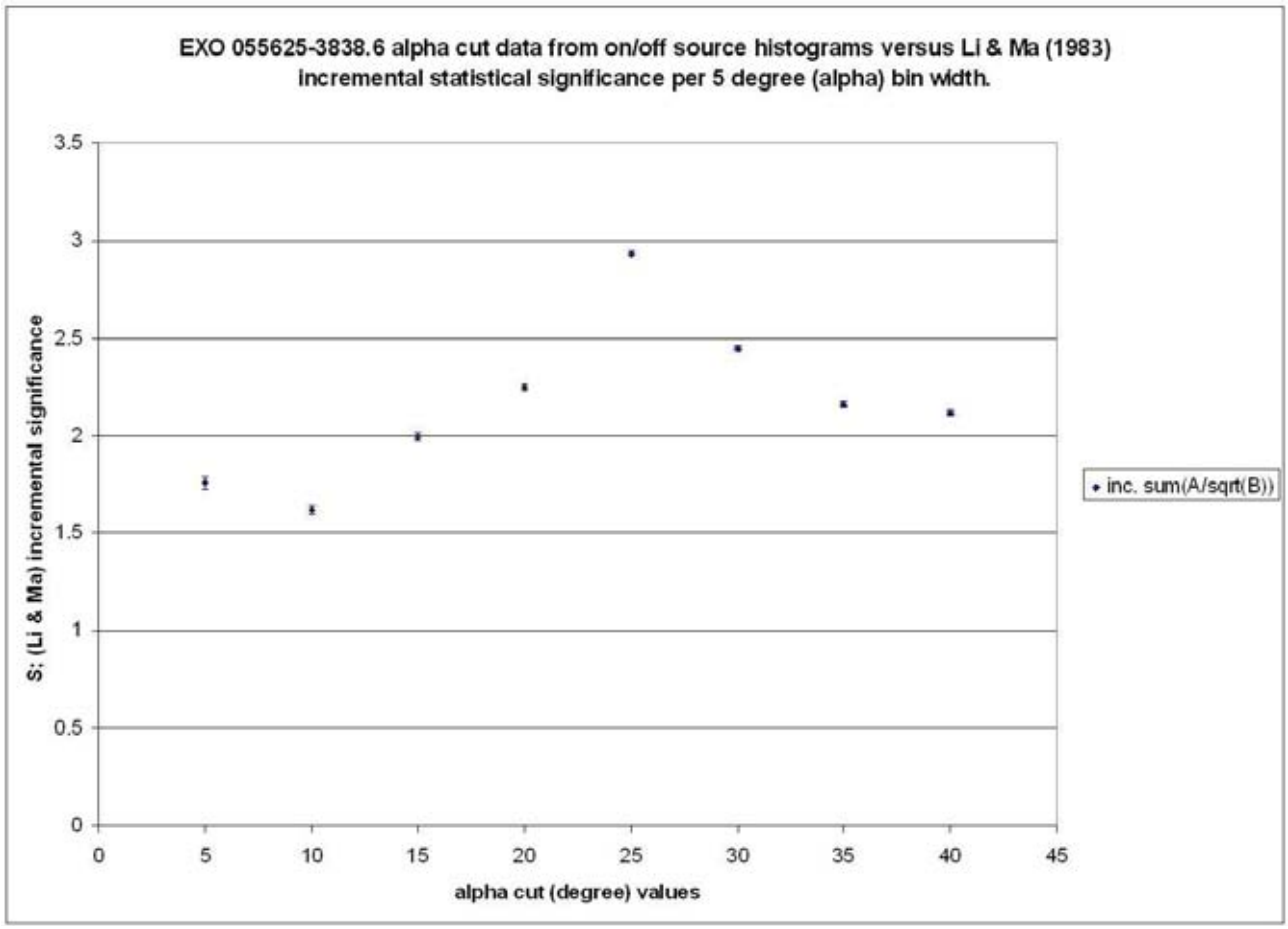

Figure K.4: Data taken directly from Table 7.3: Plot of EXO 055625-3838.6 incremental significance calculated using equation 7.3 (Li & Ma (1983), [111]) against each 5° (bin width) angle in Figure 7.14 *alpha* cut histogram. The size of the error bars (uncertainty) in this figure are explained in Section 7.1.4 and in Table 7.2 caption.

Bibliography

[1] Acciari, V.A. *et al.* (2009), *The Astrophys. J.*, **703**, 169.

[2] Aharonian, F. *et al.* (2008), *Astron.& Astrophys.*, **478(2)**, 387.

[3] Aharonian, F. *et al.* (2006), *Nature*, **440**, 1018.

[4] Aharonian, F. *et al.* (2005), *Astron.& Astrophys.*, **441**, 465.

[5] Aharonian, F. *et al.* (2005), *Astron.& Astrophys.*, **437**, 95.

[6] Aharonian, F. *et al.* (2004), *Astropart. Phys.*, **22(2)**, 109.

[7] Aharonian, F. *et al.* (2004), *The Astrophys. J.*, **614**, 897.

[8] Aharonian, F. *et al.* (2002), *Astron.& Astrophys.*, **393**, 89.

[9] Aharonian, F. *et al.* (2002), *Astron.& Astrophys.*, **384**, L23.

[10] Aharonian F. *et al.* (1999), *Astron.& Astrophys.*, **349**, 11.

[11] Albert, J. *et al.* (2008), *Nucl. Instrum. Meth. A*, **594(3)**, 407.

[12] Albert, J. *et al.* (2006), *arXiv:astro-ph/0603478v4*, Los Alamos National Laboratory of Astrophysical Abstracts, **http://xxx.lanl.gov/abs/astro-ph/0603478**.

[13] Aleksić, J. *et al.* (2010), *arXiv:1001.1291v1*, Los Alamos National Laboratory of Astrophysical Abstracts, **http://lanl.arxiv.org/abs/1001.1291v1**.

[14] Amenomori, M. *et al.* (2006), *Science*, **314**, 439.

[15] Amenomori, M. *et al.* (2003), *The Astrophys. J.*, **598**, 242.

[16] Amenomori, M. *et al.* (2003), *Proc. 28th I.C.R.C. (Tskuba, Japan)*, 3019.

[17] Arbeiter, C., Pohl, M. & Schlickeiser, R. (2005), *The Astrophys. J.*, **627**, 62.

[18] Asahara, A. *et al.* (2003), *Proc. 28th I.C.R.C. (Tskuba, Japan)*, 2807.

[19] Asakimori, K. *et al.* (1998), *The Astrophys. J.*, **502**, 278.

[20] Aschenbach, B. (1991), *Rev. Modern Astron.*, **4**, 173.

[21] Atkins, R. *et al.* (2000), *Nucl. Inst. Meths. in Phys. Research Sec. A*, **449**, 478.

[22] Atoyan, A. *et al.* (2005), *Astropart. Phys.*, **23**, 79.

[23] Atoyan, A. & Patera, J. (2004), *J. Mathematical Phys.*, **45**, 2468.

[24] Atwood, W.B. *et al.* (2009), *The Astrophys. J.*, **697**, 1071.

[25] Bass, M. *et al.* eds. (1995), *Handbook of optics/sponsored by the optical society of America*, **1**, 2nd. ed., pp. 44.2-44.33, McGraw-Hill, New York.

[26] Bastieri, D. *et al.* (2001), *Nucl. Inst. Meths. in Phys. Research Sec. A*, **461**, 521.

[27] Beddar, A.S. (2003), *et al., Phys. in Med. and Biology*, **48**(9), 1141.

[28] Bednarek, W. & Protheroe, R.J. (1999), *Monthly Not. R. Astronom. Soc.*, **310**, 577.

[29] Benbow, W. (2005), *Proc. 29th I.C.R.C. (Pune, India)*, 101.

[30] Bernlöhr, K. *et al.* (2003), *Astropart. Phys.*, **20**, 111.

[31] Bernstein, R.A., Freedman, W.L. & Madore, B.F. (2002), *The Astrophys. J.*, **571**, 56.

[32] Bevington, P.R. (1992), *Data reduction and error analysis for the physical sciences.*, 2nd. ed., McGraw-Hill, New York, pp. 11, 29, 59.

[33] Boella, G. *et al.* (1997), *Astron. & Astrophys. Suppl. Series*, **122**, 299.

[34] Boggess, N. *et al.* (1992), *The Astrophys. J.*, **397**, 420.

[35] Boone, L.M. *et al.* (2002), *The Astrophys. J. Lett.*, **579**, L5.

[36] Bracewell, R. (1999), *The Fourier Transform and Its Applications*, 3rd ed., McGraw-Hill, New York, pp. 46, 243.

[37] Bradbury, S.M. & Rose, H.J. (2002), *Nucl. Inst. Meths. in Phys. Research Sec. A*, **481** 521.

[38] Bradt, H. (2008), *Astrophysics Processes: The Physics of Astronomical Phenomena*, Cambridge University Press, Cambridge, England, pp. 260-265, 280, 336-342.

[39] Bradt, H. (2004), *Astronomy methods: a physical approach to astronomical observations*, Cambridge University Press, Cambridge, England, pp. 346.

[40] Brooks, D. (2003), *Crosstalk, Part 1. Understanding Forward vs. Backward*, UltraCAD Design Inc., Bellevue, WA, U.S.A.

[41] Burr, I.W (1974), *Applied statistical methods*, Academic Press, New York, pp. 346.

[42] Cambrésy, L. *et al.* (2001), *The Astrophys. J.*, **555**, 563.

[43] Catanese, M. *et al.* (1997), *The Astrophys. J.*, **487**, L143.

[44] Chary, R. & Elbaz, D. (2001), *The Astrophys. J.*, **556**, 562.

[45] Chudakov, A.E. *et al.* (1965), *Proc. P.N. Lebedev Phys. Inst.*, **26**, 99.

[46] Chupp, E.L. (1976), *Gamma-ray astronomy: Nuclear transition region.*, D. Reidel Pub. Co.

[47] Ciliegi, P. *et al.* (1993), *The Astrophys. J. Supp. Series*, **85**, 111.

[48] Clay, R.W. & Dawson, B. (1997), *Cosmic Bullets*, Allen & Unwin, Sydney NSW, pp. 6-30.

[49] Conner, J.P., Evans, W.D. & Belian, R.D. (1969), *The Astrophys. J.*, **157**, L157.

[50] Cornils, R. *et al.* (2003), *Astropart. Phys.* **20**, 129.

[51] Costamante, L. & Ghisellini, G. (2002), *Astron. & Astrophys.*, **384**, 56.

[52] Dazeley, S.A. (1999), *A search for Very High Energy Gamma-ray Emission From Four Galactic Pulsars*, PhD. thesis, University of Adelaide, pp. 62.

[53] de Jager, O.C. & Stecker, F.W. (2002), *The Astrophys. J.*, **566**, 738.

[54] Dwek, E & Krennrich, F. *The Astrophys. J.* (2005), **618**, 657.

[55] Elbaz, D. *et al.* (2002), *Astron. & Astrophys.*, **384**, 848.

[56] Fazio, G.G. *et al.* (1968), *Canadian J. of Phys.*, **46**, S451.

[57] Fazio, G.G. *et al.* (1972), *The Astrophys. J. Lett.*, **175**, L117.

[58] Fegan, D.J. *et al.* (1968), *Canadian J. of Phys.*, **46**, S433.

[59] Fichtel, C.E. *et al.* (1975), *The Astrophys. J.*, **198**, 163.

[60] Fixsen, D.J. *et al.* (1998), *The Astrophys. J.*, **508**, 123.

[61] Flyckt, S.O. & Marmonier, C. (2002), *Photomultiplier Tubes: Principles and applications*, Photonis, Brive, France, pp. 1-2, 1-3, 1-4, 1-5, 1-6, 1-7, 1-8, 1-9, 1-10, 1-11, 1-12, 1-13, 1-14, 1-15, 1-16, 1-17, 1-24, 1-35, 2-2, 2-8, 2-9, 2-11, 3-15.

[62] Fraß, A. *et al.* (1998), *Astropart. Phys.*, **8**, 91.

[63] Fruin, J.H. *et al.* (1964), *Phys. Lett.*, **10**, 176.

[64] Funk, S. *et al., Astropart. Phys.* (2004), **22**(3), 285.

[65] Gaidos, J.A. *et al.* (1996), *Nature*, **383**, 319.

[66] Galbraith, W. & Jelly, J.V. (1953), *Nature*, **171**, 349.

[67] Gardner, J.P., Brown, T.M. & Ferguson, H.C. (2000), *The Astrophys. J.*, **542**, L79.

[68] George, I.M. & Turner, T.J. (1996), *The Astrophys. J.*, **461**, 198.

[69] Gibson, A.I. *et al.* (1982), *Proc. Very High Energy Gamma Ray Astron. (Ootacamund, India)*, Smithsonian Inst. Pubs., 97.

[70] Giommi, P. *et al.* (1989), *Mon. Not. R. Astron. Soc.*,**236**, 375.

[71] Graff, P.B. *et al.* (2008), *The Astrophys. J.*, **689**, 68.

[72] Grindlay, J.E. *et al.* (1973), *Proc. 13th I.C.R.C. (Denver, U.S.A.)*, **1**, 36.

[73] Gunji, S. *et al.* (2006), *Cangaroo Observation Manual, Version 2006.11.09*, **http://venus.icrr.u-tokyo.ac.jp/obsmanual_html/hardware.html**, ICRR, University of Tokyo, Japan.

[74] *Hamamatsu photomultiplier tube R4124.* (1998), Technical document; **TPMH1233E01**, Hamamatsu Photonics Corp., Japan.

[75] Hartman, R.C. *et al.* (1999), *The Astrophys. J. Suppl. Series*, **123**, 79.

[76] Hauser, M. & Dwek, E. (2001), *Ann. Rev. Astron. & Astrophys.*, **39**, 249.

[77] Hauser, M. *et al.* (1998), *The Astrophys. J.*, **508**, 25.

[78] Hecht, E. (1987), *Optics*, 2nd. ed., Addison-Wesley, Reading Massachussets, pp. 80, 392, 396, 422, 447, 472, 475.

[79] Hillas, A.M. *et al.* (1998), *The Astrophys. J.*, **503**, 744.

[80] Hillas, A.M. & Patterson, J.R. (1990), *J. Phys. G*, **16**, 1271.

[81] Hillas, A.M. (1985), *Proc. 19th I.C.R.C. (La Jolla, U.S.A.)*, **3**, 445.

[82] Hinton, J.A. (2004), *Astropart. Phys.* **48**, 331.

[83] Hofmann, W. (2003), *Proc. 28th I.C.R.C. (Tskuba, Japan)*, 2811.

[84] Holder, J. *et al.* (2006), *Astropart. Phys.*, **25**, 391.

[85] Holder, J. (2001), *Proc. 27th I.C.R.C. (Hamburg, Germany)*, 2613.

[86] Horns, D., Kohnle, A & Aharonian, F.A. (2001), *Proc. 27th I.C.R.C. (Hamburg, Germany)*, 106.

[87] Illingworth, V. (ed.) (1994), *Collins Dictionary of Astronomy*, HarperCollins, Glasgow, pp. 430.

[88] Ito, C. (2000), *3. Camera design*, CANGAROO images (unpublished), CANGAROO-III, **http://icrhp9.icrr.u-tokyo.ac.jp/private/C3/images/C-iii-cam.gif**, ICRR, University of Tokyo, Japan.

[89] Jackson, J. & Vette, J.I. (1975), *OGO Program Summary*, NASA SP-7601.

[90] Jansen, F. *et. al* (2001), *Astron. & Astrophys.*, **365**, L1.

[91] Jauch, J.M. & Rohrlich, F. (1955), *The Theory of Protons and Electrons*, Addison-Wesley, Cambridge.

[92] Kabuki, S. *et al.* (2003), *Proc. 28th I.C.R.C. (Tskuba, Japan)*, 2859.

[93] Kashlinsky, A. (2005), *Physics Reports*, **409**, 361.

[94] Kawachi, A. *et al.* (2001), *Astropart. Phys.*, **14**, 261.

[95] Kirkup, L. (1994), *Experimental Methods*, John Wiley & Sons, Brisbane, pp. 85.

[96] Kneiske, T.M., Mannheim, K. & Hartmann, D.H. (2002), *Astron. & Astrophys.*, **386**, 1.

[97] Kneiske, T.M. *et al.* (2004), *Astron. & Astrophys.*, **413**, 807.

[98] Kohnle, A., Horns, D. & Krawczynski, H. (2001), *Proc. 27th I.C.R.C. (Hamburg, Germany)*, 2605.

[99] Konopelko, A. *et al.* (2003), *The Astrophys. J.*, **597**, 851.

[100] Kranich, D. *et al.* (1999), *Astropart. Phys.*, **12**, 65.

[101] Kraushaar, W. *et al.* (1965), *The Astrophys. J.*, **141**, 845.

[102] Krennrich, F. *et al.* (2002), *The Astrophys. J.*, **575**, L9.

[103] Krennrich, F. *et al.* (2001), *The Astrophys. J.*, **560**, L45.

[104] Kubo, H. *et al.* (2003), *Proc. 28th I.C.R.C. (Tskuba, Japan)*, 2863.

[105] Kubo, H. *et al.* (2001), *Proc. 27th I.C.R.C. (Hamburg, Germany)*, 2900.

[106] Kumar, R. *et al., Optics & Laser Tech.* (2007), **39**(2), 256.

[107] Lampton, M. & Raffanti, R. (1994), *Rev. Sci. Instrum.*, **65**(11), 3577.

[108] Legache, G. *et al.* (2000), *Astron. & Astrophys.*, **354**, 247.

[109] Lemière, A. (2004), *AIP Conf. Proc.*, **745**, 443.

[110] Levine, A.M. *et al.* (1996), *The Astrophys. J.*, **469**, L33.

[111] Li, T. & Ma, Y. (1983), *The Astrophys. J.*, **272**, 317.

[112] Lichti, G.G. *et al.* (2007), *AIP Conf. Proc.*, **906**, 119.

[113] Liu, M. (2006), *Demystifying switched-capacitor circuits*, Newnes, Oxford, pp. 58.

[114] Longair, M.S. (1997), *High Energy Astrophysics. Volume 2: Stars, the Galaxy and the interstellar medium*, 2nd ed., Cambridge University Press, Cambridge, England, pp. 248, 259, 261-62.

[115] Madau, P. & Pozzetti, L. (2000), *MNRAS*, **312**, L9.

[116] Martin, W.H. (1929), "DeciBel, the New Name for the Transmission Unit", *Bell System Technical Journal*, John Wiley & Sons, New York.

[117] Martínez, M. (2003), *Proc. 28th I.C.R.C. (Tskuba, Japan)*, 2815.

[118] Metcalfe, L. (2003), *et al., Astron. & Astrophys.*, **407**, 791.

[119] Michelson, P.F. (2003), *X-ray and Gamma-Ray Telescopes and Instruments for Astronomy, SPIE Proc.*, **4851**, 1144.

[120] Mori, M. (2000), *Some pictures of the telescope*, CANGAROO images (unpublished), CANGAROO-II, **http://icrhp9.icrr.u-tokyo.ac.jp/image/00Mar/10m-2.jpg**, ICRR, University of Tokyo, Japan.

[121] Mori, M. (2000), *Some pictures of the telescope*, CANGAROO images (unpublished), CANGAROO-II, **http://icrhp9.icrr.u-tokyo.ac.jp/image/552chCamera.jpg**, ICRR, University of Tokyo, Japan.

[122] Mori, M. (2000), *73. Ampbox and PMT numbering after the camera expansion*, CANGAROO images (unpublished), CANGAROO-II, **http://icrhp9.icrr.u-tokyo.ac.jp/private/C2/images/Ampbox-numbering.gif**, ICRR, University of Tokyo, Japan.

[123] Mori, M. (2002), *Some pictures of telescopes*, CANGAROO images (unpublished), CANGAROO-III, **http://icrhp9.icrr.u-tokyo.ac.jp/private/pictures/2002/2002_0315/P3150057.JPG**, ICRR, University of Tokyo, Japan.

[124] Moskalenko, I.V., Porter, T.A. & Strong, A.W. (2006), *The Astrophys. J.* **640**, L155.

[125] Mücke, A. & Protheroe, R.J. (2001), *Astropart. Phys.*, **15**, 121.

[126] Nakase, T. (2001), *PKS 2005-489 Analysis Status Report*, 2001/07/05, **http://www-cr.scphys.kyoto-u.ac.jp/member/cangaroo/analysis**, Kyoto University, Japan.

[127] Nishida, D. *et al.* (2002), *Proc. The Universe viewed in Gamma-Rays (Kashiwa, Japan)*, T17.

[128] Nolan, P.L. *et al.* (1992), *IEEE Trans. Nucl. Sci.*, **39**, 993.

[129] Ohishi, M. *et al.* (2003), *Proc. 28th I.C.R.C. (Tskuba, Japan)*, 2855.

[130] Ohishi, M. *et al.* (2003), *Report on the reflector tuning works in July 2003 for the CANGAROO-III 2nd and 3rd telescope*, CANGA-

ROO documents (unpublished), Various reports, **http://icrhp9.icrr.u-tokyo.ac.jp/private/reports/reflector_jul2003.pdf**, ICRR, University of Tokyo, Japan.

[131] Ohska, T.K. (1989), *IEEE Trans. Nucl. Sci.*, **36**, 1650.

[132] Okumura, K. (2000), *Calib 7 manual*, Instructions for the software algorithms and data banks for *calib10a*. **http://icrhp9.icrr.u-tokyo.ac.jp/private**, ICRR, University of Tokyo, Japan.

[133] Okumura, K. *et al.* (2002), *The Astrophys. J. Lett.*, **579**, L9-L12.

[134] Papoulis, A. (1962), *The Fourier Integral and Its Applications*, 3rd ed., McGraw-Hill, New York, pp. 244-245, 252-253.

[135] Papovich, C. *et al.* (2004), *The Astrophys. J. Supp.*, **154**, 70.

[136] Patterson, J.R., Swaby, D.L. & Wild, N. (2001), *AIP Conf. Proc.*, **558**, 625.

[137] Peacock, J.A. (1999), *Cosmological Physics*, Cambridge University Press, Cambridge.

[138] Petry, D. *et al.* (1996), *Astron. & Astrophys.*, **311**, L13.

[139] Primack, J.R. *et al.* (2001), *AIP Conf. Proc.*, **558**, 463.

[140] Protheroe, R.J. & Mücke, A. (2001a), *Particles and Fields in Radio Galaxies (San Francisco, U.S.A.), ASP Conf. Proc.*, **250**, 113.

[141] Protheroe, R.J. & Mücke, A. (2001b), *AIP Conf. Proc.*, **558**, 700.

[142] Puhlhofer, G. *et al.* (2003), *Astropart. Phys.*, **20**, 267.

[143] Punch, M. (1993), *New Techniques in TeV Gamma Ray Astronomy*, Ph.D. Thesis, National University of Ireland.

[144] Punch, M. *et al.* (1992), *Nature*, **358**, 477.

[145] Ravnda, S. *ed.* (1994), CERN Institute *GEANT* tutorial manual, **http://wwwasd.web.cern.ch/wwwasd/geant/tutorial/manual/tutorial_1.html**, Geneva Switzerland.

[146] Rebillot, P.F. *et al.* (2003), *Proc. 28th I.C.R.C. (Tskuba, Japan)*, 2599.

[147] Reynolds, A.P. *et al.* (1999), *Astron. & Astrophys. Supp. Series*, **134**, 287R.

[148] Reynolds, A.P. *et al.* (1993), *The Astrophys. J.*, **404**, 206.

[149] Röken, C. & Schlickeiser, R. (2009), *Astron. & Astrophys.*, **503**, 309.

[150] Rosswog, S, & Brüggen, M. (2007), *Introduction to High-Energy Astrophysics*, Cambridge University Press, Cambridge, England, pp. 151.

[151] Rowell, G.P. (1995), *A search for Very High Energy Gamma rays from PSR1706-44 using the Atmospheric Čerenkov Imaging Technique*, PhD. thesis, University of Adelaide, pp. 28-32.

[152] Rybicki, G.B & Lightman, A.P. (1979), *Radiative Processes in Astrophysics*, John Wiley & Sons, New York, pp. 169-175.

[153] Salamon, M.H. & Stecker F.W. (1998), *The Astrophys. J.*, **493**, 547.

[154] Sbarufatti, B. *et al.* (2005), *The Astronom. J.*, **129**, 559.

[155] Schroedter, M. (2005), *The Astrophys. J.*, **628**, 617.

[156] Sevilla, I., Barrio, J.A. & Fonseca, V. (2003), *Astropart. Phys.*, **19**, 495.

[157] Smith, R.J. (1987), *Electronics Circuits and Devices*, 3rd ed., John Wiley & Sons, New York, 327.

[158] Swanenburg, B.N. *et al.* (1994), *The Astrophys. J. Lett.*, **243**, L73.

[159] Tanaka, Y., Inoue H., & Holt, S.S. (1994), *PASJ*, **46**, L73.

[160] The L3 collaboration, CERN (2008), *Astron. & Astrophys.*, **488**, 1093.

[161] Ulmer *et al.* (1974), *The Astrophys. J.*, **192**, 691.

[162] Vacanti, G. *et al.* (1991), *The Astrophys. J.*, **377**, 467.

[163] Vincent, P. *et al.* (2003), *Proc. 28th I.C.R.C. (Tskuba, Japan)*, 2887.

[164] Vladimirski, B.M. *et al.* (1973), *Proc. 13th I.C.R.C. (Denver. U.S.A.)*, **1**, 456.

[165] Weekes, T.C. *et al.* (2002), *Astropart. Phys.*, **17**, 221.

[166] Weekes, T.C. *et al.* (1989), *The Astrophys. J.*, **342**, 379.

[167] Weekes, T.C. (1988), *Phys. Report*, **160**, 1.

[168] Weekes, T.C. *et al.* (1972), *The Astrophys. J.*, **174**, 165.

[169] Weisskopf, M.C. *et al.* (2000), *The Astrophys. J.*, **536**, L81.

[170] Winston, R. (1970), *J. of the Optical Soc. of America*, **60**, 245.

[171] Wright, E.L. (2001), *The Astrophys. J.*, **553**, 538.

[172] Wright, E.L. & Reese, E.D. (2000), *The Astrophys. J.*, **545**, 43.